

Aus dem Fachbereich Medizin  
der Goethe-Universität  
Frankfurt am Main

Gustav-Embden-Zentrum für Biologische Chemie  
Institut für Biochemie I - Pathobiochemie  
Direktor: Prof. Dr. Bernhard Brüne

**The role of peroxisome proliferator-activated receptor  $\gamma$   
during sepsis-induced lymphopenia**

Dissertation

zur Erlangung des Doktorgrades der theoretischen Medizin  
des Fachbereichs Medizin der Goethe-Universität  
Frankfurt am Main

vorgelegt von  
**Martina Victoria Schmidt**  
aus Haan

Frankfurt am Main 2011

Dekan:	Prof. Dr. Josef Pfeilschifter
Referent:	PD Dr. Andreas von Knethen
Korreferent:	Prof. Dr. Dr. Kai Zacharowski
2. Korreferent:	Prof. Dr. Volkhard Kempf
Tag der mündlichen Prüfung:	09.11.2011

*„So eine Arbeit wird eigentlich nie fertig,  
man muss sie für fertig erklären,  
wenn man in der Zeit und den Umständen  
das Möglichste getan hat“*

- Johann Wolfgang von Goethe -

## TABLE OF CONTENTS

<b>Table of Contents</b>	I
<b>List of Figures</b>	III
<b>List of Tables</b>	V
<b>Abbreviations</b>	VI
<b>1. Summary</b>	1
<b>2. Zusammenfassung</b>	3
<b>3. Introduction</b>	5
3.1. Sepsis	5
3.1.1. History	5
3.1.2. Epidemiology and definition	6
3.1.3. Sepsis pathophysiology	7
3.2. PPAR $\gamma$	19
3.2.1. Between transcription and transrepression	19
3.2.2. Structure	20
3.2.3. PPAR $\gamma$ ligands	23
3.2.4. Anti-inflammatory properties	24
3.3. Apoptosis	26
3.3.1. Apoptosis versus necrosis	26
3.3.2. Regulation of apoptosis	27
3.4. Preliminary data: PPAR $\gamma$ during sepsis	30
3.5. Aims of this study	31
<b>4. Material and Methods</b>	32
4.1 Material	32
4.1.1. Mice	32
4.1.2. Chemicals, Reagents and Kits	32
4.1.3. Antibodies	34
4.1.4. Oligonucleotides	35
4.1.5. Equipment & Software	35
4.2. Methods	37
4.2.1. Mouse work	37
4.2.2. Primary cell analysis	39
4.2.3. Biochemistry and molecular biology	41
4.2.4. Microbiology	46
4.2.5. Statistical analysis	46

<b>5. Results</b>	48
5.1. Phenotyping Tc-PPAR $\gamma$ <sup>-/-</sup> mice	48
5.2. LPS-induced systemic inflammation in Tc-PPAR $\gamma$ <sup>-/-</sup> vs. WT mice	49
5.3. CLP-induced sepsis in Tc-PPAR $\gamma$ <sup>-/-</sup> vs. WT mice	50
5.3.1. Absolute T-cell count	50
5.3.2. Detection of apoptotic T-cells	51
5.3.3. Survival studies	52
5.3.4. Apoptotic signaling in WT vs. Tc-PPAR $\gamma$ <sup>-/-</sup> T-cells	54
5.4. Neutralizing IL-2 impairs pro-survival signaling in Tc-PPAR $\gamma$ <sup>-/-</sup>	56
5.5. Therapeutical use of PPAR $\gamma$ the antagonist GW9662	62
5.5.1. Absolute T-cell count	63
5.5.2. Detection of T-cell apoptosis	65
5.5.3. Apoptotic signaling during sepsis after GW9662	67
5.5.4. Exploring the therapeutic window of GW9662 medication	69
<b>6. Discussion</b>	71
6.1. Problems in current sepsis therapy	71
6.2. T-cell apoptosis during sepsis	72
6.3. Apoptosis pathways during sepsis modified by PPAR $\gamma$	74
6.4. Systemic effects of PPAR $\gamma$ antagonism with GW9662	79
6.5. Systemic inflammation vs. sepsis - LPS vs. CLP	81
6.6. Possible consequences for sepsis treatment	82
6.7. Outlook	84
6.7.1. The role of PTEN during sepsis progression	84
6.7.2. Impact of GW9662 on T-cells of septic patients	85
6.7.3. Antagonism of S1P to improve peripheral T-cell counts	86
<b>7. References</b>	89
<b>8. Appendix</b>	106
<b>9. Publications</b>	109
<b>10. Acknowledgments</b>	112
<b>11. Curriculum Vitae</b>	114
<b>12. Erklärung</b>	115

## LIST OF FIGURES

#

Figure 1: Pathogenic networks during septic shock.....	11#
Figure 2: Sepsis pathophysiology. ....	14#
Figure 3: Regulation of coagulation during sepsis .....	16#
Figure 4: SIRS and CARS during inflammation .....	18#
Figure 5: PPAR $\gamma$ domain structure .....	21#
Figure 6: Chemical structure of rosiglitazone and GW9662 .....	21#
Figure 7: Effect of different ligands on the PPAR $\gamma$ -RXR $\alpha$ complex .....	22#
Figure 8: PPAR $\gamma$ -dependent repression of pro-inflammatory cytokine production. ....	26#
Figure 9: Cecum ligation and puncture sepsis model.....	38#
Figure 10: PPAR $\gamma$ expression in T-cells derived from WT or Tc-PPAR $\gamma$ <sup>-/-</sup> mice .....	48#
Figure 11: LPS-induced T-cell depletion and underlying apoptotic signals .....	50#
Figure 12: Flow cytometric quantification of spleen and blood derived T-cells .....	51#
Figure 13: Apoptosis detection in septic Tc-PPAR $\gamma$ <sup>-/-</sup> mice and WT mice .....	52#
Figure 14: Survival curves of CLP-induced death of WT and Tc-PPAR $\gamma$ <sup>-/-</sup> mice .....	53#
Figure 15: Bacterial load and end organ damage in septic WT and Tc-PPAR $\gamma$ <sup>-/-</sup> mice.....	54#
Figure 16: IL-2 mRNA expression, intracellular IL-2 protein expression and binding of NFAT to the IL-2 promoter in T-cells from WT and Tc-PPAR $\gamma$ <sup>-/-</sup> mice .....	55#
Figure 17: Bcl-2 mRNA and protein expression in septic WT and Tc-PPAR $\gamma$ <sup>-/-</sup> mice .....	56#
Figure 18: Tc-PPAR $\gamma$ <sup>-/-</sup> mice received either 500 $\mu$ g anti-IL-2 or 500 $\mu$ g IgG control antibody .....	57#
Figure 19: Evaluation of apoptosis by TUNEL and active caspase 3 staining in anti-IL-2 and IgG-treated Tc-PPAR $\gamma$ <sup>-/-</sup> mice .....	58#
Figure 20: Comparison of survival of anti-IL-2-treated and IgG-treated Tc-PPAR $\gamma$ <sup>-/-</sup> mice.....	58#
Figure 21: Bacterial clearance and end organ damage in anti-IL-2 and IgG-treated Tc-PPAR $\gamma$ <sup>-/-</sup> mice.....	59#
Figure 22: Bcl-2 mRNA and protein expression in anti-IL-2 and IgG-treated Tc-PPAR $\gamma$ <sup>-/-</sup> mice .....	59#
Figure 23: PTEN and pAkt expression in WT and Tc-PPAR $\gamma$ <sup>-/-</sup> mice.....	60#

---

Figure 24: Bim mRNA and protein expression in WT and Tc-PPAR $\gamma$ <sup>-/-</sup> mice.....	61#
Figure 25: Bim expression on mRNA and protein level in anti-IL-2 and IgG-treated Tc-PPAR $\gamma$ <sup>-/-</sup> mice.....	62#
Figure 26: Correlation of T-cell count and T-cell PPAR $\gamma$ expression upon CLP and impact of GW9662 timing regime on T-cell count.....	63#
Figure 27: Absolute T-cell count in spleens and blood of WT mice treated with 1 mg/kg GW9662 at 3 h after CLP .....	64#
Figure 28: <i>In vivo</i> PPRE reporter activity in response to GW9662 stimulation in septic mice.. ..	65#
Figure 29: Detection of apoptosis via TUNEL assay and active caspase 3 staining upon GW9662 stimulation.....	65#
Figure 30: Comparison of survival of GW9662-treated and DMSO-treated WT mice.....	66#
Figure 31: Bacterial clearance and end organ damage quantification in GW9662-treated mice.. ..	67#
Figure 32: Pro- and anti-apoptotic signaling on mRNA level in WT mice treated with GW9662 or DMSO.....	68#
Figure 33: Analysis of apoptosis pathways upon GW9662 or DMSO treatment .....	68#
Figure 34: Absolute T-cell count in WT mice treated with 3 mg/kg GW9662 or DMSO at 5 h after CLP .....	69#
Figure 35: Comparison of survival of GW9662-treated and DMSO-treated Tc-PPAR $\gamma$ <sup>-/-</sup> mice.....	70#
Figure 36: PPAR $\gamma$ binding to NFAT reduces pro-survival IL-2 transcription .....	76#
Figure 37: PPAR $\gamma$ -induced PTEN expression promotes pro-apoptotic signaling .....	79
Figure 38: Therapeutical timing regime for treatment with PPAR $\gamma$ agonists and antagonists during the course of sepsis.....	85
Figure 39: Acute thymus involution as hypothetical mechanism for decreased peripheral T-cell count.....	88

## LIST OF TABLES

Table 1: Clinical definition of sepsis .....	7
Table 2: Local and systemic effects of cytokines released by innate immune cells .....	8
Table 3: Regulation of pro- and anti-apoptotic members of the Bcl-2 protein family. ....	29
Table 4: List of animal trial permissions .....	32
Table 5: List of chemicals, reagents, kits and their providers .....	32
Table 6: List of antibodies for Western and FACS Analysis .....	34
Table 7: List of oligonucleotides .....	35
Table 8: List of instruments .....	35



## ABBREVIATIONS

13-HODE	13-hydroxyoctadecadienoic acid
15d-PGJ <sub>2</sub>	15-deoxy- $\Delta^{12,14}$ -prostaglandin J <sub>2</sub>
15-HETE	15-hydroxyeicosatetraenoic acid
9-HODE	9-hydroxyoctadecadienoic acid
aa	Amino acids
AF	Activation function
Akt	Protein kinase B
ALT	Alanine aminotransferase
Anti-IL-2	IL-2 neutralizing antibody
AP-1	Activating protein 1
APACHE	Acute physiology and chronic health evaluation
Apaf	Apoptosis protease activating factor
aPC	Activated protein C
AST	Aspartate aminotransferase
ATP	Adenosine triphosphate
Bcl-2	B-cell lymphoma 2
Bim	Bcl-2-like protein 11 (BCL2L11)
Br-dUTP	Bromolated deoxyuridine triphosphate nucleotides
BSA	Bovine serum albumin
C <sub>5a</sub>	Complement factor 5a
Ca <sup>2+</sup>	Calcium
CARS	Compensatory anti-inflammatory response syndrome
CBP	CREB binding protein
CCR	Chemokine receptor
CD	Cluster of differentiation
cDNA	Complementary DNA
CFU	Colony forming units
ChIP	Chromatin immunoprecipitation
CLP	Cecum ligation and puncture
CREB	cAMP response element binding protein
CXCR	Chemokine X receptor
DAG	Diacylglycerol
DBD	DNA binding domain
DEPC	Diethyl pyrocarbonate
DISC	Death inducing signaling molecule
DMSO	Dimethylsulfoxide
DNA	Deoxyribonucleic acid

---

DR	Death receptor
EB	Elution buffer
EDTA	Ethylendiamintetraacetate
EPCR	Endothelial protein C receptor
Erk	Extracellular signal-regulated kinase
FACS	Fluorescence-activated cell sorter
FADD	Fas-associated death domain containing protein
FasR	Fas receptor
FCS	Fetal calf serum
FOXO	Forkhead transcription factor
g	Gram
GFP	Green fluorescence protein
h	Hour(s)
H&E	Hematoxyllin and eosin staining
HAART	Highly active anti-retroviral therapy
HbA <sub>1C</sub>	Glycated (glycosylated) hemoglobin
HDACs	Histone deacetylases
HEK	Human embryonic kidney cells
HIV	Human immunodeficiency virus
HMGB	High mobility group box
HSP	Heat shock protein
i.p.	Intra-peritoneal
i.v.	Intra-venous
ICAD	Caspase-activated DNase
ICAM	Intracellular adhesion molecule
IFN	Interferon
Ig	Immunglobuline
IgG	Immunoglobulin G; isotype control antibody
IL	Interleukin
IL-1ra	IL-1 receptor antagonist
iNOS	Inducible NO-synthase
LBD	Ligand binding domain
LCMV	Lymphocyte choriomeningitis virus
LDH	Lactate dehydrogenase
LFA	Lymphocyte function-associated antigen
LPB	Lipopolysaccharide binding protein
LPS	Lipopolysaccharide
LTB <sub>4</sub>	Leukotrien B4
LXR	Liver X receptor
MAC	Membrane-activation complex

---

MAPK	Mitogen-activated protein kinase
MCP	Monocyte chemotactic protein
MHC	Major histocompatibility complex
Min	Minute
MIP	Macrophage inflammatory protein
mm	Millimetre
mmHg	Millimetre of mercury = manometric unit of pressure
MMP	Mitochondrial membrane potential
MODS	Multiple organ dysfunction syndrome
mRNA	Messenger ribonucleic acid
NaCl	Sodium chloride
NCoR	Nuclear receptor co-repressor
NFAT	Nuclear factor of activated T-cells
NF $\kappa$ B	Nuclear factor $\kappa$ B
NK cells	Natural killer cells
NO	Nitric oxide
NSAIDs	Non-steroidal anti-inflammatory drugs
oxLDL	Oxidized low-density lipoprotein
PaCO <sub>2</sub>	Arterial partial pressure of carbon dioxide
PAF	Platelet activating factor
PAI-1	Plasminogen activator inhibitor type-1
pAkt	Phosphorylated Akt
PAMP	Pathogen-associated molecular pattern
PARP	Poly-ADP-ribose polymerase
PB	Precipitation buffer
PBMCs	Peripheral blood mononuclear cells
PBS	Phosphate buffered saline
PC	Protein C
PCR	Polymerase chain reaction
PECAM	Platelet endothelial cell adhesion molecule
PFA	Paraformaldehyde
PG	Prostaglandine
PGE <sub>2</sub>	Prostaglandine E2
PI	Propidium iodide
PI3K	Phosphoinositol 3-kinase
PIP2	Phosphatidylinositol-diphosphate
PIP3	Phosphatidylinositol-triphosphate
PK	Protein kinase
PMSF	Phenylmethylsulphonylfluoride
PPAR $\gamma$	Peroxisome proliferator-activated receptor $\gamma$

---

PPRE	PPAR response element
PRR	Pattern recognition receptor
PS	Phosphatidylserine
PTEN	Phosphatase and tensin homolog
qPCR	Quantitative PCR/realtime PCR
RANTES	Regulated upon activation normal T-cell expressed and secreted
RNA	Ribonucleic acid
ROS	Reactive oxygen species
RP	Red pulp
Rpm	Rounds per minute
RXR	Retinoid X receptor
S1P	Sphingosine-1-phosphate
sCD	Soluble cluster of differentiation
SD	Standard deviation
SDS	Sodium dodecyl sulphate
siRNA	Small interfering RNA
SIRS	Systemic inflammatory response syndrome
SMRT	Silencing mediator for retinoid and thyroid hormone receptors
SOFA	Sepsis-related organ failure assessment
SphK	Sphingosine kinase
SPPARMs	Selective PPAR modulators
STAT	Signal transducer and activator of transcription
sTNFR	Soluble TNF receptor
SUMO	Small-ubiquitin related modifier
TBS	Tris-buffered saline
TCR	T-cell receptor
TF	Tissue factor
TGF	Transforming growth factor
Th	T helper cell
TNF	Tumor necrosis factor
TNF-R	TNF receptor
TRAIL	TNF-related apoptosis-inducing ligand receptor
TTBS	Tris-buffered saline and Tween 20
TUNEL	Terminal deoxynucleotidyl transferase dUTP nick end labeling
TZD	Thiazolidinedione
VEGF	Vascular endothelial growth factor
VLA	Very late antigen
WB	Western blot analysis
WP	White pulp

## 1. SUMMARY

Sepsis is one of the most common diseases on intensive care units all over the world and accounts there for the highest mortality rate. One of the hallmarks of sepsis is an accelerated T-cell apoptosis, resulting in a compromised immune state with the inability to eradicate pathogens. This promotes organ damage or even organ failure. A multiple organ dysfunction evolves, which often ends up in septic shock and death. Recently, it was shown that severe T-cell depletion correlates with sepsis mortality. When inhibiting T-cell apoptosis, an increased mouse survival was observed in experimental sepsis.

One factor that plays a potential role during sepsis is the ligand-activated transcription factor peroxisome-proliferator activated receptor  $\gamma$  (PPAR $\gamma$ ). Besides its transcriptional activity PPAR $\gamma$  confers the ability to repress other transcription factors and to reduce pro-inflammatory cytokine expression. In the context of sepsis, PPAR $\gamma$  is upregulated in T-cells derived from septic patients and a PPAR $\gamma$  ligand was identified in septic patient's serum. Furthermore, applying PPAR $\gamma$  agonists to activated T-cells provokes their apoptosis. The present thesis appoints PPAR $\gamma$  to be responsible for T-cell death during sepsis and introduces PPAR $\gamma$  as a potential target to achieve protection against the deleterious consequences of T-cell depletion.

The first aim of my thesis was to discover the role of PPAR $\gamma$  in T-cells during non-lethal endotoxemia. When injecting 1 mg/kg lipopolysaccharide (LPS) to wild type mice (WT) and mice bearing a conditional depletion of PPAR $\gamma$  in T-cells (Tc-PPAR $\gamma^{-/-}$ ), a massive depletion of WT T-cells was observed, whereas no T-cells were depleted in the Tc-PPAR $\gamma^{-/-}$  population. In these experiments, I identified the pro-survival cytokine IL-2 as highly important for T-cell survival by initiating anti-apoptotic Bcl-2 signaling. Although the LPS-model induces a systemic inflammation it is not very similar to human sepsis. Therefore, I made use of a polymicrobial sepsis model that mimics a ruptured appendicitis, the cecum ligation and puncture model (CLP). Analyzing T-cell counts thereafter demonstrated an abrogated T-cell depletion in the Tc-PPAR $\gamma^{-/-}$  group. Furthermore, high T-cell counts of Tc-PPAR $\gamma^{-/-}$  mice correlated with significantly

higher survival rates after CLP-sepsis, accompanied by an improved bacterial clearance and less end organ damage. Pathway analyses identified high IL-2 and anti-apoptotic Bcl-2 expression levels in Tc-PPAR $\gamma$ <sup>-/-</sup> T-cells, conferring reduced T-cell apoptosis. This pathway was corroborated by experiments limiting the pro-survival effects of Tc-PPAR $\gamma$ <sup>-/-</sup> mice by using an IL-2 neutralizing antibody. This setup reduced Bcl-2 expression and provoked apoptosis resulting in lower T-cell counts and a higher mortality rate. Secondly, I identified PPAR $\gamma$ -induced PTEN expression to counteract the pro-survival PI3K/Akt pathway and induce pro-apoptotic Bim expression. Next, I questioned whether PPAR $\gamma$  displays a therapeutic target that could be modified by synthetic inhibitors, such as the specific, irreversible antagonist GW9662. I confirmed the potential of GW9662 to inhibit PPAR $\gamma$  activity by using *in vivo* PPRE reporter analysis. Time kinetics for application of GW9662 resulted in an optimal timing regime when 1 mg/kg GW9662 was applied at 3 h following CLP. GW9662 application provoked complete abrogation of T-cell depletion, even an increase of peripheral blood T-cells was observed. Again, a high T-cell count correlated to increased survival of the GW9662-treated population and was accompanied by improved bacterial clearance and less end organ damage. In order to identify which T-cell subpopulation (CD4<sup>+</sup> or CD8<sup>+</sup>) is responsible for survival and to determine the optimal time frame to therapeutically apply the inhibitor, 3 mg/kg GW9662 was applied at 5 h after CLP. The dose of 1 mg/kg applied at 5 h after CLP revealed no benefit. The higher dose provoked no depletion of the CD8<sup>+</sup> subpopulation, but CD4<sup>+</sup> T-cells were reduced to untreated control levels. Survival studies for 7 days resulted in a mortality rate of 50%, which is not significantly better than survival of control mice. This result proposes CD4<sup>+</sup> cells to promote survival and to correlate with a better outcome of sepsis.

In conclusion, I identified PPAR $\gamma$  to be crucial for T-cell apoptosis during sepsis by modifying two apoptosis pathways. In addition, I established pharmacological blocking of PPAR $\gamma$  as an option to improve experimental sepsis and propose this treatment as possible target for sepsis therapy in humans.

## 2. ZUSAMMENFASSUNG

Sepsis ist eine der häufigsten Erkrankungen auf Intensivstationen weltweit und verursacht dort die höchste Mortalitätsrate. Ein besonderes Kennzeichen der Sepsis ist der rapide Verlust von T-Zellen durch Apoptose. Dies hemmt den Immunstatus des Patienten und bewirkt ein Unvermögen gegen Pathogene anzukämpfen. Eine Organdysfunktion oder sogar ein multiples Organversagen wird hervorgerufen. Die T-Zelldepletion korreliert mit der hohen Sepsismortalität und ihre Hemmung führte zu einem verbesserten Überleben in experimenteller Sepsis.

Ein Faktor, der während der Sepsis eine wichtige Rolle spielt ist der Ligand-aktivierte Transkriptionsfaktor Peroxisom Proliferator-aktivierter Rezeptor  $\gamma$  (PPAR $\gamma$ ). Neben seiner transkriptionellen Aktivität vermag PPAR $\gamma$  andere Transkriptionsfaktoren zu binden und somit die Expression von proinflammatorischen Zytokinen zu inhibieren. PPAR $\gamma$  ist in T-Zellen septischer Patienten induziert und die Zugabe eines PPAR $\gamma$  Agonisten zu aktivierten T-Zellen löst bei diesen Apoptose aus. Die vorliegende Arbeit identifiziert PPAR $\gamma$  als verantwortliches Protein für die massive T-Zellapoptose während der Sepsis und definiert PPAR $\gamma$  als potenzielles Target zur Hemmung der verhängnisvollen Konsequenzen der T-Zellapoptose septischer Patienten.

Das erste Ziel meiner Arbeit war es, die Rolle von PPAR $\gamma$  in T-Zellen während der nicht-letalen Endotoxinämie zu analysieren. Dafür verwendete ich Mäuse, die eine konditionelle Depletion von PPAR $\gamma$  in T-Zellen (Tc-PPAR $\gamma^{-/-}$ ) aufweisen. Diesen und Wildtyp (WT) Mäusen wurde 1 mg/kg Lipopolysaccharid (LPS) verabreicht, das zu einer massiven Apoptose von WT T-Zellen jedoch nicht von Tc-PPAR $\gamma^{-/-}$  T-Zellen führte. In WT T-Zellen hemmte PPAR $\gamma$  die Expression des T-Zell-Überlebensfaktors IL-2 und verringerte dadurch die Expression von anti-apoptotischem Bcl-2. Das LPS Modell imitiert zwar eine systemische Inflammation, jedoch wird mit diesem Modell keine Sepsis ausgelöst. Darum etablierte ich ein polymikrobielles Sepsismodell, das einen Blinddarmdurchbruch nachahmt, das Zökum Ligations- und Punktionsmodell (ZLP). Die Analyse der T-Zellzahl nach ZLP ergab ebenfalls eine Aufhebung

der T-Zelldepletion in Tc-PPAR $\gamma$ <sup>-/-</sup> Mäusen. Zudem zeigten diese Mäuse ein signifikant verbessertes Überleben, das mit verstärkter Bakterienbeseitigung und weniger Organschäden korrelierte. Wiederrum war die T-Zell Apoptose durch induziertes IL-2 und Bcl-2 gehemmt. Dieser Signalweg wurde durch Versuche mit einem IL-2 neutralisierenden Antikörper bestätigt, der den Überlebensvorteil der Tc-PPAR $\gamma$ <sup>-/-</sup> Mäuse aufhob. Als nächstes untersuchte ich den PI3K/Akt Signalweg, der in meinem Modell durch PPAR $\gamma$ -induziertes PTEN gehemmt wurde und die Expression von pro-apoptotischem Bim erwirkte. Um PPAR $\gamma$  als therapeutisches Angriffsziel zu verifizieren verwendete ich den irreversibel bindenden, spezifischen Antagonist GW9662. Das Potenzial von GW9662 PPAR $\gamma$  zu inhibieren bestätigte ich in *in vivo* Reporteranalysen. Durch die Applikation von 1 mg/kg GW9662 3 h nach ZLP wurde die T-Zelldepletion in WT Mäusen verhindert und es konnte sogar ein Anstieg der peripheren Blut-T-Zellzahl festgestellt werden. Die hohe T-Zellzahl korrelierte auch in diesem Versuchsansatz mit einer hohen Überlebensrate, einer verbesserten Bakterienbeseitigung sowie weniger Organschäden. Zur Identifikation des T-Zellsubtyps (CD4<sup>+</sup> oder CD8<sup>+</sup>), der für das Überleben notwendig ist, sowie um das therapeutische Fenster genau zu etablieren, wurden Versuche mit einer GW9662-Dosis von 3 mg/kg appliziert nach 5 h ZLP durchgeführt, da die Dosis von 1 mg/kg gegeben nach 5 h ZLP in Vorversuchen keine Wirkung zeigte. Die höhere Dosis führte zu einer Vermehrung der CD8<sup>+</sup> T-Zellsubpopulation, jedoch zeigte sich eine starke Verringerung der CD4<sup>+</sup> Zellzahl. In diesem Versuchsansatz überlebten 50% der Mäuse. Dies stellte keinen signifikanten Überlebensvorteil im Vergleich zu den Kontrollen dar und identifiziert CD4<sup>+</sup> Zellen als überlebensnotwendig während der Sepsis-induzierten Immunsuppression.

Zusammenfassend war es mir im Rahmen dieser Arbeit möglich PPAR $\gamma$  als entscheidenden apoptose-auslösenden Faktor für T-Zellen herauszustellen und zwei durch PPAR $\gamma$  modifizierte Apoptose-Signalwege zu identifizieren. Die pharmakologische Hemmung von PPAR $\gamma$  konnte ich als Therapieoption während der experimentellen Sepsis identifizieren und damit einen potentiellen neuen Angriffspunkt im Rahmen der Sepsistherapie vorstellen.



### 3. INTRODUCTION

#### 3.1. Sepsis

##### 3.1.1. History

Though the term sepsis is linked closely to modern intensive care, the medical concept is rather older. The word *sepsis* has its origin with Hippokrates (~460-370 BC), who suggested two forms of tissue breakdown: *Pepsis* as a process represented by fermentation of wine or the digestion of food. It was associated with life and good health; *sepsis*, on the contrary, described a process of deterioration and decay and was associated with death and disease. With the identification that microorganisms were the agents of deterioration, the word 'sepsis' was applied to the clinical condition resulting from bacterial infection (1). In 1847 Ignaz Semmelweis (1818-1865) was the first researcher who developed a modern view of sepsis. He discovered that cases of puerperal fever, a form of sepsis, also known as childbed fever, could be decreased drastically if doctors washed their hands in a chlorine solution before gynaecological examinations. The result was that the mortality rate of women in childbed dropped from 35% to 1%. The French chemist Louis Pasteur (1827-1912) revealed that tiny single cell organisms caused putrefaction. He called them bacteria or microbes and correctly deducted that these microbes could be causing diseases. In 1914, Hugo Schottmüller (1867-1937) paved the way for a modern definition of sepsis: "*Sepsis is present if a focus has developed from which pathogenic bacteria, constantly or periodically, invade the blood stream in such a way that this causes subjective and objective symptoms*". Thus, for the first time, the source of infection as a cause of sepsis came into focus and the etiology and pathophysiology of sepsis became more and more clear. In 1989, Roger C. Bone (1941-1997) established a simple definition for sepsis syndrome, which was based on specific clinical symptoms and included a known source of infection that is still valid until today: "*Sepsis is defined as an invasion of microorganisms and/or their toxins into the bloodstream, along with the organism's reaction against the invasion*" (2).

### 3.1.2. Epidemiology and definition

According to the “Kompetenznetzwerk Sepsis” (SepNet) sepsis provokes an annual incidence of 154,000 cases in Germany. Despite advances in critical care and antimicrobial therapy, the disease displays a mortality rate of 54% for septic shock and severe septic conditions, and 20% for sepsis (3) making the disease one of the most prevalent causes of death on intensive care units (ICUs). Even with intensive and successful investigations and promising preclinical treatment trials, so far efforts to reduce the mortality rate of sepsis in patients have failed. Increasing costs of critical care treatment exert pressure to better understand the molecular mechanisms of sepsis pathophysiology in order to generate new therapeutic strategies (4).

One needs to differentiate between an infection (invasion of bacteria, viruses, fungi in the host) and a sepsis (response of the host to the infection). The clinical picture of “sepsis” can be divided into different phases: the *systemic inflammatory response syndrome* (SIRS), sepsis, severe sepsis, septic shock and *multiple organ dysfunction syndrome* (MODS) (6-7) (Table 1).

While most of the patients survive the first SIRS with intensive medical care without developing MODS they might develop a *compensatory anti-inflammatory response syndrome* (CARS). This state is characterized by a suppressed immunity with less possibility to fight the infections thus, being called immunoparalysis. If the primary infection is getting dominant again, or if a secondary infection arises, MODS might develop and eventually provokes death of the patient.

Gram-positive or gram-negative bacteria mostly cause sepsis, but also fungi (especially candida infections), and less often viruses or parasites. Patients that are most prominent to develop a sepsis are old people, patients with metabolic or neoplastic diseases or immunodeficiency. Further, immunosuppressed patients i.e. after organ transplantation and those who rely on catheter or other invasive material (“plastic”) belong to high-risk patients (8-10). Parallel to the different sepsis states, a risk evaluation can be achieved by different laboratory parameters (oxygen consumption, arterial pH-value, sodium and potassium concentrations in serum, creatinin, hematokrit, bilirubin). Therefore, the APACHE (acute physiology and chronic health evaluation) III Score (9, 11) and

the SOFA (Sepsis-related Organ Failure Assessment) Score (9, 12) were developed.

Table 1: Clinical definition of sepsis (5).

SIRS	Systemic immune response to a non-infectious state, with at least two of the following parameters: Temperature <36° or >38.3°C Heart rate >90 beats/min Respiratory rate >20 breaths/min or paCO <sub>2</sub> < 32 mmHg White blood cell count <3500 or >12,000 cells/ml or >10% immature band forms
Sepsis	Systemic response to infection, manifested by two or more of the conditions mentioned under SIRS (SIRS+evidence of infection)
Severe sepsis	Sepsis associated with organ dysfunction, hypoperfusion, or hypotension including lactic acidosis, oliguria, or acute alteration in mental state.
Septic shock	Sepsis-induced hypotension (e.g. systolic blood pressure <90 mmHg or a reduction of >40 mmHg from base line) despite adequate fluid resuscitation, along with the presence of perfusion abnormalities that may include lactic acidosis, oliguria, or an acute alteration in mental state. Vasopressor- or inotropic-treated patients may not be hypotensive at the time of measurement.
MODS	The presence of altered organ function in an acutely ill patient such that homeostasis cannot be maintained without intervention.

### 3.1.3. Sepsis pathophysiology

Upon release of bacteria to the peritoneum, the immune system is confronted with bacteria specific antigen. First instance for defense is the innate immune system, the first recognition of bacterial pathogens. Local macrophages and granulocytes possess an evolutionary old repertoire of receptors (PRR=pattern recognition receptors), that recognize constant molecular patterns of microbial pathogen (such as LPS or peptidoglykanes), so called PAMPs (pathogen-associated molecular patterns). Recognition of PAMPs provokes, on the one hand, an activation of the confronted cell (macrophages, granulocytes) that phagocytoses the pathogens. On the other hand, a signal cascade in the nucleus

is activated producing inflammatory cytokines and chemokines (i.e. IL-1, IL-6, IL-8, IL-12, TNF $\alpha$ , RANTES) (9, 13-14). This secretion of inflammatory cytokines provokes an activation of surrounding innate immune cells and later on activation of adaptive immune cells (local effects). Furthermore, cytokines induce systemic effects to activate the host against pathogens (systemic effects) (9, 15) (Table 2).

Table 2: Local and systemic effects of cytokines released by innate immune cells (9, 15).

	Local effects	Systemic effects
IL-1	Activates endothelium	Fever
IL-6	Activates lymphocytes Promotes antibody production	Fever Produces acute phase proteins
IL-8	Chemotactic on leukocytes (neutrophils)	
IL-12	Activates NK-cells Differentiation of CD4 <sup>+</sup> T-cells to Th1 cells	
TNF $\alpha$	Activates endothelium promotes permeability of vessel wall	Fever Shock Anergy

## Innate Immunity

It is the goal of the organism to prevent infections as early, effective, and fast as possible to limit a generalisation and spreading throughout the body. To achieve this, numerous mediators that affect the endothelium of local blood vessels are released. Five cardinal signs characterize a typical clinical inflammation that is initiated by effects of mediators: *rubor* (redness), *dolor* (pain), *calor* (heat), *tumor* (swelling) and *functio laesa* (loss of function) (9).

All innate immune cells derive from hematopoietic stem cells in the bone marrow that produce lymphatic or myeloid precursor cells. Cells of the innate immunity derive from myeloid precursors. These are granulocytes, also called polymorphnucleic leukocytes (PMN) that are further differentiated in neutrophils, eosinophils, basophils, and monocytes, which extravasate into tissue and are by then called macrophages. They form the first defensive front against invaded

microorganisms. Approximately 99% of all infections are eliminated by the innate immune system (8).

The most important receptors of the innate immune system are CD14 and the Toll-like receptors (TLR). CD14 is a glycoprotein, which exists in 2 forms: membrane-bound and soluble (sCD14). The membrane-bound form is expressed on i.e. monocytes, macrophages, PMN, B-cells, and liver parenchym cells. The expression rate rises with maturation and contact with LPS. CD14 is not only the receptor for LPS, but also for other microbial ligands. The transfer of LPS to CD14 is catalysed by LBP (LPS-binding protein). LBP is an acute phase protein, which is secreted by the liver, the lung and the kidneys. IL-6 and IL-1 induce the production of LBP. CD14 is a glycosylphosphatidylinositol-fixed receptor without transmembrane domain. Therefore, signal transduction is accomplished by another molecule, TLR4. TLR4 is a family member of the Toll-like receptors (TLR). The TLR family consists of 10 family members so far (TLR1-10). The TLR belong to the TIR-superfamily that is characterized by a Toll/IL-1-receptor domain (TIR). TLR2-5 and TLR9 take part in recognizing microbial products, but differ in their ligands. TLR1 and TLR6 have modulatory functions. They do also differ in their expression patterns. The TLR have an important role in recognizing and differentiate between numerous microbial products (8).

Upon recognition of microbial products phagocytes are activated. LPS-activated macrophages produce free oxygen radicals and other mediators (lysozym, kationic proteins, lactoferrin) with microbicidal potential. Furthermore, pro-inflammatory cytokines are released (tumor necrosis factor  $\alpha$  (TNF $\alpha$ ), IL-1, IL-6, IL-12, HMGB1), chemokines (MCP-1, IL-8, MIP-1 $\alpha$  and  $\beta$ ) as well as lipid mediators (platelet-activating factor (PAF), prostaglandins (PG), leukotriens) that modify the surrounding tissue (8). TNF $\alpha$  is the key enzyme for inflammation, inducing the inducible nitric oxide (NO)-synthase (iNOS) and the release of NO, provoking a local vasodilatation. This results in higher, but slower blood flow (causing *rubor* and *calor*). Similar to TNF $\alpha$ , the prostaglandin E<sub>2</sub> (PGE<sub>2</sub>) is produced by products of cell membranes and further promotes vasodilatation. Microorganisms and LPS also turn on the humoral innate immune response. The complement system activates the membrane-activation

complex (MAC) by cleaving the anaphylatoxins  $C_{5a}$  and  $C_{3a}$ . They in turn can induce degranulation of basophilic granulocytes and mast cells. Thereby released histamine, serotonin, and leukotriene  $B_4$  ( $LTB_4$ ) provoke pain (*dolor*) and further increase vasodilatation. Due to vasodilatation and increased endothelial damage, liquid leaks into the surrounding tissue and into the peritoneum with an accumulation of complement factors, immunoglobulines, and serum proteins. This phenomenon is clinically manifested as tissue edema (*tumor*) or ascites. The lymphoid vessels and the lymph nodes cause drainage of this fluid and initiation of the adaptive immune system. Endothelial damage in the site of infection causes exposition of the tissue thromboplastin to the coagulation system. The coagulation cascade, boosted by  $TNF\alpha$  and platelet activated factor (PAF) derived from macrophages and neutrophils, is activated on site. Thrombin is produced and blocks small blood vessels by fibrin formation thus, preventing further spreading of pathogens.

Neutrophils and macrophages recognize microorganisms by PRR or by complement factor  $C_{3b}$  marking and destroy them in their phagolysosomes. By production of reactive oxygen radicals and hydrogen peroxide ("oxidative burst", stimulated by IL-8 and  $TNF\alpha$ ), DNases, lipases, proteases and defensins they eliminate pathogens. Upon phagocytosis, these cells secrete more and more cytokines and chemokines that recruit more immune cells to the site of infection. The adhesion molecules selectins are expressed on the surface in response to  $LTB_4$ , complement factor  $C_{5a}$  or histamine released from mast cells upon contact with the vessel wall. Selectins bind to ligands on leukocytes, the Sialyl-Lewis-Unit of glycoproteins, and reversibly stick to the endothelium. Due to the low blood flow leukocytes can roll on the vessel endothelium (*leukocyte rolling*). MIP-1a and  $TNF\alpha$  further provoke expression of the adhesion molecule intercellular adhesion molecule-1 (ICAM-1). On all leukocytes, the  $\beta$ -integrin LFA-1 (CD11a:CD18) is expressed and recognizes ICAM-1 and ICAM-2. The  $\beta$ -integrin Mac-1 (CD11b:CD18, CR3) is expressed by macrophages, PMN and lymphocytes and recognizes membrane bound  $C_{3bi}$  and fibrinogen. CR4 (CD11c:CD18) found on macrophages and monocytes binds membrane bound fibrinogen (9).

IL-8 (mouse functional analogs: MIP-2 and KC), promotes rearrangement of LFA-1 and Mac-1 on the leukocyte to form a high affinity product for ICAM-1. Leukocytes are bound stronger to the vessel wall and begin to migrate through the vessel wall (extravasation, leukocyte diapedesis). This is mainly provoked by LFA-1/ICAM-1 interaction and by platelet endothelial cell adhesion molecule-1 (PECAM-1, CD31) that is expressed by leukocytes as well as in-between endothelial cells. In tissue, leukocytes follow the concentration gradient of chemokines (i.e. IL-8, MCP-1, RANTES) to the site of infection (9). How diverse mechanisms of the innate immunity regulate defense against LPS and other microbial products to promote sepsis and multiple organ dysfunction is summarized in Figure 1.

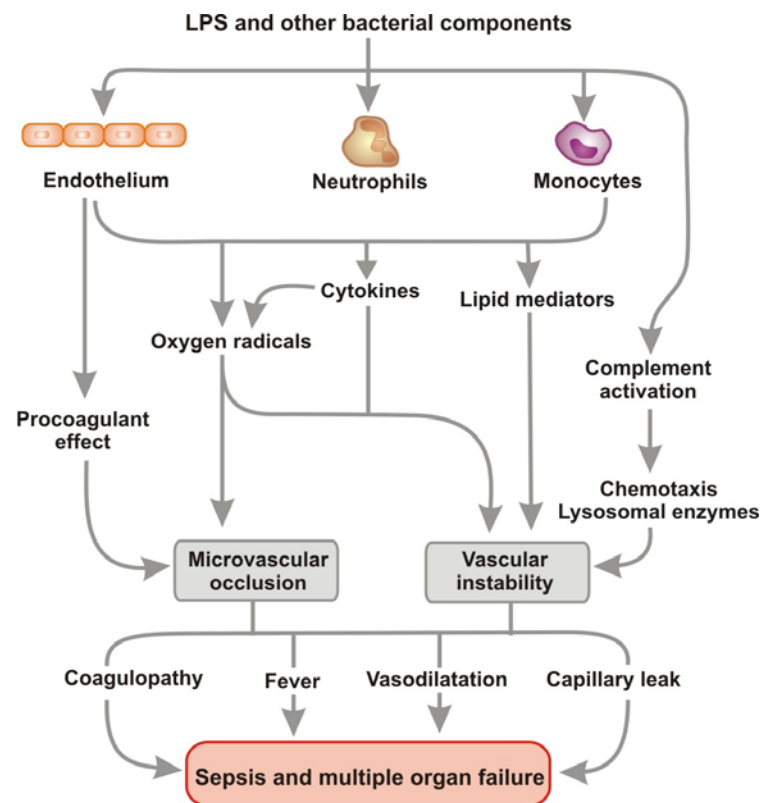


Figure 1: Pathogenic networks during sepsis. LPS and other microbial products simultaneously activate multiple parallel cascades that contribute to the pathophysiology of sepsis and septic shock. Reduced vascular stability and microvascular occlusion lead to coagulation, fever, vasodilatation, and capillary leakage provoking hypoperfusion and inadequate oxygenation and thus organ failure (16).

## Adaptive Immunity

In some cases the innate immune system alone is not able to eliminate all pathogens. However, it is still important to delay spreading of the infection until the adaptive immune response is activated. As antigen-presenting cells (APC) dendritic cells and macrophages present peptide fragments of phagocytosed microorganisms to CD4<sup>+</sup> cells by their major histocompatibility complex II (MHCII). Thereby, the antigen-specific immune defense is activated. The T-cell receptor (TCR) of CD4<sup>+</sup> cells recognizes the specific peptide antigen by its variable region. The TCR-associated CD3-complex activates CD4<sup>+</sup> cells to induce a specific gene expression profile. Of special interest hereby is the induced secretion of IL-2. IL-2 in turn triggers autocrine activation of CD4<sup>+</sup> cells. This effect is further promoted by expression of surface molecules of the B7-family on APCs, which bind to CD28 of lymphocytes, leading to an increased IL-2 mRNA stability and higher expression levels of the IL-2 receptors. IL-2 induces proliferation of CD4<sup>+</sup> cells that now expand clonally. CD4<sup>+</sup> cells differentiate to effector cells that lack L-selectin so that they cannot be held back in lymph nodes. Now, they express Very Late Antigen-4 (VLA-4) and bind to vascular cell adhesion molecule-1 (VCAM-1) on the endothelial wall and migrate to the site of infection. By interferon  $\gamma$  (IFN $\gamma$ ) and IL-12, CD4<sup>+</sup> cells develop to inflammatory Th1-effector cells that in turn activate macrophages. By IL-4 and IL-6 in contrast they develop to become Th2-helper cells. The latter induce differentiation of B-lymphocytes to plasma cells and modulate the Th1-response. Plasma cells in turn produce antigen-specific antibodies. As early as the first interaction of pathogen with cytokine-producing macrophages, the fate of the adaptive immune system to become cellular (Th1) or humoral (Th2) is defined. This in turn is important for the course of infection and the ability to eliminate pathogens. However, most protein antigens that are presented by MHCII complexes induce a mixed Th1 and Th2 cellular response. The differentiation of CD4<sup>+</sup> cells to a Th1 or Th2 phenotype is not only defined by secretion of different cytokines (Th1: mainly TNF $\alpha$  and IFN $\gamma$  versus Th2: mainly IL-4, IL-5, IL-10, and transforming growth factor  $\beta$  (TGF $\beta$ )), but also by different surface markers. Th1 cells are characterized by CXCR3 and CCR5. Th2 cells



express CCR4, CCR8 and less CCR3. This results in different chemotactic behaviour (9).

To effectively combat invaded microorganisms and execute them, activated macrophages are necessary. Macrophage activation is the main duty of Th1-cells. This activation is promoted by the cytokine  $\text{IFN}\gamma$  or by direct cell-cell contact. Th2 cells are not capable of activating macrophages; they secrete the macrophages inhibiting cytokine IL-20. On the one hand, macrophages are necessary to eliminate pathogens, however they might as well be harmful for the surrounding tissue by their ability to produce products of the “oxidative burst”. Therefore, activated macrophages need to be deactivated to decrease overwhelming self-harmful reactions. For this issue, three mechanisms are known so far: Cytokine production stops as soon as cell-cell contact of T-cell and macrophage is interrupted. Further,  $\text{IFN}\gamma$ -mRNA possesses a relatively short half-life and is rapidly degraded by a simultaneously expressed RNase. Third, Th2 cells secrete macrophage-inhibiting cytokines, such as  $\text{TGF}\beta$ , IL-4, IL-10 and IL-13. By  $\text{TGF}\beta$  (direct) or by IL-10 (indirect) Th2 cells also decelerate activation and proliferation of Th1 cells. The presence of Th2 cells is therefore important for controlling and limiting effector mechanisms of activated macrophages (9). However, this mechanism might as well be deleterious when effector mechanisms of macrophages are highly needed to defend against pathogens.

A scheme of the pathophysiological mechanisms of the innate and adaptive immune system during sepsis as a state of systemic inflammation is presented in Figure 2.

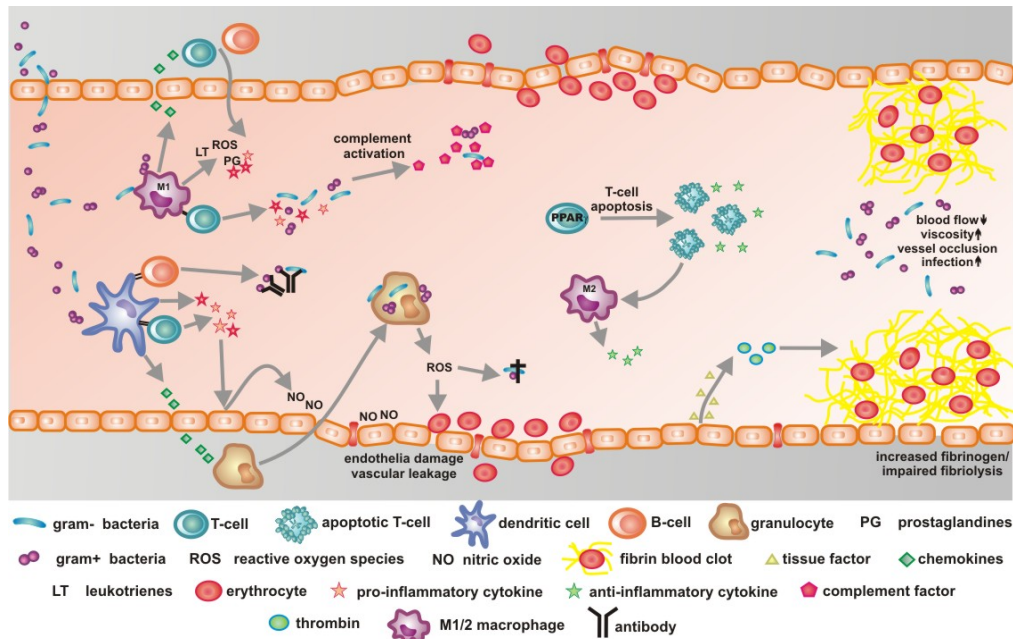


Figure 2: Sepsis pathophysiology. When bacteria enter the systemic circulation, they are detected and phagocytosed by innate immune cells, such as dendritic cells or macrophages. They in turn activate adaptive immune cells, such as B- and T-cells and promote complement activation. Immune cells secrete cytokines and chemokines, which provoke invasion of additional immune cells. Endothelial cells and granulocytes induce nitric oxide (NO) and reactive oxygen species (ROS) production, provoking dilatation of vessels, as well as endothelial damage and vascular leakage. Cell damage provokes the release of anti-inflammatory mediators and T-cell apoptosis to limit self-harmful effects. Apoptotic T-cells in turn switch macrophages to an anti-inflammatory phenotype thus, inhibiting further ROS formation and bacterial clearance. In addition, the endothelial cells secrete tissue factor that promotes thrombin formation to increase fibrinogen and impair fibrinolysis. Blood flow is reduced, blood viscosity increased, vessels further occlude and the infection gets dominant again or even a secondary infection might arise.

## The coagulation cascade

Cytokines are also important in inducing a procoagulant effect in sepsis. LPS and other microbial components initiate coagulation pathways leading to induced expression of tissue factor (TF) on PMN and endothelial cells. TF activates a series of proteolytic cascades, which result in the conversion of prothrombin to thrombin, which in turn generates fibrin from fibrinogen. Simultaneously, normal regulatory fibrinolytic mechanisms (fibrin breakdown by plasmin) are impaired because of high plasma levels of plasminogen-activator inhibitor type-1 (PAI-1) that prevents the generation of plasmin from the

precursor plasminogen. The result is enhanced production and reduced removal of fibrin leading to the deposition of fibrin clots in small blood vessels, inadequate tissue perfusion and organ failure. Pro-inflammatory cytokines, especially IL-1 and IL-6, are important inducers of coagulation (17). Conversely, IL-10 regulates coagulation by inhibiting tissue factor expression on monocytes (16).

An additional cause of the procoagulant state in sepsis is the downregulation of three naturally occurring anticoagulant proteins: antithrombin (AT), protein C (PC) and tissue factor pathway inhibitor (TFPI). These anticoagulants are of interest because in addition to their inhibitory effect on thrombin generation, they also have anti-inflammatory properties, including effects on release of monocyte-derived  $\text{TNF}\alpha$  by inhibiting activation of the transcription factors  $\text{NF}\kappa\text{B}$  and activator protein (AP)-1 (17).

Attention has focused on PC, which is converted to the activated form (aPC) when thrombin complexes with thrombomodulin, an endothelial transmembrane glycoprotein. Once aPC is formed it dissociates from an endothelial protein C receptor (EPCR) before binding protein S, resulting in inactivation of factors Va and VIIIa and thus blocking the coagulation cascade. In sepsis aPC levels are reduced and expression of endothelial thrombomodulin and EPCR are impaired, providing evidence for successful therapeutic value of aPC replacement therapy (16, 18) (Figure 3).

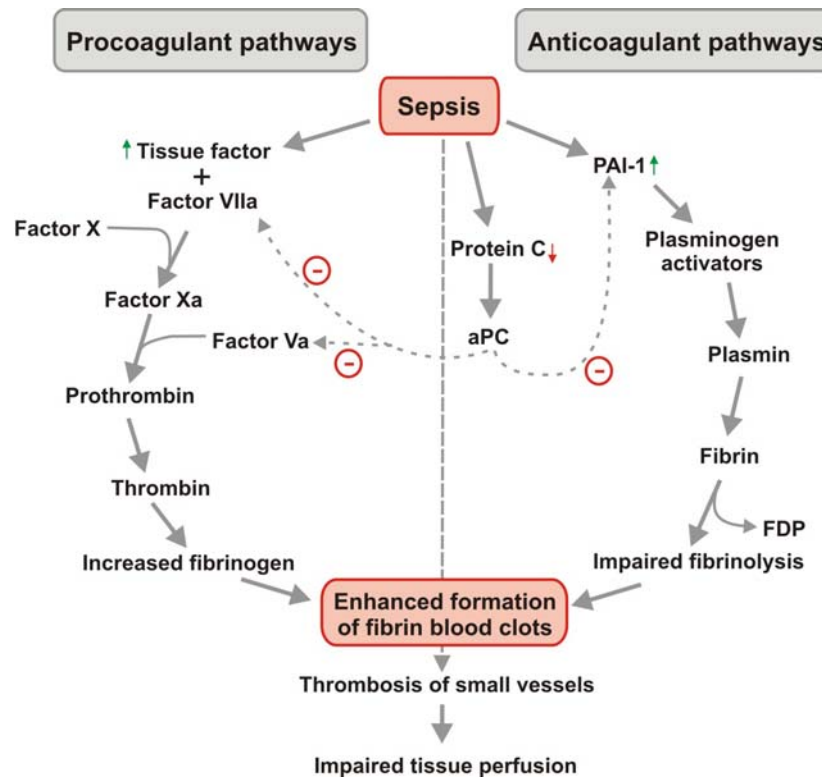


Figure 3: Regulation of coagulation during sepsis. Normal homeostatic balance between procoagulant and anticoagulant mechanisms are disturbed during sepsis. Expression of tissue factor and plasminogen-activator inhibitor 1 (PAI-1) are enhanced, leading to increased production of prothrombin that is converted to thrombin which in turn generates fibrin from fibrinogen. PAI-1 impairs production of plasmin thus, fibrinolytic mechanisms by which fibrin is degraded to FDP fail. Low levels of protein C and activated protein C (aPC) cause inactivation of factors Va and VIIa and inhibit PAI-1 which results in further procoagulant effects. Resulting fibrin clots in the microvasculature impair tissue oxygenation and promote cell damage (16).

### Compensatory anti-inflammatory response syndrome (CARS)

Pathogens that invade the circulation cause an excessive production of inflammatory mediators. They in turn trigger systemic inflammation, provoking a vicious circle by increasing tissue damage and vascular leakage (19). To counteract the deleterious effects of the pro-inflammatory response, anti-inflammatory mediators, such as soluble tumor necrosis factor receptor (sTNF-R), IL-10, IL-1 receptor antagonist (IL-1ra) and TGF $\beta$  (20) are released. Described as most deleterious during CARS is the immune cell apoptosis that is unevenly observed in sepsis and mostly affects lymphocytes in blood and spleen. Apoptosis can cause immunosuppression by two mechanisms:

depletion of various immune cells resulting in the loss of key anti-microbial function and inducing immunosuppressive effects in surviving cells. As a consequence of T-cell apoptosis an immunoparalysis occurs, which renders the septic host susceptible to secondary or opportunistic infections (21) and correlates with sepsis mortality (19, 22-23). This concept of compensatory anti-inflammatory response syndrome (CARS) was proposed by Roger Bone in 1997 to describe the consequences of the counter-regulatory mechanisms initiated to limit the overwhelming inflammatory process in patients with infectious (sepsis) or non-infectious (SIRS) diseases. One major consequence of CARS is the modification of the immune status that could favor the enhanced susceptibility of intensive care patients to nosocomial infections (20). Some studies indicate a correlation between the severity of the immunosuppression and an increased probability of developing severe sepsis. In line, several “two hit” animal models suggested that following a first insult, an enhanced susceptibility to infection occurs. For example, a first infection, usually a peritonitis, which is experimentally induced either by i.p. injection of *E.coli* or by CLP, renders the animals more susceptible to a secondary bacterial or fungal lung infection (24). In fact, most of the patients with sepsis or septic shock undergoing an immunosuppression do not die from the initial systemic infection, but from a second or third hit, that they acquire during their ICU stay (25). Furthermore, it is hypothesized that the increased risk of death or rehospitalization following sepsis survival correlates with a prolonged state of immunosuppression and persistent infections (25).

Among other studies, Hotchkiss et al. (26-27) have clearly demonstrated that extensive T-cell apoptosis in animal models of sepsis and in septic patients is an important pathogenic event. Results from animal models exhibit improved sepsis survival rates due to abrogation of T-cell apoptosis (28). However, CARS is not a general phenomenon that dampens all immune function, it is rather an adaptation depending on the compartments (i.e. blood or tissue), the type of primary or secondary infection, the nature of the studied function, the nature of the produced mediators, and the nature of the leukocytes. For example, apoptosis can either be enhanced in e.g. lymphocytes and dendritic cells, remain unchanged in e.g. monocytes, or be decreased in neutrophils (29-30).

Recent clinical studies primarily targeted the initial pro-inflammatory immune response, since correlations between production of pro-inflammatory mediators and severity and mortality of the disease exist (31). However, clinical trials attenuating the inflammatory response, using high-dose corticosteroids, tumor necrosis factor antagonists, anti-endotoxin antibodies and interleukin-1-receptor antagonists were so far disappointing, potentially through suppression of the host's ability to fight primary or secondary infections (25, 29, 32-33). Thus, preventing lymphopenia by inhibition of T-cell apoptosis can be envisioned as an option to improve long-term morbidity after sepsis by advancing the host's ability to fight against secondary infections.

In the beginning of sepsis, the pro-inflammatory answer (SIRS mediators) and the anti-inflammatory response (CARS mediators) are balanced, once SIRS mediators or once CARS mediators are more abundant. However, during septic shock, this balance is disrupted and exaggerated thus, provoking the severe symptoms of sepsis such as organ dysfunction, septic shock and eventually death (Figure 4).

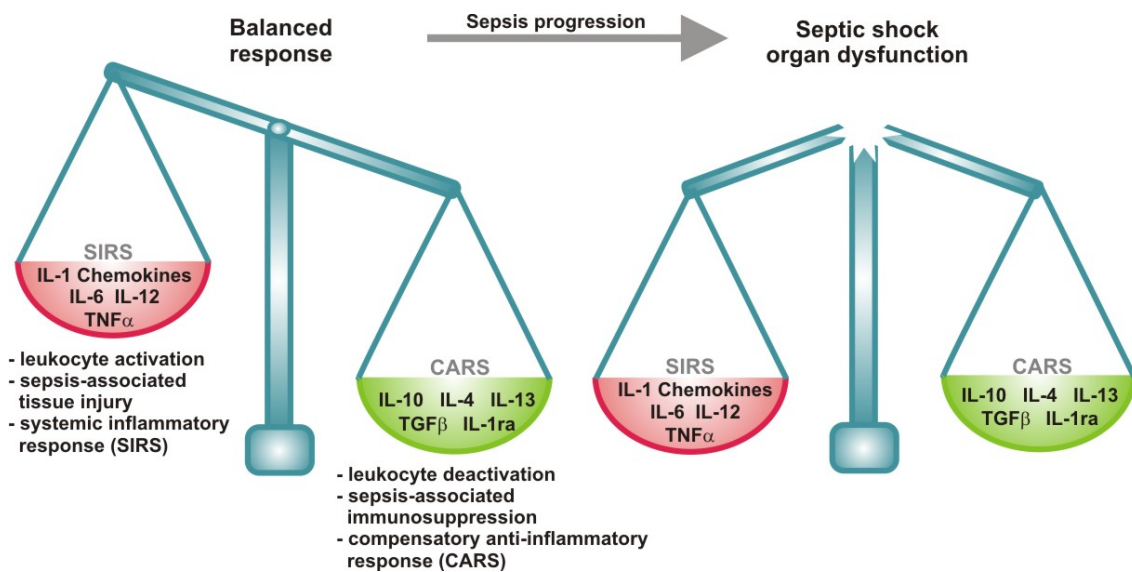


Figure 4: SIRS and CARS during inflammation. The inflammatory response can be envisioned as a balanced response of pro-inflammatory mediators (during SIRS) and anti-inflammatory mediators (during CARS). SIRS mediators are IL-1, IL-6, IL-12, TNF $\alpha$ , and diverse chemokines. They in turn activate CARS mediators, such as IL-1 receptors antagonist (IL-1ra), TGF $\beta$ , IL-4, IL-10, and IL-13. During septic shock, the balanced regulation of SIRS and CARS mediators is dysregulated and exaggerated and it comes to a dysfunctional inflammatory response (34).

## 3.2. PPAR $\gamma$

### 3.2.1. Between transcription and transrepression

The peroxisome is a subcellular organ with several important functions including the removal of molecular oxygen and subsequent breakdown of hydrogen peroxide, glycerolipid synthesis, cholesterol biosynthesis and decomposition, as well as fatty acid oxidation. An orphan nuclear receptor that is activated by peroxisome proliferators provided further insights into the molecular mechanisms by which peroxisomes promote their pleiotropic effects. This receptor, namely peroxisome proliferator-activated receptor (PPAR), belongs to the nuclear hormone receptor superfamily that further includes estrogen receptors, thyroid hormone receptors, retinoic acid and vitamin D3 receptors as well as retinoid X receptors (RXRs) (35). Since the discovery of the first PPAR by Issemann and Green in 1990 (36), the role of this class of nuclear receptors in normal physiology and pathophysiology has become more and more relevant. Similar to other members of the nuclear receptor superfamily, PPARs possess a central DNA-binding domain that recognizes PPAR response elements (PPREs) in the promoter region of their target genes. The transcriptional regulation of target genes by PPARs is achieved by heterodimerization of PPARs with RXR and binding to PPREs. RXR also forms heterodimers with other members of the nuclear receptor superfamily, provoking competition between the heterodimerization partners and interaction with PPAR-dependent transcription. PPAR-RXR heterodimers can also bind to a PPRE in the absence of a ligand. Although the presence of ligand-bound PPAR-RXR at the PPRE is typically associated with transcriptional activation, the presence of unliganded PPAR-RXR at a PPRE has effects that vary depending on the promoter context and cell type. There are three isoforms described: PPAR $\alpha$ , PPAR $\gamma$ , and PPAR $\delta$ . PPAR $\alpha$  was the first identified isoform and responds to several compounds inducing peroxisome proliferation, where this subfamily was named after. The other PPARs do not share this functionality.

PPAR $\gamma$  is expressed most abundant in adipose tissue and is a master regulator of adipogenesis. PPAR $\gamma$  activation promotes adipocyte differentiation and is

associated with induction of lipogenic enzymes and glucoregulatory molecules (37). However, PPAR $\gamma$  is also found in other cell types, including fibroblasts, hepatocytes, myocytes, colon and breast epithelial cells, the white and red pulp of the spleen, activated T-cells, human bone marrow precursors, and macrophages/monocytes (38). For some PPAR $\gamma$  target genes in adipocytes, unliganded PPAR $\gamma$ -RXR heterodimers recruit corepressor complexes, resulting in active repression, whereas other gene corepressors are not recruited by unliganded PPAR $\gamma$ -RXR (39).

### 3.2.2. Structure

#### Structure of the PPAR $\gamma$ protein

Three isoforms of the PPAR family were identified so far, encoded by separate genes: PPAR $\alpha$ , PPAR $\delta$ , and PPAR $\gamma$ . These three isotypes display dissimilar patterns of tissue distribution and differ in their ligand-binding domains (36). PPAR $\gamma$  expression is controlled by different promoters, leading to the PPAR $\gamma$ 1 isoform (475 amino acids) and PPAR $\gamma$ 2 isoform (additional 30 amino acids at the N-terminus) that differ mainly in their expression patterns. PPAR $\gamma$ 1 isoform expression is found in nearly all tissues except muscle, and the PPAR $\gamma$ 2 isoform is primarily expressed in adipose tissue and the intestine. Alternative transcription is accomplished by the use of three established promoters, whereas transcript variant 1 and 3 code for protein PPAR $\gamma$ 1 and transcript variant 2 codes for PPAR $\gamma$ 2 (40). Besides these three, another 5 transcript variants have been identified in the last decade (41-42), but it remains elusive whether they have further and distinct function.

The structure of the PPAR $\gamma$ 1 protein was first discovered by Nolte et al. using X-ray-Raman scattering. Likewise other nuclear receptors, PPAR $\gamma$  consists of five domains (Figure 5). The N-terminus contains the ligand-independent activation domain (A/B), also known as AF1 (activation function 1). The DNA-binding domain (DBD) consists of two zinc-finger-motifs, which allow the protein to interact with the PPRE on the DNA. Next, the hinge domain (HD) assigns flexibility in concerns of ligand and DNA binding. Thus, the protein is able to interact directly with other proteins. By this ability, PPAR $\gamma$  promotes effects that



are independent of its transcriptional potential, and modifies different signaling pathways. At the C-terminus of the PPAR $\gamma$  protein the ligand binding domain (LBD) is localized, as well as the ligand-dependent activation domain AF2 (activation function 2) (43).

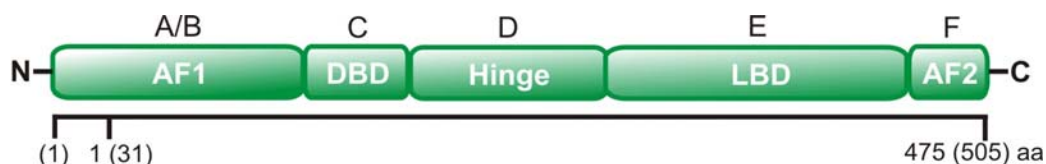


Figure 5: PPAR $\gamma$  domain structure. The structure of PPAR $\gamma$  shows the characteristic nuclear receptor configuration of five domains (A/B, C, D, E, F). The DNA-binding domain (DBD; domain C) and the ligand-binding domain (LBD, domain E) are highly conserved. The amino-terminal A/B domain represents the ligand-independent activation domain 1 ('activation function 1', AF1). At the C-terminal site, the ligand-dependent domain ('activation function 2', AF2, domain F) and the LBD are localized. The domain D consists of a variable Hinge-domain and plays an important role for conformational changes.

### Structure of synthetic ligands and their mode of action

The most prominent synthetic PPAR $\gamma$  ligands are the thiazolidinediones (TZDs). All TZDs feature a similar 2,4-thiazolidinedione-structure motif. This structure can be basically divided into three parts: an acidic head-group (blue), a central aryl-spacer (red) and a lipophilic end part (yellow). This structure reminds, at least in part, of a fatty acid derivate, similar to the previously reported natural ligands (Figure 6).

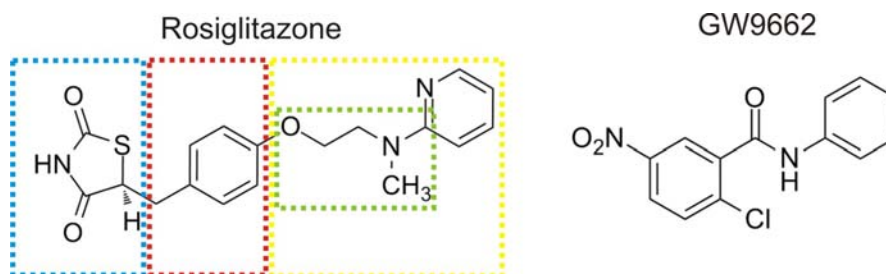


Figure 6: Chemical structure of rosiglitazone and the synthetic antagonist GW9662. The general structure of a TZD displays a thiazolidinedione head group (blue), a central aryl-spacer (red) that is attached by a linker (green) to a lipophilic end part (yellow).

The structure of the TZDs was chemically modified to improve selectivity and affinity. It was shown that introducing a heterocyclic N-atom in the lipophilic part (yellow), as seen in rosiglitazone (Figure 6), significantly improves the affinity to the receptor. This is due to formation of a covalent hydrogen bond of the N-atom to Cys<sup>285</sup> in the LBD of PPAR<sub>γ</sub> (44). GW9662 is a specific inhibitor of PPAR<sub>γ</sub> with only minor effects on the other PPARs (IC<sub>50</sub> PPAR<sub>γ</sub>: 3.3 nM; IC<sub>50</sub> PPAR<sub>α</sub>: 30 nM; IC<sub>50</sub> PPAR<sub>δ</sub>: 2000 nM) (45). GW9662 mediates its inhibitory potential by effects on receptor organization. Leesnitzer et al. (2002) explored the mode of binding of GW9662 by biochemical experiments using samples with GW9662-modified PPAR<sub>γ</sub> and mass spectrometry. They found GW9662 to covalently bind to Cys<sup>285</sup> in the LBD (45). However, in 2006 Hamuro et al. described this finding as “not well understood” and reported that unlike full agonists (TZDs), no conformational or dynamic change occurs in this region upon the antagonist GW9662 binding to PPAR<sub>γ</sub>. It remains as dynamic as the ligand-free form, proposing no covalent binding of GW9662 in the LBD to Cys<sup>285</sup> (46). In line, in 2008 Chandra et al. underlined this result by reporting that GW9662, compared to rosiglitazone, does not bind to Cys<sup>285</sup>, but resides in the pocket without having made the covalent bond in the intact PPAR<sub>γ</sub> (Figure 7).

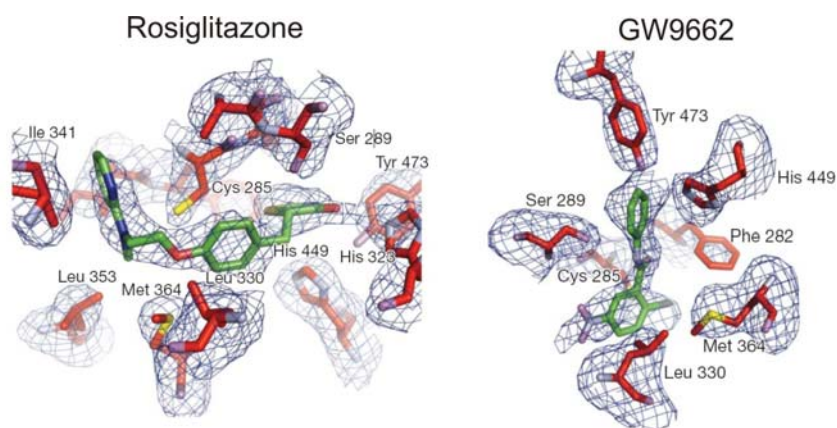


Figure 7: Effect of different ligands on the PPAR<sub>γ</sub>-RXR<sub>α</sub> complex. Comparison of the binding mode of rosiglitazone with that of GW9662 within the PPAR<sub>γ</sub>-LBD pocket. GW9662 does not form a covalent bond with Cys<sup>285</sup> in the ligand binding pocket of PPAR<sub>γ</sub> (adapted from Chandra et al. 2008).

Nevertheless, the positioning of the nitro-aryl chloride portion of GW9662 shows this ligand is ready to form a covalent adduct, given the proximity of its displaceable chloride group to the cysteine sulphur (47). Another possible binding site for GW9662 within the LBD of PPAR $\gamma$  was not proposed in the literature so far. In general, it is hypothesized that binding of agonists within the ligand-binding site causes a conformational change where coactivator binding is stabilized. In contrast, binding of antagonists results in a conformation that favors binding of corepressors.

### 3.2.3. PPAR $\gamma$ ligands

PPAR $\gamma$  ligands include a surprisingly diverse set of natural ligands (37). In the context of sepsis the PPAR $\gamma$  agonist needed for the induction of cell death may be provided by endothelial cells or macrophages under inflammatory or septic conditions, most likely as a by-product of cyclooxygenase-2 activity (48). Enhanced levels of the physiological PPAR $\gamma$  agonist 15-deoxy- $\Delta^{12,14}$ -prostaglandin J2 (15d-PGJ<sub>2</sub>) have been detected in blood samples of septic patients (49). Other factors that are likely to be generated during sepsis with a high affinity to PPAR $\gamma$  are lipoxygenase products such as 15-hydroxyeicosatetraenoic acid (15-HETE), 9-hydroxyoctadecadienoic acid (9-HODE), and 13-hydroxyoctadecadienoic acid (13-HODE). Especially the identification of fatty acid derivatives as selective PPAR $\gamma$  ligands that are generated during inflammatory processes, proved special importance for PPAR $\gamma$  in regulating immunological processes. Furthermore, it has been described that LPS increases the susceptibility of low-density lipoprotein (LDL) towards oxidation, generating oxidized-LDL as a specific PPAR $\gamma$  agonist (50). The isolation and identification of these endogenous ligands during sepsis has yet to be performed. Moreover, we cannot exclude that multiple factors are responsible for PPAR $\gamma$  activation during sepsis. In fact, the volume of the ligand-binding cavity of PPAR $\gamma$  is much larger than pockets of other nuclear hormone receptors (PPAR $\gamma$ : 1619 Å versus vitamin D receptor: 871 Å, retinoid X receptor  $\alpha$ : 687 Å, progesterone receptor: 557 Å and estrogen receptor: 476 Å). This relatively large ligand binding pocket in PPAR $\gamma$  can bind a broad

range of endogenous ligands (51) that are likely to be produced during sepsis. Further findings raise the possibility that PPAR $\gamma$  can bind two ligand molecules at once. This could explain why its ligand binding pocket is unusually large compared to that of other nuclear receptors. The proposed simultaneous ligand binding would also underline the hypothesis that PPAR $\gamma$  is not a specific target for one particular ligand, but it is a sensor molecule that scans the intracellular mixture of various fatty acid molecules (52).

Synthetic ligands are the insulin sensitizing thiazolidinediones (TZDs, such as englitazone, ciglitazone, pioglitazone, rosiglitazone, troglitazone), non-steroidal anti-inflammatory drugs (NSAIDs, i.e. indomethacin, fenoprofen, flufenarnic acid), tyrosine derivatives (farglitazar, GW7845), and a variety of new chemical classes (37, 39). In humans, TZDs enhance insulin action, improve glycemic control with a significant reduction in the level of glycated haemoglobin (HbA<sub>1C</sub>), and have variable effects on serum triglyceride levels in patients with type 2 diabetes. Despite their proven efficacy and widespread use, these drugs possess a number of deleterious side effects, including significant weight gain and peripheral edema (37). These side effects emphasize the critical need for the discovery and characterization of alternative PPAR modulators that would retain the antidiabetic properties while avoiding the side effects. PPAR $\gamma$  modulators so-called SPPARMs (selective PPAR modulators) have been designed displaying different binding properties to the PPARs compared to full agonists (51, 53). The “dual”, “balanced” or “pan” PPAR ligands are a group of drugs, which bind two or more PPAR isoforms. These drugs are currently under investigation for treatment of a larger subset of symptoms of the metabolic syndrome. These include the experimental compounds aleglitazar, muraglitazar and tesaglitazar (51). Known synthetic PPAR $\gamma$  antagonists are i.e. biphenol A diglyceridyl ether (BADGE), GW9662, SR-202, CDDO-Me, PD068235, Diclofenac, and T0070907 (48).

#### **3.2.4. Anti-inflammatory properties**

PPAR $\gamma$  acts as a transcriptional activator of many adipocyte-specific genes involved in lipid synthesis, handling and storage of lipids, growth regulation, insulin signaling, and adipokine production (54). In addition to the transcriptional

activity, recent observation showed that PPAR $\gamma$  can directly bind to other proteins and inhibits signal transduction (Figure 8). This ability is called transrepression and assigns PPAR $\gamma$  the capability to inhibit pro-inflammatory signaling and induce an anti-inflammatory response (55-56). Transrepression is mainly mediated by direct protein-protein interactions between PPAR $\gamma$  and other transcription factors, such as NF $\kappa$ B (57-59), NFAT (60), AP-1 (59, 61), or STAT (62). In contrast to direct sequence-specific interaction of PPAR $\gamma$  with DNA itself this mechanism scavenges transcription factors from binding to their responsive elements. PPAR $\gamma$  inhibits pro-inflammatory signaling and induces an anti-inflammatory response. Of special importance is this ability in immune cells, where PPAR $\gamma$  activation reduces expression of pro-inflammatory cytokines, such as IL-2, TNF $\alpha$ , IL-1 $\beta$ , and IL-12. Further PPAR $\gamma$ -dependent transrepression is mediated by PPAR $\gamma$  binding to co-activator complexes, which are essential for transcription factor-dependent transactivation, such as steroid receptor co-activator 1 (SRC1) and cAMP response element binding protein (CREB)-binding protein (CBP)/p300. These complexes confer histone acetyltransferase activity and reorganize the chromatin packaging, to allow the transcriptional machinery gaining access to the promoter region (63). Thus, NF $\kappa$ B and AP1-mediated gene induction (64-65) and pro-inflammatory cytokine expression is inhibited. In its SUMOylated form, PPAR $\gamma$  transrepresses gene expression by preventing removal of the co-repressor complex nuclear receptor co-repressor/silencing mediator for retinoid and thyroid hormone receptors (NCoR/SMRT) from the promoter region of pro-inflammatory transcription factors (NF $\kappa$ B), which, through association with histone deacetylases (HDACs), attenuates gene transcription (66-67). Besides transrepression PPAR $\gamma$  inhibits mitogen-activated protein kinase (MAPK) by a so far unknown mechanism (68-70). This prevents MAPK from phosphorylating and thereby activating downstream pro-inflammatory transcription factors. In addition, cytosolic PPAR $\gamma$  directly binds protein kinase C  $\alpha$  (PKC $\alpha$ ). Subsequently its translocation to the cell membrane is inhibited, leading to attenuated activation and further depletion. In monocytes/macrophages this provokes desensitization in response to apoptotic cell phagocytosis, where attenuated PKC $\alpha$  signaling blocks NADPH-oxidase-dependent ROS formation (71).

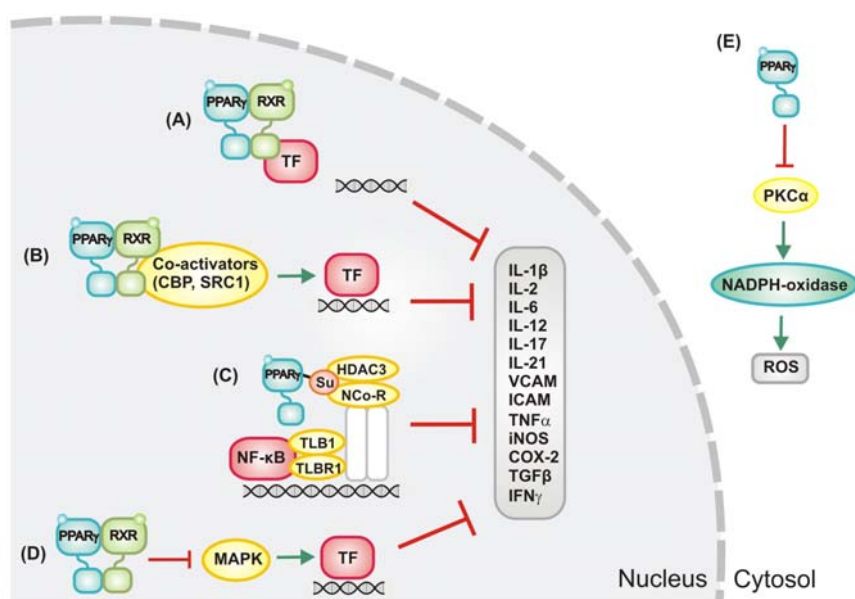


Figure 8: PPAR $\gamma$ -dependent repression of pro-inflammatory cytokine production. Ligand-activated PPAR $\gamma$  dimerizes with the retinoid X receptor (RXR)  $\alpha$ . In this state, (A) PPAR $\gamma$  can directly associate with pro-inflammatory transcription factors, such as STAT, NFAT, AP-1, or NF $\kappa$ B thus, preventing pro-inflammatory gene expression. Further, (B) PPAR $\gamma$  scavenges co-activators from binding to pro-inflammatory transcription factors (TF) or (C) inhibits degradation of co-repressors. E.g. it was shown that SUMOylated PPAR $\gamma$  reduces degradation of NCo-R/HDAC3/TLB1/TLBR1 complex and prevents NF $\kappa$ B-dependent gene expression. Besides these mechanisms of transrepression PPAR $\gamma$  directly inhibits MAPK and downstream signaling. By inhibiting PKC $\alpha$  translocation, PPAR $\gamma$  attenuates NADPH oxidase activation. Heterodimerization with RXR $\alpha$  is not required in the latter two cases (38).

### 3.3. Apoptosis

#### 3.3.1. Apoptosis versus necrosis

Throughout the entire life of an organism, besides cell proliferation also a controlled cell death takes place. We differentiate between two major forms of cell death: apoptosis and necrosis. Necrosis occurs in cells that were severely damaged. Necrotic cells release toxic substances into the surrounding, which promotes inflammatory reactions. Markers for necrosis are: swelling, loss of membrane integrity, release of cell contents, loss of cell organelles, and decomposition of DNA by endonucleases and exonucleases. The inducible form

of cell death, apoptosis, also known as programmed cell death or non-necrotic cellular suicide, is described in the following (72-73).

### **3.3.2. Regulation of apoptosis**

#### **The extrinsic way (death receptor pathway)**

Apoptosis can be initiated by different stimuli that all end up in activation of caspases (“cystein-specific aspartate proteases”). On the one hand, apoptosis is mediated by binding of extracellular ligands on transmembrane receptors. Under physiologic conditions this is mostly mediated by stimulation of death receptors such as TNF-receptor 1 (TNF-R1), Fas-receptor (Fas-R), death receptor 4 or 5 (DR4/DR5), TNF-related apoptosis-induction ligand receptor 1 (TRAILR1) and TRAILR2. Ligand binding provokes formation of a multimeric complex, the death inducing signaling complex (DISC) that contains the death-receptor (e.g. Fas-R), adaptor molecules, such as Fas-associated death domain-containing protein (FADD) and caspase 8. Caspases are a class of cysteine proteases that includes several representatives involved in apoptosis. They convey the apoptotic signal in a proteolytic cascade cleaving and activating other caspases that then degrade other cellular targets provoking cell death. Caspase 8 is the initial caspase involved in response to receptors with a death domain like Fas. Active caspase 8 results from proteolytic splicing and in turn activates effector-caspases, such as caspase 3. Substrates of the caspase cascade are i.e. structural proteins such as  $\beta$ -actin and nuclear laminine, DNA repairing enzymes such as poly-ADP-ribose polymerase 1 (PARP1), as well as anti-apoptotic Bcl-2 family members. Another typical substrate for caspases is the inhibitor of caspase-activated DNase (ICAD). ICAD splices chromosomal DNA during apoptosis in between nucleosomes, which results in fragmented DNA (72-73).

#### **The intrinsic pathway (mitochondrial-mediated pathway)**

Caspases can as well be activated by cell intrinsic signals, such as damage of DNA and activation of p53. Other factors inducing intrinsic apoptosis are loss of nutrition or oxygen supply. Major players during intrinsic apoptosis regulation

are mitochondria. This mitochondrial stress pathway is initiated by the release of cytochrome c, a protein of the respiratory chain, from mitochondria membranes. In the cytoplasm, cytochrome c interacts with the adapter molecules apoptosis protease activating factor-1 (Apaf-1), causing self-cleavage and, in cooperation with desoxy-ATP, activation of caspase 9. This complex is called apoptosome. At this stage apoptosis can be inhibited by interaction of the apoptosome with heat-shock proteins (HSP). In presence of ATP, downstream caspases 3, 6, and 7 are activated by the upstream proteases and act themselves to cleave cellular targets, fragmentate DNA and induce cell death. Caspases can be inhibited by inhibitors of apoptosis proteins (IAPs). As described above, cytochrome c is released from the mitochondrial membrane through pores to the cytosol. These pores are built by pro-apoptotic members of the Bcl-2-family. Members of the Bcl-2 family belong to three subclasses: one anti-apoptotic class, and two pro-apoptotic classes. The two pro-apoptotic classes are the multiple-domain-proteins (Bax and Bak) and proteins that have only one single regulatory domain (BH3-only proteins, such as Bid, Bad, Noxa, Puma, Bim) (Table 3). Upon injury, the pro-apoptotic members, such as Bad and Bax, translocate to mitochondria where they bind Bcl-2 and Bcl-xl, neutralize their anti-apoptotic properties by building pores in the mitochondrial membrane thus, inducing changes in mitochondrial membrane potential (MMP) (74). The structure of the Bcl-2 proteins shows a striking similarity to the overall fold of the pore-forming domains of bacterial toxins (75). Anti-apoptotic members are important to ensure membrane integrity and inhibit cytochrome c release by binding Bax and Bad, which are responsible for cytochrome c release. The membrane potential is therefore maintained by a balance between anti-apoptotic Bcl-2 family proteins, notably Bcl-2 and Bcl-xl, and pro-apoptotic family members such as Bad, Bim and Bax (72-73). A series of stimuli regulate the amount and activity of every Bcl-2 protein family member. Main regulatory proteins are the tumor-suppressor protein p53 as well as Bax, Puma, Noxa and proteins of the PI3K/Akt pathway (73) (Table 3).



Table 3: Regulation of pro- and anti-apoptotic members of the Bcl-2 protein family (73).

<b>Protein</b>	<b>Regulation</b>
<b>Proapoptotic</b> (Multiple domain proteins)	
Bax, Bak	Transcription induced by p53
<b>Proapoptotic</b> (BH3-only-protein)	
Bid	Activated upon enzymatic splicing of caspase 8
Bad	Inactivated by phosphorylation by Akt-kinase
Noxa, Puma	Transcription induced by p53
Bim	Transcription inhibited by Akt-kinase
<b>Antiapoptotic</b>	
Bcl-2	Transcription

### Apoptosis during sepsis

Defining death pathways during sepsis is important because insight provided into the mechanisms of cell death might present potential therapies. For example, involvement of the death receptor pathway points to members of the TNF receptor family, and several specific receptor antagonists are capable of blocking these sites. Involvement of the mitochondrial-mediated pathway suggests stress-induced mitochondrial injury, which occurs during oxidative stress. Antioxidant therapy proved to be promising in some models of apoptosis. Hotchkiss et al. found in 2005 an increase in activation of caspases 8 and 9, which indicates that lymphocyte apoptosis may be occurring by both extrinsic and intrinsic pathways. Further, they determined active caspase 3-positive, Bcl-2-negative lymphocytes as well as active caspase 3-positive, Bcl-2-positive lymphocytes, which suggests mitochondrial-mediated apoptosis and death receptor-mediated apoptosis (76). Studies in animal models of sepsis support the concept that lymphocyte apoptosis in sepsis is a result of both pathways. Ayala et al. showed that sepsis-induced lymphocyte apoptosis can be attenuated and survival of mice can be improved by administration of compounds that block the Fas death receptor (77). However, studies from three other independent laboratories have shown that lymphocytes from Bcl-2 overexpressing mice are resistant to sepsis-induced apoptosis and provoking improved survival (78-80).

Of special importance during sepsis are the Bcl-2 protein family members Bcl-2 and Bim. It was shown that overexpression of Bcl-2 prevented apoptosis and improved outcome in sepsis. These findings showed that lymphocytes from Bcl-2 transgenic mice were resistant to sepsis-induced apoptosis, and that these mice had a threefold improvement in survival compared to controls (80). Subsequently, several groups have shown that sepsis decreases the level of expression of Bcl-2 by lymphocytes which might be one mechanism responsible for, or that contributes to, the apoptosis of lymphocytes (76, 81-82). Bcl-2 protects against apoptosis by binding to and neutralizing the pro-apoptotic family members, such as Bim, Puma, and Noxa (83). Bim is the most extensively studied one of these proteins and is required for cell death secondary to cytokine withdrawal, death of autoreactive T-cells, and for termination of acute T-cell responses to viral infections (84-86). Hotchkiss et al. showed that Bim knockout mice have nearly complete protection against sepsis-induced lymphocyte apoptosis and a distinct survival advantage in a cecum ligation and puncture model of septic peritonitis (87). In line, RNA interference (with small interfering RNA, siRNA) provided a way to transiently imitate a genetic knockout in a clinical setting. Further they proposed that this siRNA-induced decrease in Bim expression results in liberation of sufficient Bcl-2 to effectively bind to and inhibit Bax/Bak channel formation, thereby blocking apoptosis (88). In special regard to these important studies, this thesis focusses on regulation of Bcl-2 and Bim by PPAR $\gamma$ .

#### **3.4. Preliminary data: PPAR $\gamma$ during sepsis**

T-cells of septic patients showed an up-regulation of PPAR $\gamma$  and their sera contained a PPAR $\gamma$  agonist. The up-regulation was shown to sensitize T-cells of septic patients towards apoptosis. This implies that PPAR $\gamma$  plays a significant role in T-cell apoptosis, contributing to lymphocyte loss in sepsis and an inhibition of PPAR $\gamma$  may turn out to be beneficial for patients suffering from lymphopenia during sepsis (89). While there were indications that PPAR $\gamma$  activation modulates T-cell fate, the importance of PPAR $\gamma$  for T-cell apoptosis, sepsis outcome and the underlying mechanisms remained elusive.

### 3.5. Aims of this study

The present thesis aims at elucidating the role of PPAR $\gamma$  during sepsis progression and especially focusses on its role in apoptosis induction, the underlying mechanisms and its potential as a new therapeutic target during sepsis.

Based on previous results, I hypothesized that activation of PPAR $\gamma$  during sepsis induces apoptosis of peripheral T-cells in spleen and in blood. Consequently, this T-cell depletion contributes to an immune paralysis and impairs the host susceptible to secondary infections, leading to high mortality rates. Therefore, in my experiments I first aimed at clarifying the question whether manipulating PPAR $\gamma$  functionality by genetical ablation of the PPAR $\gamma$  gene in mice prevents T-cells from apoptosis and increases survival. My next aim was to elucidate the underlying pathway for PPAR $\gamma$ -dependent apoptosis. In this regard I specifically focused on regulatory proteins that have been described in the literature to be important during T-cell apoptosis. Special interest was given on the investigation of the therapeutic potential of PPAR $\gamma$ . Therefore, experimental sepsis using a specific PPAR $\gamma$  inhibitor that is supplied post-sepsis to prevent PPAR $\gamma$  activation and eventually T-cell depletion should be performed. Additionally, I intended to clarify whether this treatment regime results in higher survival rates in my experimental sepsis model. Further, I was intrigued to investigate the underlying pathway of apoptosis prevention in T-cells in this setup of pharmacological PPAR $\gamma$  inhibition. Finally, I intended to elucidate whether higher T-cell counts improved survival by executing effects on classical sepsis-related parameters, such as bacterial clearance and end organ damage.

## 4. MATERIAL AND METHODS

### 4.1. Material

#### 4.1.1. Mice

C57BL/6N-PPAR $\gamma^{fl/fl}$	kindly provided by Dr. Frank Gonzalez, NCI, Bethesda, USA
C57BL/6NTac-(Tg)(lck-Cre)	Taconic, Germantown, USA

C57BL/6N-PPAR $\gamma^{fl/fl}$  and C57BL/6NTac-(Tg)(lck-Cre) were crossed to breed C57BL/6N-lck-Cre;PPAR $\gamma^{fl/fl}$  containing a conditional depletion of the PPAR $\gamma$  protein in T-cells.

Mice were kept in a temperature-controlled room with 12 h light and 12 h dark diurnal cycle. They were housed in filter-topped cages and were fed standard laboratory chow and water *ad libitum*. All animal experiments followed the guidelines of the Hessian animal care and use committee (Table 4).

Table 4: List of animal trial permissions

Short title of animal trial permission	Authorization number
„T-Zelldepletion“	F144/01
„T-Zelldepletion bei ZLP“	F91/51
„Hemmung der T-Zelldepletion bei Sepsis“	F144/06

#### 4.1.2. Chemicals, Reagents and Kits

Table 5: List of chemicals, reagents, kits and their providers

Chemical/Reagent/Kit	Provider
Absolute™ qPCR SYBR® Green Mix	ABgene (Hamburg)
Acid washed glass beads	Stratagene (Heidelberg)
Agarose	Sigma-Aldrich (Steinheim)
APO-BRDU TUNEL kit	Phoenix Flow Systems (San Diego)

Bepanthen® (Dexpanthenol)	Bayer (Leverkusen)
Brefeldin A	Sigma Aldrich (Steinheim)
BSA (bovine serum albumin)	Roth (Karlsruhe)
Catalyzed Signal Amplification kit	Dako Inc. (Glostrup)
Chelex®100	BioRad (Munich)
Columbia Agar	Hypha Diagnostica (Heidelberg)
CytokineBeadArray Mouse Inflammation kit	BD Bioscience (Heidelberg)
DAB (diaminobenzidine tetrahydrochloride)	Dako Inc. (Glostrup)
Deoxynucleotide Solution Mix (dNTPs)	New England Biolabs (Frankfurt)
EDTA (ethylenediaminetetraacetic acid)	AppliChem (Darmstadt)
Endo Agar	Hypha Diagnostica (Heidelberg)
Eosin G	Merck (Darmstadt)
Ethanol	Sigma-Aldrich (Steinheim)
FCS (fetal calf serum)	PAA Laboratories (Cölbe)
Formaldehyd	Riedel-de-Haen (Seelze)
GeneRuler™	Fermentas (St. Leon-Rot)
Glycine	Merck (Darmstadt)
GW9662	Cayman Chemical (Ann Arbor)
H <sub>2</sub> O <sub>2</sub> (Hydrogenperoxide)	Merck (Darmstadt)
iScript™ cDNA Synthesis Kit	BioRad (Munich)
Ketavet® (Ketamine)	Pfizer vet. (Zurich)
Lipopolysaccharide (from <i>E. coli</i> , 0127:B8)	Sigma-Aldrich (Steinheim)
Maxer's hematoxyllin	Roth (Karlsruhe)
NaCl (sodium chloride)	Sigma-Aldrich (Steinheim)
Needles (18-27 gauge)	BD Bioscience (Heidelberg)
NP-40 (nonyl phenoxy/polyethoxyethanol)	Sigma-Aldrich (Steinheim)
Nuclear ORANGE	eBioscience (Frankfurt)
Pan T-cell Isolation kit for AutoMACS	Miltenyi Biotec (Bergisch-Gladbach)
Paraformaldehyd	Merck (Darmstadt)
PCR Purification kit	Qiagen (Hilden)
peqGOLD RNAPure™	PeqLab Biotechnologie (Erlangen)
PPRE lentivector	System Biosciences (Mountain View)
Prolene® 5-0	Ethicon Inc (Norderstedt)
Protease Inhibitor Cocktail Mix (PIM)	Roche (Basel)
Protein G-Agarose Beads	Roche (Basel)
Protein Ruler	Fermentas (St. Leon-Rot)
Proteinase K	Invitrogen (Darmstadt)
PureLink® PCR Purification Kit	Invitrogen (Darmstadt)
Rompum® (Xylazine)	Bayer vet. (Leverkusen)
RPMI (Rosswell Park Memorial Institute)	PAA Laboratories (Cölbe)
Salmon Testes DNA	Invitrogen (Darmstadt)

SDS (sodium dodecyl sulfate)	Roth (Karlsruhe)
Syringes (2-20 ml)	B.Braun (Melsungen)
Taq DNA Recombinant PCR kit	Invitrogen (Darmstadt)
Temgesic® (Buprenorphine)	Essex Chemie AG (Clifton)
Thioglycollate-G	Hypha Diagnostica (Heidelberg)

### 4.1.3. Antibodies

Table 6: List of antibodies for Western and FACS analysis

Antigen	Source	Provider
Actin	Rabbit	Sigma Aldrich (Steinheim)
Akt	Mouse	Cell Signaling Technology (Danvers)
Anti-rabbit-IgG	Rabbit	Vector laboratories Inc. (Burlingame)
Bcl-2	Rabbit	BD Bioscience (Heidelberg)
Bim	Mouse	Cell Signaling Technology (Danvers)
Biotinylated-IgG	Rabbit	Vector Laboratories Inc. (Burlingame)
CD3 $\epsilon$ -APC	Mouse	EuroBioScience (Friesoythe)
CD3 $\epsilon$ -FITC	Mouse	EuroBioScience (Friesoythe)
CD45-pacific blue	Mouse	BD Bioscience (Heidelberg)
CD4-PE	Mouse	EuroBioScience (Friesoythe)
CD8a-APC	Mouse	Miltenyi Biotec (Bergisch-Gladbach)
Cleaved caspase 3	Rabbit	Cell Signaling Technology (Danvers)
Fc-Block	Mouse	BD Bioscience (Heidelberg)
IgG	Rabbit	Upstate Biotechnology (Billercia)
IL-2-PE	Mouse	BD Bioscience (Heidelberg)
LEAF <sup>TM</sup> Purified IgG isotype control	Rat	BioLegend (Uithoorn)
LEAF <sup>TM</sup> Purified anti-mouse IL-2	Rat	BioLegend (Uithoorn)
Mouse-IRDye680	Donkey	LI-COR (Lincoln)
Mouse-IRDye800CW	Donkey	LI-COR (Lincoln)
NFAT	Rabbit	Santa Cruz (Santa Cruz)
pAkt	Rabbit	Cell Signaling Technology (Danvers)
PPAR $\gamma$	Rabbit	Santa Cruz (Santa Cruz)
Rabbit-IRDye680	Donkey	LI-COR (Lincoln)
Rabbit-IRDye800CW	Donkey	LI-COR (Lincoln)

#### 4.1.4. Oligonucleotides

Oligonucleotides were purchased from Biomers.net GmbH (Ulm) and described in Table 7. For amplification of mouse IL-2, Actin, PPAR $\gamma$ , and Bcl-2 QuantiTect Primer Assay from Qiagen GmbH (Hilden) were used.

Table 7: List of oligonucleotides

Name	upsteam primer	downstream primer
Bim	5'-GGCCAAGCAACCTTCTGATG-3'	5'-GCCTTCTCCATACCAGACGG-3'
ChIP-IL-2	5'-TTTGTCCACCACAACAGGCT-3'	5'-CGAGCTGCATGCTGTACATG-3'
Lck-Cre	5'-TCCTGTGAACTTGGTGCTTG-3'	5'-AAAAGAAAACGTTGATGCCG-3'
PPAR $\gamma^{fl/fl}$	5'-CTCCAATGTTCTCAAACCTTAC-3'	5'-GATGAGTCATGTAAGTTGACC-3'
PTEN	5'-CTGTTCTAACCGGGCAGCTT-3'	5'-CGTGTGGAGGCAGGAGAAG-3'

#### 4.1.5. Equipment & Software

Table 8: List of instruments

Instruments&Software	Provider
AIDA Image Analyzer	Raytest GmbH (Straubenhardt)
AutoMACS <sup>TM</sup> Separator	Miltenyi Biotech GmbH (Bergisch-Gladbach)
AxioVision 40 V4.7.0.0 Software	Carl Zeiss AG (Jena)
B250 Sonifier	Branson Ultrasonics (Danbury)
CASY <sup>®</sup> cell counter	Schärfe System (Reutlingen)
Centrifuge 5415 R	Eppendorf GmbH (Hamburg)
Centrifuge CR 3.22 and MR23i	Jouan GmbH (Unterhaching)
CFX Cyclor system	BioRad (Munich)
CFX Manager Software	BioRad (Munich)
FACS Diva Software	BD Bioscience (Heidelberg)
FACSFortessa	BD Biosciences (Heidelberg)
Flo Jo Software	Tree Star inc. (Ashland)
Holten Lamin Air clean bench	Jouan GmbH (Unterhaching)
IG 150 (cell culture incubator)	Jouan GmbH (Unterhaching)
Mastercycler <sup>®</sup>	Eppendorf GmbH (Hamburg)
NanoDrop ND-1000	Peqlab Biotechnologie GmbH (Erlangen)
Odyssey 2.1 Software	LiCOR Biosciences GmbH (Bad Homburg)
Odyssey infrared imaging system	LI-COR Biosciences GmbH (Bad Homburg)

---

Thermomixer 5436	Eppendorf GmbH (Hamburg)
Trans-Blot SD blotting machine	BioRad (Munich)
UV-Transilluminator gel documentation system	Raytest GmbH (Straubenhardt)
Zeiss Axioskop 40	Carl Zeiss AG (Jena)

---



## 4.2. Methods

### 4.2.1. Mouse work

#### Genotyping of mice

Conditional T-cell PPAR $\gamma$  knockout (Tc-PPAR $\gamma^{-/-}$ ) mice were generated by crossing C57BL/6N mice, bearing loxP-flanked alleles of PPAR $\gamma$  (PPAR $\gamma^{fl/fl}$ ) (90), with C57BL/6NTac-(Tg) *lck*-Cre transgenic mice, in which the Cre recombinase has been knocked in behind the *lck* promoter (91-92). PPAR $\gamma^{fl/fl}$  mice were used as control WT mice.

Genotypes of mice were determined by PCR of tail genomic DNA. To prepare the genomic DNA, tail-tips (~0.5 cm) were cooked in 75  $\mu$ l of lysis buffer (see Appendix), cooled down to room temperature and neutralized with 75  $\mu$ l of neutralizing buffer (see Appendix). 3  $\mu$ l were taken for PCR to analyze the expression of the *Cre* under control of the *lck*-promoter (*lck*-Cre primer) and the expression of loxP-sites in the PPAR $\gamma$  gene (PPAR $\gamma^{fl/fl}$  primer).

Setup of genotyping PCR reaction:

Enzyme activation		95 °C	15 min	
Denaturation	33 cycles	}	95 °C	15 s
Annealing			55 °C	30 s
Extension			72 °C	30 s

PCR products were analyzed on 1.5 % agarose gels.

#### Lipopolysaccharide (LPS)-induced systemic inflammation

To induce systemic inflammatory conditions, WT mice and conditional Tc-PPAR $\gamma^{-/-}$  mice were injected i.p. with 1 mg/kg lipopolysaccharide (LPS) from *Escherichia coli*, (serotype 0127:B8). After 24 h, mice were sacrificed and spleens were dissected.

### Cecum ligation and puncture (CLP) sepsis model

The cecum ligation and puncture (CLP) model was used to mimic septic conditions in mice. The CLP model has many pathophysiological similarities to the clinical situation where a bowel perforation-induced peritonitis results from an infection that is caused by mixed intestinal flora. The CLP model is one of the most widely used models of sepsis and septic shock. It satisfies many of the criteria for an appropriate sepsis model: it is polymicrobial, has focal infection origins, produces septicemia, and releases bacterial products into the periphery (93).

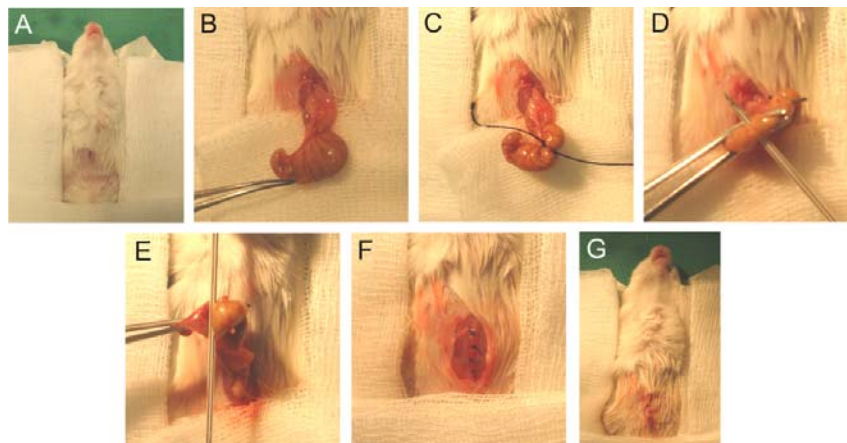


Figure 9: Cecum ligation and puncture sepsis model. (A) After anesthetization, shaving, and disinfection, (B) the abdomen of the mouse is opened and the cecum is exposed. Further, (C) the cecum is ligated, carefully not to disturb the ileocecal flow. (D) The ligated cecum is punctured once 'through-and-through' with a 20-gauge needle and (E) a small amount of faeces is extruded from each puncture site. At last, (F) the abdominal cavity is closed in two layers. (G) The mouse receives 1 ml of 0.9% NaCl for fluid resuscitation as well as analgetics after the procedure and when needed and is monitored regularly.

For CLP surgery, mice were anesthetized with 0.4 mg/kg ketamin (Ketavet<sup>®</sup>) and 0.02 mg/kg xylazine (Rompun<sup>®</sup>). The abdominal hairs were shaved and the area disinfected with 70% ethanol. The abdominal cavity is opened via a midline laparotomy incision of about 3 cm in an aseptic fashion and the cecum was exposed. The cecum is ligated distal to the ileocecal valve, taking care to maintain bowel continuity. The ligated cecum was punctured twice with a 20-

gauge needle. Next, sufficient pressure was applied to the cecum to extrude a single droplet of fecal material from each puncture site. The abdomen is closed in two layers, and mice are resuscitated with 1 ml of 0.9% NaCl. Until mice wake up from narcosis they are kept warm on a heater mat. Mice subjected to sham laparotomy (sham) underwent the same procedure without ligation and puncture. Animals received s.c. 0.05 mg/kg buprenorphine (Temgesic<sup>®</sup>) after surgery and in the following time as needed. Mice were sacrificed after 24 h or monitored regularly for seven days to determine survival (Figure 9).

### **Antagonizing PPAR $\gamma$ with GW9662**

To antagonize PPAR $\gamma$ , WT mice were treated with 1 or 3 mg/kg GW9662. To verify the time point, when GW9662 exerts the most prominent effect, a time kinetic administrating GW9662 at 1 h, 3 h, or 5 h following CLP surgery was performed. 50  $\mu$ l DMSO (10% in PBS) was supplied as solvent control.

### **Neutralizing IL-2**

*In vivo* IL-2 neutralization was accomplished with an i.p. injection of 500  $\mu$ g LEAF<sup>™</sup> purified anti-mouse IL-2 neutralizing antibody (anti-IL-2) 1 h post-CLP. To determine unspecific effects of the antibody, a control group was treated with 500  $\mu$ g LEAF<sup>™</sup> purified IgG isotype control antibody (IgG) 1 h after CLP.

## **4.2.2. Primary cell analysis**

### **T-cell isolation**

After 24 h following CLP surgery or LPS treatment, mice were sacrificed, spleens and blood were dissected and a single cell suspension of splenocytes was prepared. Whole blood and splenocytes were incubated for 5 min with erythrocyte lysing buffer (see Appendix), and subsequently centrifuged for 5 min at 4°C, 500 x g. T-cells were enriched to >90% by autoMACS separation from

spleens using the Pan T-cell Isolation Kit. Therefore, splenocytes were counted using the Casy Counter.  $1 \times 10^8$  cells were washed and suspended in 400  $\mu$ l of running buffer (see Appendix). Next, cells were incubated with biotin-labeled antibodies against all cell populations besides T-cells for 10 min at 4°C (Pan T-cell kit solution 1). Afterwards, 300  $\mu$ l of running buffer and 200  $\mu$ l of anti-biotin magnetic beads (Pan T-cell kit solution 2) were added and cells were incubated for 15 min at 4°C. Subsequently, the antibody-biotin-labeled cells were washed with 8 ml running buffer, centrifuged at 300 x g for 5 min at 4°C and resuspended in 2 ml of running buffer. Isolation using the autoMACS separator was performed by negative isolation in the sensitive mode (<depletes>). The elution fraction was centrifuged at 300 x g for 10 min and supernatant was discarded. Cells were resuspended in 10 ml of running buffer and counted using the Casy Counter. After another centrifugation at 300 x g for 10 min, the cell pellet was frozen at -20°C for subsequent protein or mRNA isolation as described. Purification was verified by FACS analysis using an anti-CD3 $\epsilon$ -FITC-labeled antibody.

### **FACS analysis**

Splenocyte suspensions were prepared from freshly dissected spleens following standard procedures. Incubating cell suspensions for 5 min with erythrocytes lysis buffer (see Appendix) lysed erythrocytes.  $10^6$  cells were incubated with fluorophore-conjugated antibodies against the following cell-surface proteins: anti-CD45-pacific blue, anti-CD4-PE, anti-CD3 $\epsilon$ -FITC, and anti-CD8a-APC for 30 min at 4°C in PBS, 0.5% BSA. Following incubations, labeled cells were washed with PBS. 15 min prior to analysis with FACSFortessa, cells were incubated with Nuclear ORANGE to mark living cells. For analysis of specific cell populations, gates were set with appropriate controls.

### **Intracellular IL-2 analysis**

To analyze intracellular levels of IL-2,  $10^6$  splenic T-cells were suspended in 500  $\mu$ l culture medium. Cells were incubated for 2.5 h with 50  $\mu$ M brefeldin A to block anterograde protein transport. The reaction was stopped with 50  $\mu$ l of 20 mM EDTA. Next, cells were stained with antibodies to cell-surface proteins as described. Subsequently, cells were fixed in 3% PFA at room temperature for 30 min and afterwards permeabilized with 1% NP-40 for 1 h. To prevent unspecific binding, cells were blocked with 1% BSA for 20 min before staining with anti-IL-2-PE on a rotating platform in the dark at 4°C for 1 h. Intracellular IL-2 was visualized using FACS analysis. FACS Diva software and Flow Jo Software were used for analysis.

### **4.2.3. Biochemistry and molecular biology**

#### **Chromatin immunoprecipitation (ChIP) assay**

ChIP assay was performed with  $1 \times 10^7$  primary T-cells derived from sham or CLP mice with different treatments. Cells were resuspended in 5 ml culture medium, crosslinked by adding 45  $\mu$ l 37% formaldehyde/ml and shaken at 200 rpm for 5 min at RT. Afterwards, 80  $\mu$ l 1 M glycine/ml medium was added and incubated for another 5 min with shaking. Cells were washed with PBS and resuspended in 1 ml ChIP lysis buffer (see Appendix) directly followed by centrifugation for 1 min at 4°C at 12,000 x g. Sedimented nuclei were resuspended in 400  $\mu$ l ChIP lysis buffer and incubated for 15 min on ice. To shredder whole genomic DNA, glass beads were added to the lysate and sonicated three fold with 18 x 8 pulses. To determine DNA fragmentation and for input control, the sonicated lysate was analyzed by agarose gel electrophoresis. 120  $\mu$ l of each lysate containing fragmented soluble chromatin was immunoprecipitated with 2  $\mu$ g of anti-NFAT antibody. For mock-IP, lysates were incubated with 1  $\mu$ g of normal rabbit IgG over night at 4°C on a rotating platform. 50  $\mu$ l of protein G agarose beads were preincubated with 5  $\mu$ l salmon testes DNA (10.6 mg/ml) and 25  $\mu$ l BSA (10 mg/ml). The next day 10  $\mu$ l of PIM was added. 30  $\mu$ l of prepared protein G agarose beads were added to the

immunoprecipitated probe and incubated over night at 4°C on a rotating platform. To wash away non-bound proteins, agarose beads were washed 5 times with 1 ml ChIP lysis buffer followed by centrifugation for 1 min at 2,000 x g. Afterwards, 100 µl Chelex 100 were added, briefly vortexed and boiled at 99°C for 10 min. To digest proteins, 1 µl of proteinase K (20 µg/ml) was added and incubated at 37°C for 1 h followed by another 10 min at 99°C. Tubes were then centrifuged for 1 min at 12,000 x g. To finally isolate the DNA, 80 µl of elution buffer (EB) were added, vortexed for 10 sec and centrifuged for 1 min at 12,000 x g. The isolation step was repeated and supernatants were combined in a new tube. DNA was extracted using the PCR Purification Kit from Qiagen. Therefore, supernatants were precipitated with 5 volumes of precipitation buffer (including ethanol). Precipitation was performed for at least 30 min at 4°C or over night at -20°C. The precipitated sample was applied to a purification column and centrifuged for 1 min at 12,000 x g. After washing the column 3 times with precipitation buffer, the DNA is eluted. Therefore, 200 µl elution buffer was prewarmed to 50°C and 100 µl were put on the column, let stand for 1 min and centrifuged at 12,000 x g for 1 min. The elution step was repeated with another 100 µl elution buffer. A 423-bp fragment of the IL-2 promoter spanning an established NFAT response element (94) was amplified using 5 µl of DNA and the ChIP-IL-2 primer. For input controls 20% fragmented DNA of each probe was used. Resulting fragments were separated on a 1.5% agarose gel containing ethidium bromide (0.5 mg/l). Bands were visualized by UV excitation.


### **RNA isolation, reverse transcription and realtime PCR**

Primary T-cells were isolated from spleens as described. Total RNA from T-cells was isolated using PeqGold RNAPure following manufacturer's description. In brief, 1 ml of PeqGold was applied to  $5 \times 10^6$  cells. After 10 min incubation the lysate was transferred to 1.5 ml vials, supplemented with 200 µl chloroform and mixed thoroughly for 15 s. The mixture was incubated for 5 min at room temperature, followed by 5 min centrifugation with 12,000 x g at room temperature. During this step, the mixture separated into a chloroform phase,


and a water phase, divided by a small phase with debris. The upper water phase was transferred to a fresh 1.5 ml vial, was mixed with 500  $\mu$ l isopropanol and incubated 30 min at room temperature for RNA precipitation. RNA was sedimented by centrifugation (15 min, 12,000  $\times$  g, 4°C) and washed twice with 1 ml 70% ethanol in DEPC-treated distilled H<sub>2</sub>O. The RNA pellet was air dried at 60°C and resuspended in DEPC-treated distilled H<sub>2</sub>O. RNA concentration was determined with the NanoDrop ND-1000.

Reverse transcription was performed with 1  $\mu$ g RNA using iScript cDNA synthesis kit. In brief, 1  $\mu$ g of isolated mRNA was mixed with 4  $\mu$ l 5x reaction buffer, 1  $\mu$ l iScript reverse transcriptase and filled up with nuclease-free H<sub>2</sub>O to 20  $\mu$ l. The reaction mix was incubated for 5 min at 25°C, 30 min at 42°C and finally 5 min at 85°C for enzyme inactivation. The resulting cDNA was diluted 1:5.

Quantitative PCR was performed with Absolute QPCR SYBR Green mix according to manufacturer's instructions. 4  $\mu$ l of cDNA were mixed with either 1  $\mu$ l QuantiTect Primer Assay or 0.5  $\mu$ l forward and reverse primer (5  $\mu$ M) each, 10  $\mu$ l Absolute™ qPCR SYBR Green Fluorescein Mix and filled up with distilled H<sub>2</sub>O to 20  $\mu$ l. The mixtures were transferred to a 96-well plate, spinned down and the plate sealed with an optical adhesive seal sheet. qPCR was performed using the MyiQ Single-Colour Real-time PCR Detection System and the following thermal cycling program:

Enzyme activation		95 °C	15 min	
Denaturation	45 cycles		95 °C	15 s
Annealing			55 °C	30 s
Extension			72 °C	30 s

To confirm the specificity of the reaction, a melt curve was created using the following program:

Denaturation		95 °C	30 s	
Starting temperature		60 °C	30 s	
Melting step	80 cycles		60 °C	10 s
			+ 0.5°C per cycle	

Relative mRNA expression was calculated using the BIO-RAD GeneEx gene expression macro based on the ddCt method.

### **Protein determination (Lowry) and SDS-PAGE/Western blot (WB) analysis**

For Western analysis, primary mouse T-cells were isolated as indicated, pelleted by centrifugation and resuspended in 100-200  $\mu$ l Urea Lysis Buffer (see Appendix) and sonicated. After shaking the lysate for 30 min at 4°C, the lysate was cleared by centrifugation (15,000 x g, 15 min, 4 °C). The protein concentration was determined using DC Protein Assay Kit, based on the Lowry method. Briefly, a standard dilution series of bovine serum albumin (BSA) in Urea Lysis Buffer was prepared (0.625 to 10 mg/ml). 2  $\mu$ l of the samples and the standard dilutions were pipetted in duplicates into a 96-well plate, 20  $\mu$ l of solution A, and 160  $\mu$ l of solution B were added. The colorimetric reaction was detected after incubation for 10 min at RT with shaking. The extinction was measured at 750 nm using the Mithras LB 940 multimode reader. 80  $\mu$ g of protein were denatured using 4 x sample buffer (see Appendix) and resolved on 10% SDS-polyacrylamide gels (see Appendix). Proteins were blotted onto nitrocellulose membrane, blocked with Rockland Blocking Buffer for IRDye Fluorescence Western Blotting and treated with primary antibodies in Blocking Buffer/50% TTBS (see Appendix). After overnight incubations at 4°C membranes were washed 3 times for 5 min with TTBS. For protein detection, blots were incubated with IRDye800CW-labeled secondary antibody for 45 min and washed 3 times for 5 min each with TTBS. Detection was performed using Odyssey Infrared Imaging System. Densitometry of the Western blots was performed using the LI-COR Odyssey 2.1 software.

### **TUNEL Assay**

TUNEL assay was performed according to the manufacturer's instructions using the APO-BRDU TUNEL kit.  $10^6$  freshly isolated splenocytes were labeled with anti-CD3 $\epsilon$ -APC for 30 min in 100  $\mu$ l PBS. Afterwards, cells were fixed in 1 ml



1% PFA for 1 h, washed with 1 ml PBS and resuspended in 1 ml 70% (v/v) ethanol. Cells were stored at -20°C until experiments were performed. For labeling of apoptotic cells, cells were incubated with Br-dUTP for 60 min at 37°C, followed by 30 min incubation with the FITC-labeled secondary antibody. To label total cellular DNA propidium iodide (PI) dye was supplied 15 min before analysis by flow cytometry using the FACSFortessa.

### **Immunohistochemistry**

Spleens were collected and fixed in zinc fixation buffer (see Appendix) for 6 h at room temperature. Next, tissue was dehydrated in a graded ethanol series and embedded in paraffin. Paraffin sections were processed with standard histology procedures using the catalyzed signal amplification kit according to the manufacturer's instructions. In brief, 4 µm paraffin-embedded sections were deparaffinized, rehydrated in a graded ethanol series and washed in PBS. For antigen retrieval sections were soaked in target retrieval solution (TRS) and cooked for 10 min. Slides were washed, blocked and stained with rabbit anti-cleaved caspase 3 antibody in antibody diluent over night at 4°C. Next, slides were incubated with a biotinylated anti-rabbit antibody for 1 h, followed by incubation with 0.5% H<sub>2</sub>O<sub>2</sub> in PBS for 15 min to block endogenous peroxidase activity. Further, sections were incubated with horseradish peroxidase-conjugated anti-biotin for 15 min. For color development, 3,3'-diaminobenzidine tetrahydrochloride (DAB) chromogen was used and counterstained with Mayer's hematoxyllin (1:10) and Eosin G (H&E). Sections were analyzed using the Zeiss Axioskop 40 with the AxioVision 40 V4.7.0.0 Software. The magnification of images shown is 100 x.

### ***In vivo* PPRE reporter analysis**

3x10<sup>6</sup> HEK293T cells were seeded in 5 ml DMEM high glucose medium on a 10 cm cell culture dish. The next day, transfection was performed using 6 µl JetPei and 200 µl 150mM NaCl in combination with 3 µg of the versatile HIV-

based PPRE lentivector plasmid that co-expresses mRuby and Firefly Luciferase in response to PPRE activation, 26  $\mu$ l lentiviral packaging mix and 200  $\mu$ l NaCl. After 2 days, the medium was changed. Another 3 days later, the supernatant medium contains lentiviruses with the PPRE reporter plasmid.

For *in vivo* PPRE reporter experiments, T-cells were isolated from GFP<sup>+/+</sup> mice. Next, GFP<sup>+/+</sup> T-cells cells were transduced with the lentiviruses containing the PPRE reporter plasmid by two centrifugations for 100 min at 300 x g. After transduction, cells were washed four times with 10 ml PBS, diluted in 200  $\mu$ l of sterile 0.9% NaCl and injected into the tail vein of WT mice. 36 h later, mice were subjected to CLP with subsequent treatment with 1 mg/kg GW9662 at 3 h or left untreated. After 24 h, mice were sacrificed and blood T-cells were analyzed by flow cytometry. Lymphocytes were gated for CD3<sup>+</sup> cells and GFP<sup>+/+</sup> cells. In the GFP<sup>+/+</sup> population, mRuby expression was quantified, which mirrors PPRE reporter activation.

#### **4.2.4. Microbiology**

##### **Bacteriologic analysis of peritoneal lavage**

After sacrificing mice 24 h after CLP, the peritoneum was washed with 4 ml of Thioglycollate-M solution. A dilution series of 1:10, 1:100, 1:1000 with PBS was produced. 100  $\mu$ l of each dilution was plated on either Columbia-Agar plates or Endo-Agar plates for gram-positive or gram-negative bacterial colony detection, respectively. After cultivation for 24 h at 37°C, gram-negative and gram-positive colony-forming-units (CFU) were counted for each dilution, multiplied with the dilution factor and displayed as CFU/100 $\mu$ l peritoneal lavage. Bacterial load measurements were performed by Prof. Dr. Volkhard Kempf of the Institute of Microbiology and Infection Control, Goethe-University Frankfurt.

#### **4.2.5. Statistical analysis**

All data are expressed as means  $\pm$  SD and each experiment was performed at least three times. Statistical significance was determined by unpaired student's

*t*-test or the fisher's exact *P*-test. For Western analysis, ChIP analysis, and immunohistological stainings representative data of at least three independently performed experiments are shown. Differences were considered significant if: \**p*<0.05; \*\**p*<0.01; \*\*\**p*<0.001.

## 5. RESULTS

### 5.1. Phenotyping Tc-PPAR $\gamma$ <sup>-/-</sup> mice

I first investigated whether the newly generated conditional T-cell PPAR $\gamma$  knockout mice (Tc-PPAR $\gamma$ <sup>-/-</sup>) have sufficient ablation of PPAR $\gamma$  in T-cells. Isolated T-cells of Tc-PPAR $\gamma$ <sup>-/-</sup> mice express significantly lower PPAR $\gamma$  mRNA and protein as WT mice (Figure 10). For T-cells it was shown that PPAR $\gamma$  expression is induced upon activation, such as upon sepsis (95). However, even under septic conditions provoked by CLP, PPAR $\gamma$  protein expression is not upregulated in Tc-PPAR $\gamma$ <sup>-/-</sup>, whereas the protein is highly abundant in WT mice during septic conditions (Figure 10B).

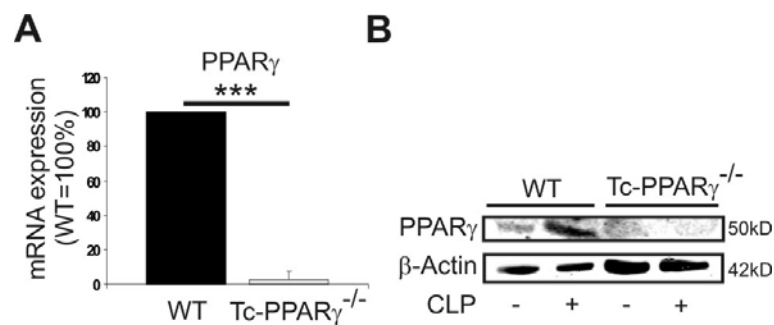


Figure 10: PPAR $\gamma$  expression in T-cells derived from WT or Tc-PPAR $\gamma$ <sup>-/-</sup> mice. (A) Real-time PCR analysis of PPAR $\gamma$  mRNA expression. PPAR $\gamma$  expression in WT T-cells was set to 100%. Data is shown as mean  $\pm$ SD. (B) Western analysis of PPAR $\gamma$  protein expression in T-cells derived from 24 h sham- or CLP-treated mice. Data are representative of at least three independent experiments. \*\*\*p<0.001.

These data proved PPAR $\gamma$  to be sufficiently ablated in T-cells by genetic depletion of the PPAR $\gamma$  gene using loxP flankation and Cre expression upon Ick-promoter activation in T-cells.

## 5.2. LPS-induced systemic inflammation in Tc-PPAR $\gamma$ <sup>-/-</sup> vs. WT mice

To examine the effects of PPAR $\gamma$  in T-cells during systemic inflammation, I challenged WT and Tc-PPAR $\gamma$ <sup>-/-</sup> mice with i.p. injection of 1 mg/kg LPS. 24 h thereafter mice were sacrificed and analyzed for relative splenic T-cell count. As seen in Figure 11A, I noticed severe T-cell depletion in the WT group after LPS, whereas in Tc-PPAR $\gamma$ <sup>-/-</sup> spleens, the T-cell count was not affected by LPS. Moreover, after isolation of splenic T-cells I questioned whether apoptotic signals regulated by important cell death regulating proteins are differently expressed in T-cells with or without PPAR $\gamma$ . At first, I analyzed expression levels of the most prominent T-cell survival factor, namely IL-2. IL-2 is expressed by T-cells and autocrine IL-2 receptor activation promotes T-cell proliferation and cell cycle control. I recognized an increased expression of IL-2 mRNA in the Tc-PPAR $\gamma$ <sup>-/-</sup> population (Figure 11B). A downstream target of autocrine IL-2 receptor stimulation is the anti-apoptotic protein Bcl-2. When determining expression levels of anti-apoptotic Bcl-2 mRNA I recognized again a strong increase in the Tc-PPAR $\gamma$ <sup>-/-</sup> group, whereas WT mice showed no upregulation (Figure 11B). As a pro-apoptotic protein, the Bcl-2 family member Bim was previously shown to be upregulated during sepsis and is specifically highly expressed in T-cells during sepsis, and its knockout provoked better survival of septic mice (88). Thus, I investigated Bim expression levels. In my model using LPS-treated WT and Tc-PPAR $\gamma$ <sup>-/-</sup> mice, I proved pro-apoptotic Bim mRNA expression to be decreased in isolated T-cells derived from LPS-stimulated Tc-PPAR $\gamma$ <sup>-/-</sup> in contrast to T-cells from WT mice (Figure 11B). This result proposes that WT mice treated with LPS contain induced apoptotic signals in their T-cells, which correlates to lower T-cell counts compared to mice with genetical ablation of PPAR $\gamma$ .

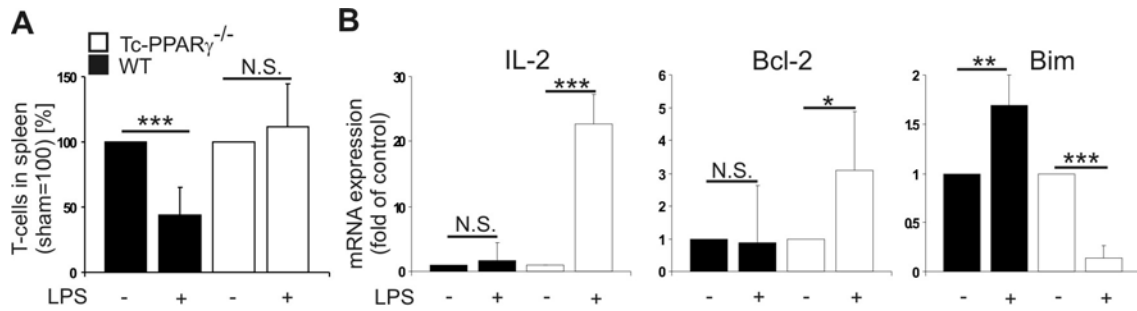


Figure 11: LPS-induced T-cell depletion and underlying apoptotic signals. (A) Relative T-cell count in Tc-PPAR $\gamma^{-/-}$  (white bars) and WT (black bars) mice 24 h after LPS or without treatment. T-cell counts in untreated controls were set to 100%. (B) X-fold induction of mRNA expression of IL-2, Bcl-2 and Bim relative to untreated controls detected by real-time PCR. Graphs show mean values  $\pm$  SD. \*  $p < 0.05$ ; \*\*  $p < 0.01$ ; \*\*\*  $p < 0.001$ ; N.S., not significant.

Inducing systemic inflammation with LPS does not represent a high clinical relevance thus, in order to further verify importance of PPAR $\gamma$  during sepsis progression I decided to continue my research using an animal model of sepsis with great similarities to human sepsis pathophysiology.

### 5.3. CLP-induced sepsis in Tc-PPAR $\gamma^{-/-}$ vs. WT mice

#### 5.3.1. Absolute T-cell count

Additionally to the LPS model, I used the cecum ligation and puncture (CLP) model to mimic septic conditions in mice. This model closely resembles the situation of a ruptured abdominal anastomosis leading to sepsis in humans (96) and is described in detail in 4.2.1. Previous studies have shown that T-lymphocyte depletion was most prominent at 24 h following CLP (97). To characterize differences during sepsis progression of WT and Tc-PPAR $\gamma^{-/-}$  mice subjected to CLP, I evaluated the amount of viable T-cells in the spleen and blood 24 h after CLP. As seen in Figure 12, FACS analysis of T-cell populations in the spleen and blood showed a marked decrease in T-cell numbers of WT animals. Regarding T-cell subpopulations, especially the CD4 $^{+}$  cell count was reduced in blood and spleens, whereas the CD8 $^{+}$  cell count was only reduced in blood. In contrast, T-cells in spleens of Tc-PPAR $\gamma^{-/-}$  mice exhibited no depletion

compared to sham-operated controls. In blood, CD4<sup>+</sup> as well as CD8<sup>+</sup> cells even increased in number. Interestingly, in untreated Tc-PPAR $\gamma$ <sup>-/-</sup> mice, I detected lower T-cell counts in the spleen and in the blood (Figure 12). This phenotype suggests PPAR $\gamma$  to be involved in T-cell development.

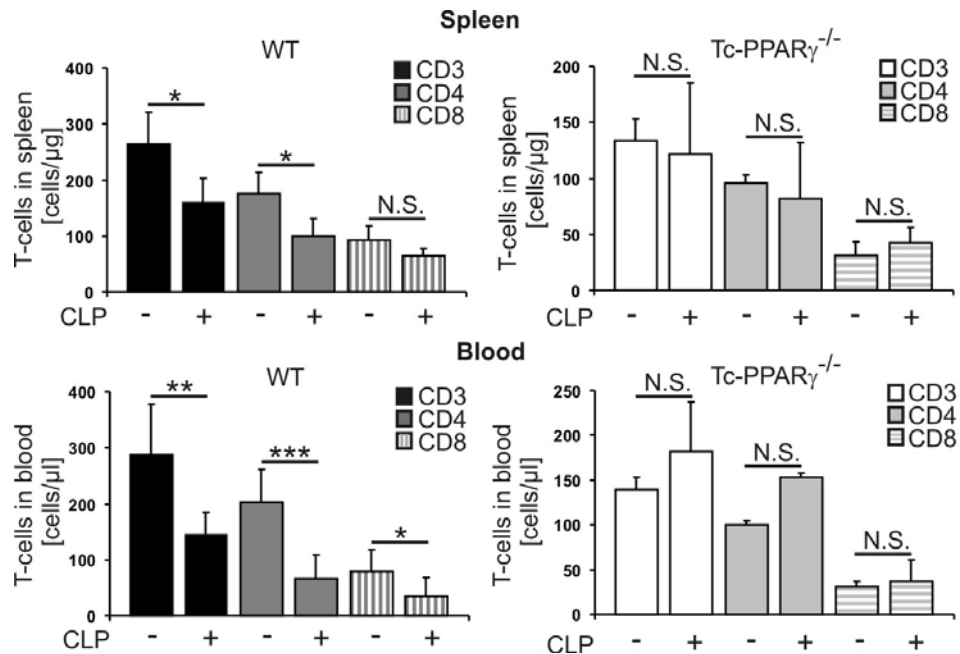


Figure 12: Flow cytometric quantification of spleen and blood derived T-cells and subpopulations from WT and Tc-PPAR $\gamma$ <sup>-/-</sup> mice at 24 h post CLP compared to sham controls. For identification, cells were stained with anti-CD3 $\epsilon$ , anti-CD4, as well as anti-CD8a and co-stained using anti-CD45 and Nuclear ORANGE to detect living lymphocytes. Data are means  $\pm$  SD. \* $p$ <0.05; \*\* $p$ <0.01; \*\*\* $p$ <0.001; N.S., not significant.

### 5.3.2. Detection of apoptotic T-cells

To analyze whether decreased T-cell counts are provoked by increased apoptosis in the spleen, I established two methods to detect different apoptosis markers. First, I identified apoptosis by histological analysis staining active caspase 3 in spleens. These experiments revealed that at 24 h following CLP, apoptotic cells accumulated in the T-cell enriched white pulp (WP) of WT mice spleens, whereas almost no splenocytes of Tc-PPAR $\gamma$ <sup>-/-</sup> contained active caspase 3 (Figure 13A). Although caspase activation is often assumed to be synonymous with cell death, they are multifunctional enzymes that convey a

number of actions, including regulation of lymphocyte proliferation, differentiation and cell cycle regulation (29, 76). Thus, the fact that there is an increase in caspase activation does not a priori signify that lymphocytes are undergoing apoptosis. In the present case, however, there is additional evidence that strongly suggests that the increased caspase 3 activation results in cell death. The staining of the degradation of intact chromatin structures into DNA fragments (TUNEL staining), determined by flow cytometry analysis, envisions an important hallmark of apoptosis. Septic T-cells from WT mice presented significantly more TUNEL positive cells compared to Tc-PPAR $\gamma$ <sup>-/-</sup> T-cells (Figure 13B). Thus, it is likely that caspase activation in the setting of sepsis is indicative of its role in cell death.

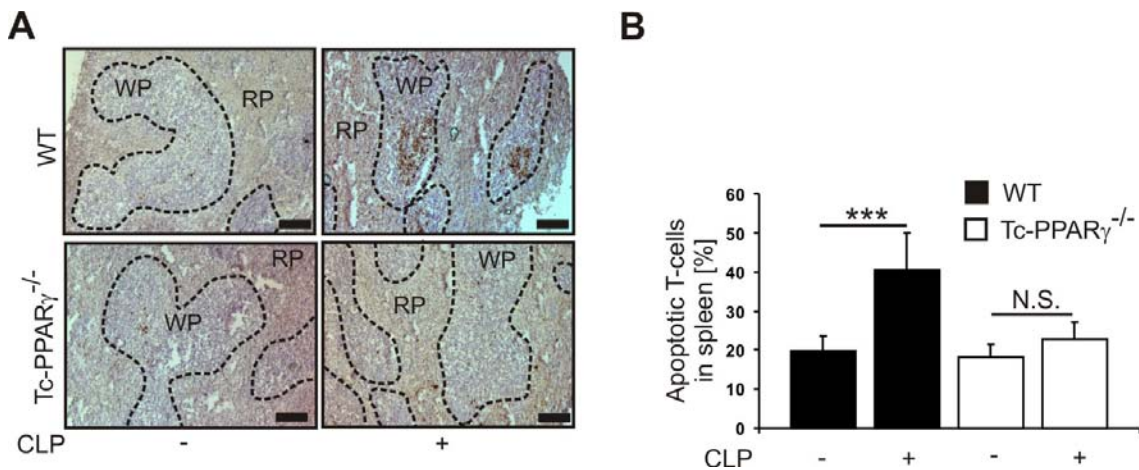


Figure 13: Apoptosis detection in septic Tc-PPAR $\gamma$ <sup>-/-</sup> mice and WT mice by caspase 3 staining and TUNEL assay. (A) Histological analysis of CLP-induced splenocyte apoptosis. Spleen sections were stained for active caspase 3 (brown) and counterstained with H&E (red and blue). Dashed line surrounds T-cell enriched white pulp (WP). RP, red pulp. Data are representative for at least three independent experiments. Scale bars=100  $\mu$ m. (B) Quantification of apoptotic T-cells in spleens by anti-CD3 $\epsilon$  and TUNEL staining using flow cytometry. Values are expressed as a mean percentage  $\pm$  SD of apoptotic T-cells relative to the total amount of T-cells in spleens of sham or CLP-treated mice. \*\*\*  $p < 0.001$ ; N.S., not significant.

### 5.3.3. Survival studies

Next, survival of septic mice observed for 7 days should clarify the question, whether increased T-cell counts in Tc-PPAR $\gamma$ <sup>-/-</sup> mice account for better survival. As seen in Figure 14, no WT mouse survived 7 days of severe septic conditions



initiated by CLP, whereas 60% of the Tc-PPAR $\gamma^{-/-}$  mice survived the observation time. Statistical analysis approved the survival advantage of the knockout population to be significant at 7 days after CLP. Previous investigations confirmed this result demonstrating a 100% mortality of WT mice occurring in 4 days if >30% of the cecum is ligated (same in our model) and a double puncture with a 20-gauge needle is performed (93).

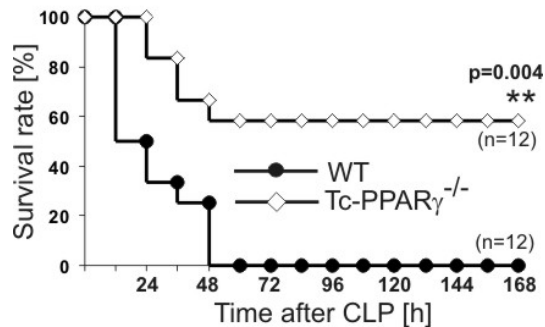


Figure 14: Survival curves of CLP-induced death of WT and Tc-PPAR $\gamma^{-/-}$  mice observed for 7d. \*\*p<0.01.

These differences in survival support my assumption that PPAR $\gamma$  exerts apoptosis of T-cells during sepsis thus, reducing survival during peritonitis-induced sepsis.

Next, I aimed at elucidating how this increased T-cell count contributes to improved survival. Therefore, the potential of T-cells to affect other cells, such as phagocytes, and to improve the bacterial clearance was assessed by peritoneal colony forming units (CFU) counts of CLP-treated mice. The peritoneal cavity contains multiple microbes that can be cultured, such as *Escherichia coli*, *Proteus mirabilis*, *Enterococcus*, *Bacteroides fragilis*, etc. (93). When analyzing the kind and amount of bacteria found in the peritoneum, I discovered higher levels (not significant) of gram-positive as well as gram-negative bacteria in WT mice, compared to Tc-PPAR $\gamma^{-/-}$  mice (Figure 15A). To detect whether this result also accounts for less organ damage and thus, decreases mortality, specific organ damage markers in the serum were envisioned. In my experiments, these markers were aspartate aminotransferase (AST, a nonspecific marker for hepatic injury), alanine aminotransferase (ALT, a specific marker for hepatic

parenchymal injury) and lactate dehydrogenase (LDH, unspecific organ damage marker) (98-99). AST, ALT and LDH were significantly increased in WT mice and mirror the poor survival of these mice in comparison to Tc-PPAR $\gamma$ <sup>-/-</sup> mice (Figure 15B).

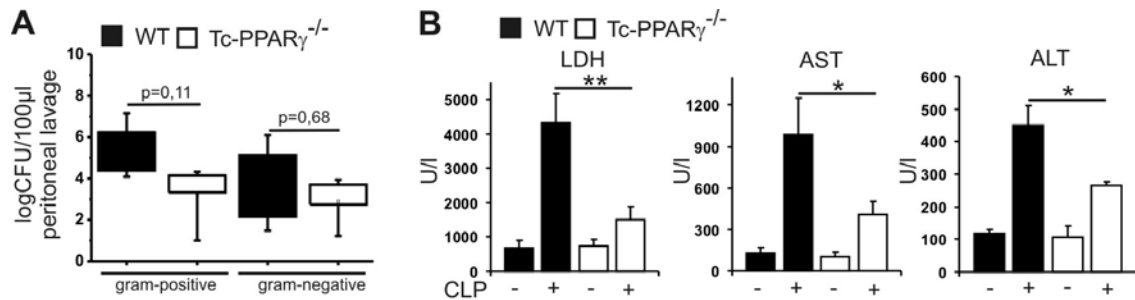


Figure 15: Bacterial load and end organ damage in CLP-treated WT and Tc-PPAR $\gamma$ <sup>-/-</sup> mice after 24 h. (A) Gram-negative and gram-positive bacterial load in peritoneum of mice. After sacrificing the mice, their peritonea were washed with 4 ml thioglycollate-G solution. Data shown are gram-positive and gram-negative bacteria colony forming units (CFU) in 100  $\mu$ l of peritoneal lavage fluid. (B) Serum activities of lactate dehydrogenase (LDH), alanine aminotransferase (ALT) and aspartate aminotransferase (AST) in mice subjected to CLP or sham. Data are means  $\pm$  SD. \* $p$ <0.05; \*\* $p$ <0.01.

#### 5.3.4. Apoptotic signaling in WT vs. Tc-PPAR $\gamma$ <sup>-/-</sup> T-cells

##### Modification of the pro-survival NFAT/IL-2/Bcl-2 pathway

To outline the molecular pro-survival effect of PPAR $\gamma$  deficiency, I investigated whether the ability of PPAR $\gamma$  to repress cytokine production in T-cells during sepsis accounts for increased apoptosis. IL-2 is known to be the most relevant cytokine for T-cell survival by increasing the expression of anti-apoptotic proteins, including Bcl-2 (100-101). IL-2 gene expression is transcriptionally regulated by nuclear factor of activated T-cells (NFAT), but complex formation with active PPAR $\gamma$  inhibits NFAT interaction with DNA (60, 102).

Therefore, I propose that in my model PPAR $\gamma$  inhibits IL-2 expression by binding to NFAT and consequently limits anti-apoptotic Bcl-2 signaling. To prove this assumption, I first examined IL-2 expression in splenic T-cells. I found elevated IL-2 mRNA expression in Tc-PPAR $\gamma$ <sup>-/-</sup> cells, but not in WT T-

cells (Figure 16A). Since IL-2 protein is mainly but not exclusively secreted by T-cells (103), I next analyzed T-cell-specific IL-2 formation by intracellular IL-2 staining instead of analyzing serum levels of IL-2. In correlation with the detected mRNA quantity, the amount of intracellular IL-2 was as well significantly higher in cells of Tc-PPAR $\gamma$ <sup>-/-</sup> mice compared to cells of WT mice after CLP (Figure 16B). As referred to in 3.2.4 and mentioned above, the PPAR $\gamma$  protein is able to bind other transcription factors and indirectly inhibits their transcriptional potential (mechanism of transrepression). Thus, diminished IL-2 mRNA expression can result from PPAR $\gamma$  ligating the transcription factor NFAT and thus, preventing IL-2 transcription (102). This ligation can be visualized and quantified by the amount of (unligated) NFAT binding to the IL-2 promoter in T-cells. A method that is capable of quantifying protein-DNA interaction is the chromatin immunoprecipitation (ChIP) assay. Using this method, I observed enhanced NFAT binding to the IL-2 promoter in Tc-PPAR $\gamma$ <sup>-/-</sup> T-cells, but none in WT T-cells after peritonitis induction or under unstimulated conditions (Figure 16C).

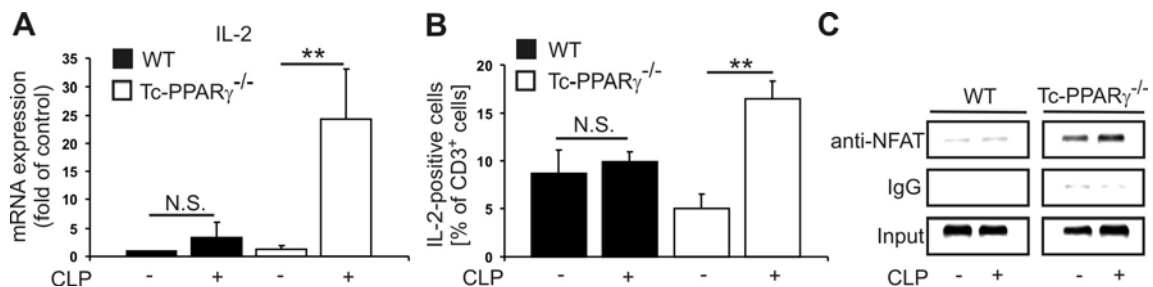


Figure 16: IL-2 mRNA expression, intracellular IL-2 protein expression and binding of NFAT to the IL-2 promoter in T-cells from WT and Tc-PPAR $\gamma$ <sup>-/-</sup> mice. Mice were sacrificed after 24 h following CLP or sham surgery. Spleens were dissected and T-cells were isolated. (A) Relative IL-2 mRNA expression in T-cells related to WT sham expression levels. (B) Intracellular IL-2 protein amount in T-cells. Percentage values indicate IL-2 expressing T-cells. (C) Association of NFAT with its response element within the IL-2 promoter analyzed by ChIP analysis. IgG was used to identify unspecific binding of the antibody. Data are representative of at least three independent experiments. \*\*p<0.01; N.S., not significant.

Hotchkiss et al. described that overexpression of anti-apoptotic proteins, such as Bcl-2, prevents lymphocyte cell death during sepsis and improves survival of septic mice (80). Taking this report into consideration, I quantified Bcl-2

expression as downstream target of IL-2 receptor stimulation during polymicrobial sepsis. Similar to the results of the LPS-model shown in Figure 11, I herein display a significant anti-apoptotic Bcl-2 mRNA induction in Tc-PPAR $\gamma$ <sup>-/-</sup> T-cells for the CLP model as well. In contrast, Bcl-2 mRNA was not induced in WT mice (Figure 17A). To check whether this is also true for the resulting Bcl-2 protein, I performed Western analysis. Importantly, Bcl-2 protein levels increased in Tc-PPAR $\gamma$ <sup>-/-</sup> after CLP in contrast to WT T-cells (Figure 17B).

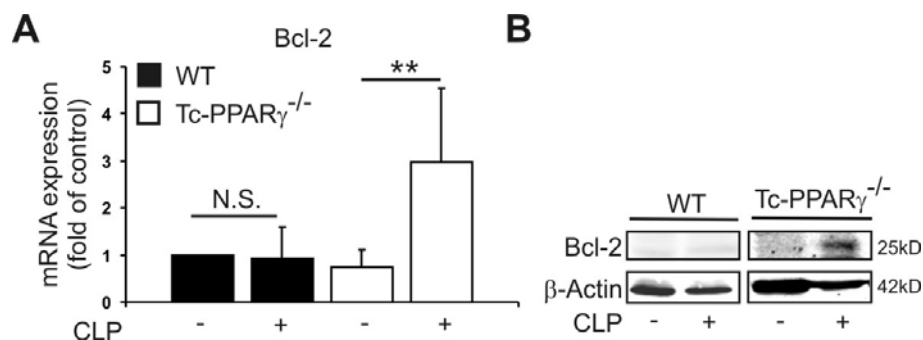


Figure 17: Bcl-2 mRNA and protein expression in septic WT and Tc-PPAR $\gamma$ <sup>-/-</sup> mice. Mice were sacrificed after 24 h following cecum ligation and puncture (CLP) or sham surgery. Spleens were dissected and T-cells were isolated. (A) Relative Bcl-2 mRNA expression in T-cells related to WT sham expression levels. Values are the means  $\pm$  SD of at least three independent experiments. (B) Western analysis of Bcl-2 expression in T-cells. \*\* $p$ <0.01; N.S., not significant.

#### 5.4. Neutralizing IL-2 impairs pro-survival signaling in Tc-PPAR $\gamma$ <sup>-/-</sup>

The above mentioned experiments present an IL-2-dependent Bcl-2 protein expression in Tc-PPAR $\gamma$ <sup>-/-</sup> mice, however, the final prove for this apoptosis pathway in PPAR $\gamma$ -lacking mice is still missing. A prove would be given if “overproduced” IL-2 is neutralized in Tc-PPAR $\gamma$ <sup>-/-</sup> mice, making them, in regard to IL-2 expression, similar to WT mice. Less pro-survival IL-2 receptor signaling, should then in turn also repress Bcl-2 and hence, reverse the pro-survival effects associated with increased IL-2 expression as described for Tc-PPAR $\gamma$ <sup>-/-</sup> mice.

The IL-2 neutralizing antibody (anti-IL-2) strongly reduced the count of Tc-PPAR $\gamma$ <sup>-/-</sup> T-cells in spleens and blood of Tc-PPAR $\gamma$ <sup>-/-</sup> mice after CLP compared to application of an isotype control (IgG). Especially CD4<sup>+</sup> T-cells decreased, whereas CD8<sup>+</sup> cells were only slightly reduced in peripheral blood (Figure 18).

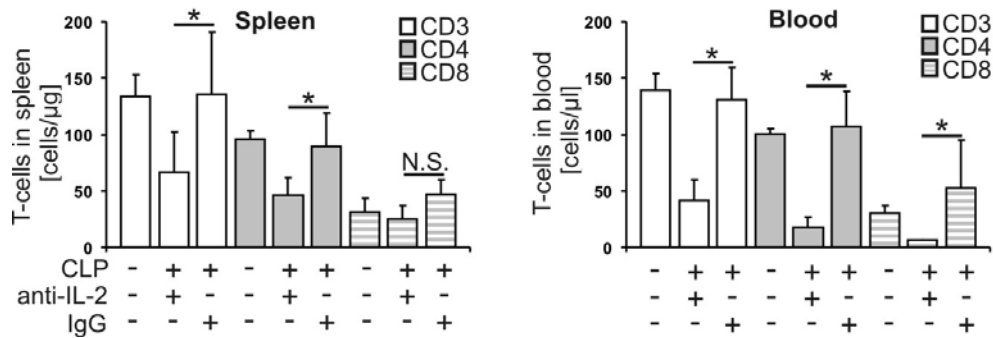


Figure 18: Absolute T-cell count in spleens and blood of anti-IL-2 or IgG-treated Tc-PPAR $\gamma$ <sup>-/-</sup> mice. Mice received either 500  $\mu$ g anti-IL-2 or 500  $\mu$ g IgG control antibody (IgG) at 1 h after CLP. Tc-PPAR $\gamma$ <sup>-/-</sup> sham mice were used as controls. T-cell quantification in spleen and blood was performed using flow cytometry. T-cells were stained with anti-CD3 $\epsilon$ , anti-CD4, as well as anti-CD8a and co-stained using anti-CD45 and Nuclear ORANGE to detect living lymphocytes. Values are the means  $\pm$  SD. \*  $p < 0.05$ ; N.S., not significant.

Also for the experimental setup neutralizing IL-2, I aimed at proving that the T-cell count correlates with apoptosis. Apoptosis detection (as previously performed) should clarify if anti-IL-2 depleted T-cells are dying by apoptosis. Anti-IL-2 treated mice presented an increase in TUNEL-positive (Figure 19A) and active caspase 3-positive T-cells (Figure 19B) after CLP. Antibody control (IgG) treatment did not exhibit apoptosis of splenic T-cells. IgG treatment provoked similar apoptosis patterns as untreated Tc-PPAR $\gamma$ <sup>-/-</sup> mice.

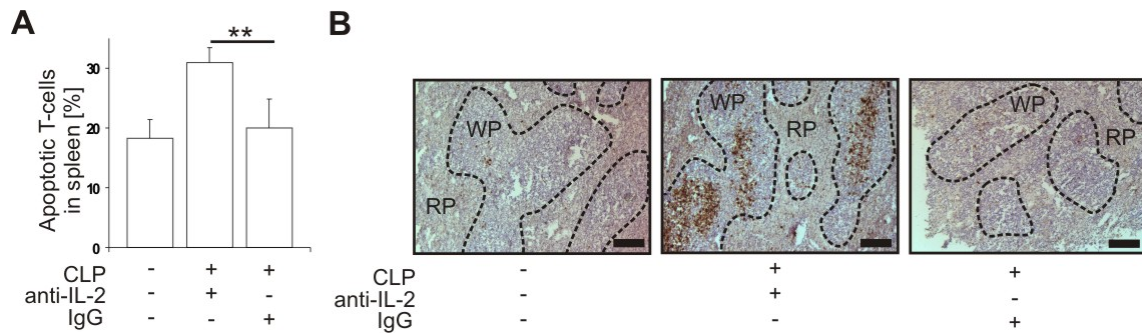


Figure 19: Evaluation of apoptosis by TUNEL and active caspase 3 staining in anti-IL-2 and IgG-treated Tc-PPAR $\gamma^{-/-}$  mice. Mice received either 500  $\mu$ g anti-IL-2 or 500  $\mu$ g IgG control antibody (IgG) at 1 h after cecum ligation and puncture (CLP). Tc-PPAR $\gamma^{-/-}$  sham mice were used as controls. (A) Quantification of apoptotic T-cells in spleens using anti-CD3 $\epsilon$  and TUNEL staining by flow cytometry. Values are expressed as the mean percentage  $\pm$  SD of apoptotic T-cells of total T-cell amounts in spleens. (B) Histological analysis of CLP-induced splenocyte apoptosis. Spleen sections were stained for active caspase 3 (brown) and counterstained with H&E (blue and red). Dashed line surrounds T-cell-enriched white pulp (WP). RP, red pulp. \*\* $p < 0.01$ . N.S., not significant.

If the lower T-cell count referred to in Figure 18 provokes less survival, anti-IL-2-treated mice should have a higher mortality rate compared to IgG-treated mice. I observed a poor 7-day survival upon anti-IL-2 treatment (10%) compared to IgG-treated littermates (60%) (Figure 20).

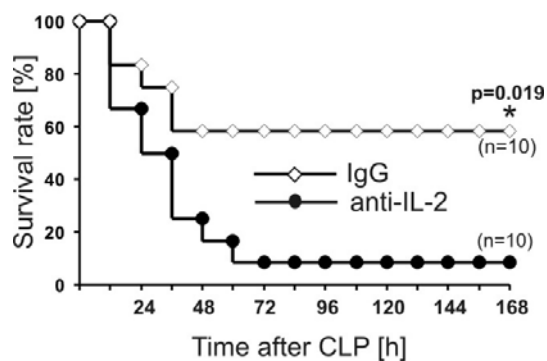


Figure 20: Comparison of survival of anti-IL-2-treated and IgG-treated Tc-PPAR $\gamma^{-/-}$  mice. Mice received either 500  $\mu$ g anti-IL-2 or 500  $\mu$ g IgG control antibody (IgG) at 1 h after CLP. Survival of mice was observed for 7d. \* $p < 0.05$ .

As shown for WT and Tc-PPAR $\gamma^{-/-}$  mice, I next questioned whether lower T-cell counts detected upon anti-IL-2 treatment correlate with lower bacterial clearance and higher end organ damage. Anti-IL-2 treatment tended to exhibit

more gram-negative and gram-positive CFU as antibody control treatment (Figure 21A). In line, lower T-cell counts pointed to worse end organ damage as indicated by LDH, AST, and ALT (Figure 21B).

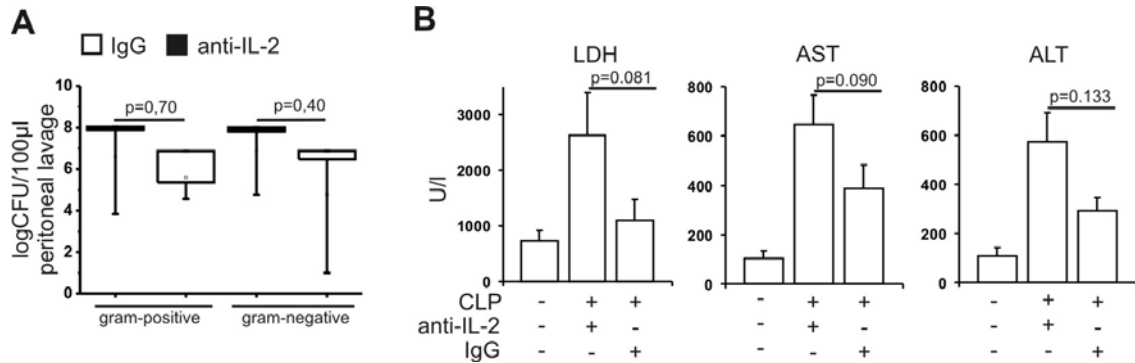


Figure 21: Bacterial clearance and end organ damage in anti-IL-2 and IgG-treated Tc-PPAR $\gamma^{-/-}$  mice. (A) Gram-negative and gram-positive bacterial load in peritoneum of mice. After sacrificing the mice, their peritonea were washed with 4 ml thioglycollate-G solution. Data shown are gram-positive and gram-negative bacteria colony forming units (CFU) in 100  $\mu$ l of peritoneal lavage fluid. (B) Serum activities of lactate dehydrogenase (LDH), alanine aminotransferase (ALT) and aspartate aminotransferase (AST) in mice subjected to CLP or sham. Data are means  $\pm$  SD.

If IL-2 receptor stimulation provokes Bcl-2 expression, this anti-apoptotic protein should be expressed less in anti-IL-2 treated mice. Bcl-2 mRNA (Figure 22A) and protein expression (Figure 22B) were diminished upon neutralizing IL-2 in Tc-PPAR $\gamma^{-/-}$  mice when compared to IgG-treated controls.

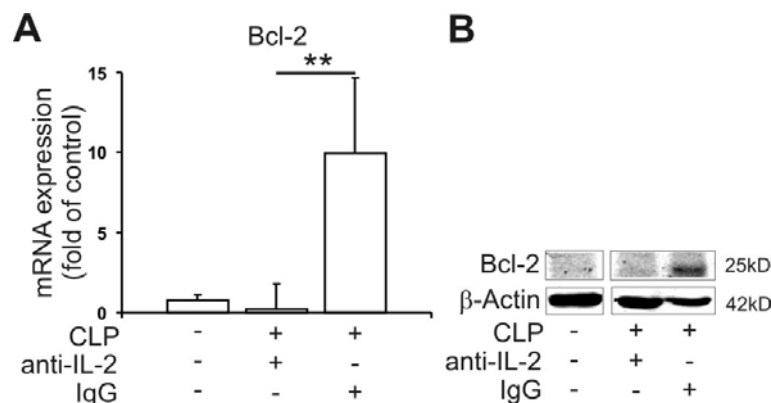


Figure 22: Bcl-2 mRNA and protein expression in anti-IL-2 and IgG-treated Tc-PPAR $\gamma^{-/-}$  mice. Mice received either 500  $\mu$ g anti-IL-2 or 500  $\mu$ g IgG control antibody (IgG) at 1 h after cecum ligation and puncture (CLP). Tc-PPAR $\gamma^{-/-}$  sham mice were used as controls. 24 h later, mice

were sacrificed, spleens were harvested and T-cells were isolated. Values are the means  $\pm$  SD. \*\* $p < 0.01$ . (A) Fold induction of Bcl-2 mRNA detected by real-time PCR and (B) Bcl-2 protein expression in T-cells detected by Western analysis.

### Modification of the PTEN/PI3K/Akt pathway

So far, I was able to confirm a PPAR $\gamma$ -dependent apoptosis that is initiated by reduced transcription of IL-2 by NFAT. However, there is another highly important molecular pathway that has a great impact on apoptosis with a so far unclear, but possible influence of PPAR $\gamma$ . This is the PI3K/Akt pathway, which modifies cell survival i.e. by regulation of pro-apoptotic Bim. Upstream of Akt, the tumor suppressor protein PTEN inhibits PI3K signaling by its lipid phosphatase activity, dephosphorylating phosphatidylinositol-triphosphate (PIP3), which impairs Akt phosphorylation (104-105). Phosphorylated Akt (pAkt) counteracts apoptosis and induces proliferation (106-107). A PPAR $\gamma$  responsive element was detected in the PTEN promoter region previously (105). Consequently, PPAR $\gamma$ -induced PTEN stalls cell division and causes cells to undergo programmed cell death. Therefore, I investigated PPAR $\gamma$ -dependent PTEN expression and downstream signaling in my experimental model of sepsis. PTEN expression was upregulated in septic T-cells from WT mice, whereas Tc-PPAR $\gamma$ <sup>-/-</sup> T-cells showed no induction (Figure 23A). Subsequently, PTEN activation inhibits the PI3K pathway thus, lowering Akt phosphorylation (pAkt) after CLP in WT T-cells. Knockout of PPAR $\gamma$  abolished this effect and increased Akt phosphorylation (Figure 23B).

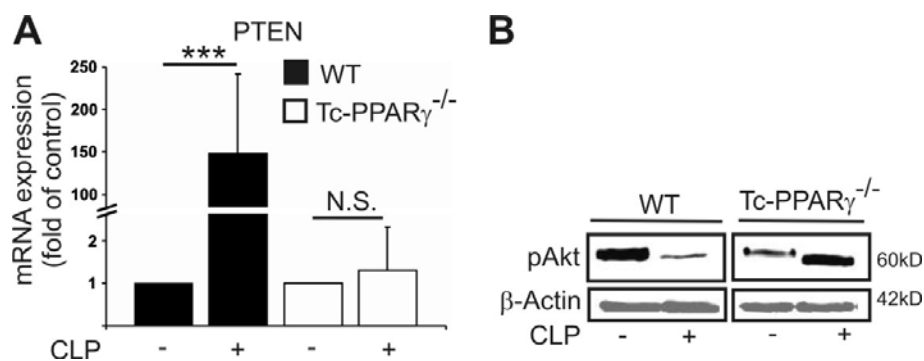


Figure 23: PTEN and pAkt expression in WT and Tc-PPAR $\gamma$ <sup>-/-</sup> mice. Mice were sacrificed after 24 h following CLP or sham surgery. (A) PTEN mRNA expression detected in T-cells of WT and



Tc-PPAR $\gamma$ <sup>-/-</sup> mice after CLP with real-time PCR. Values are the means  $\pm$  SD. \*\*\* $p$ <0.001. N.S., not significant. (B) Western analysis of phosphorylated Akt (pAkt) in WT vs. Tc-PPAR $\gamma$ <sup>-/-</sup> mice.

One major target gene that is expressed following an inhibition of the PI3K/Akt pathway is the pro-apoptotic BH3-only protein Bim. Bim activation and apoptosis induction in T-cells is established and considered as one of the most critical pathogenic mechanisms in sepsis (88, 108-109). In line, the delivery of siRNA to Bim during sepsis resulted in an increased survival of mice, due to an inhibition of T-cell apoptosis (88). Having shown that PPAR $\gamma$  induces PTEN expression and inhibits downstream pAkt, therefore I proceeded my research with examining the expression of pro-apoptotic Bim in T-cells. I noticed that Bim protein and mRNA were induced in T-cells of WT mice, whereas its expression in Tc-PPAR $\gamma$ <sup>-/-</sup> T-cells was negligible (Figure 24). In the Bcl-2 family, the disequilibrium of pro-apoptotic and pro-survival proteins leads to the translocation of pro-apoptotic proteins, such as Bim, to the mitochondria, causing cytochrome c release, caspase 3 activation, and subsequent apoptosis induction.

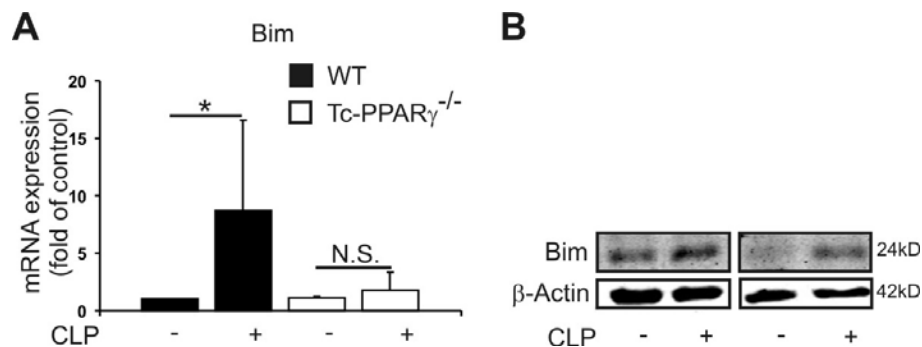


Figure 24: Bim mRNA and protein expression in WT and Tc-PPAR $\gamma$ <sup>-/-</sup> mice. Mice were sacrificed after 24 h following cecum ligation and puncture (CLP) or sham surgery. (A) Bim mRNA expression detected in T-cells of WT and Tc-PPAR $\gamma$ <sup>-/-</sup> mice after CLP with real-time PCR. Graphs show mean values  $\pm$  SD. \* $p$ <0.05. (B) Western analysis of Bim in WT vs. Tc-PPAR $\gamma$ <sup>-/-</sup>.

Previously IL-2 receptor stimulation was shown to activate the PI3K/Akt pathway (110). In line, in my experiments using the IL-2 neutralizing antibody, less IL-2 receptors stimulation should reduce PI3K/Akt signaling and provoke higher Bim expression. As hypothesized, neutralizing IL-2 in Tc-PPAR $\gamma$ <sup>-/-</sup> increased Bim mRNA as well as protein expression after CLP (Figure 25).

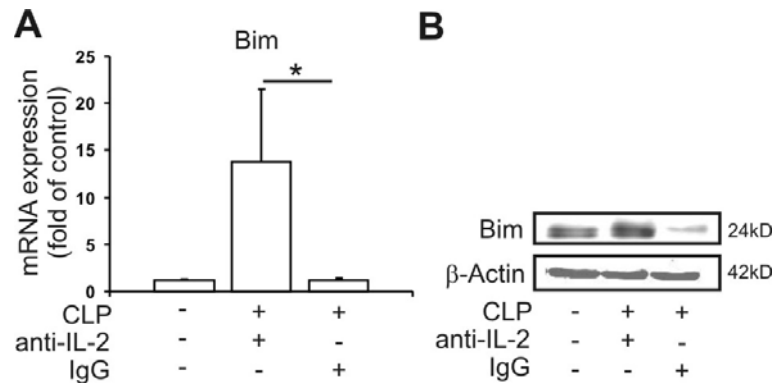


Figure 25: Bim expression on mRNA and protein level in anti-IL-2 and IgG-treated Tc-PPAR $\gamma$ <sup>-/-</sup> mice. Mice received either 500  $\mu$ g anti-IL-2 or 500  $\mu$ g IgG at 1 h after CLP. Tc-PPAR $\gamma$ <sup>-/-</sup> sham mice were used as controls. (A) Fold Bim expression at mRNA level compared to sham control and (B) protein expression in T-cells following anti-IL-2 treatment. Graphs show mean values  $\pm$  SD. \* $p$ <0.05.

This result proposes that the IL-2 receptor mediated modification of the PI3K pathway might be of high importance and that the regulation via PTEN is only secondary. To analyze this proposal further studies need to be performed which are outlined in the outlook of this thesis.

### 5.5. Therapeutical use of PPAR $\gamma$ the antagonist GW9662

To assess the therapeutic potential of PPAR $\gamma$  inhibition, I administered the specific antagonist GW9662 to septic WT mice. Mice were treated with a concentration of 1 mg/kg GW9662 (111-112) to irreversibly inhibit PPAR $\gamma$  for up to 24 h. To determine the optimal timing regime, mice were treated after 1, 3 or 5 h following CLP (Figure 26A). This experimental setup is depicted in Figure 26A. Herein, the hypothetical PPAR $\gamma$  expression pattern (green line) is plotted in correlation to the T-cell count (red dotted line). Along this setup, administrating the antagonist too early, such as already 1 h after CLP might not be beneficial as PPAR $\gamma$  is not expressed in naïve, unstimulated T-cells (95). In contrast, administered too late (5 h after CLP), T-cell depletion might have already proceeded excessively. In preliminary studies the most prominent T-cell depletion was observed at 24 h after CLP (97). At this particular time point, the antagonist should be most effective in abrogating T-cell depletion.

Examining the results of treating mice with 1 mg/kg GW9662 at 1, 3, or 5 h following CLP, I discovered  $CD3^+$  T-cell counts in spleens of  $160 \pm 42$  cells/ $\mu$ g,  $238 \pm 20$  cells/ $\mu$ g or  $130 \pm 25$  cells/ $\mu$ g, respectively. Highest T-cell counts were accomplished upon treatment at 3 h after CLP. Treatment at 1 and 5 h post-CLP lowered T-cell counts to below DMSO-control levels (Figure 26B).

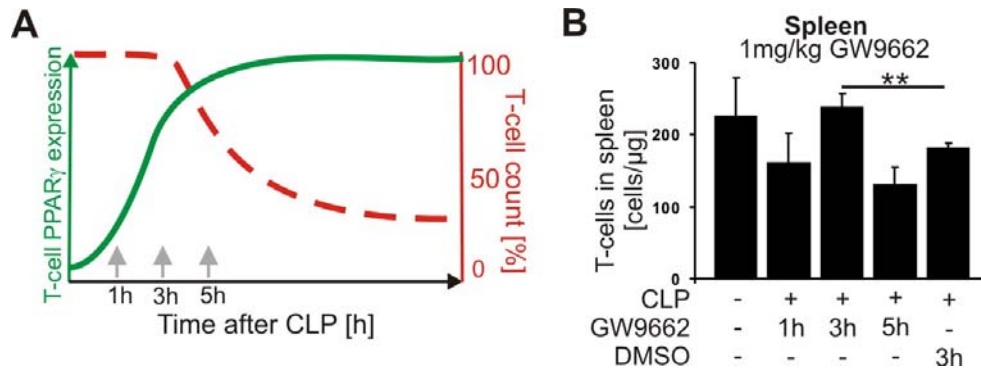


Figure 26: Correlation of T-cell count and T-cell PPAR $\gamma$  expression upon CLP and impact of GW9662 timing regime on T-cell count. (A) Hypothetical 24 h time-course of PPAR $\gamma$  expression in T-cells (green line) and T-cell count (red dashed line) during mouse polymicrobial sepsis. (B) WT mice were treated with 1 mg/kg GW9662 at 1, 3, or 5 h or with 50  $\mu$ l DMSO (10%) at 3 h or left untreated as controls. Absolute T-cell numbers in spleens and blood of WT mice after different treatments were analyzed by FACS analysis. Splenocytes were stained with anti-CD3 $\epsilon$  and co-stained using anti-CD45 and Nuclear ORANGE to detect living lymphocytes. Graphs show mean values  $\pm$  SD. \*\* $p < 0.01$ .

### 5.5.1. Absolute T-cell count

T-cells and subpopulations were further quantified in the group treated with GW9662 at 3 h post-CLP. Herein, I observed significantly higher absolute T-cells counts for  $CD3^+$  T-cells mirroring increased  $CD4^+$  and  $CD8^+$  subpopulations in spleen and blood compared to solvent (DMSO) control groups (Figure 27). In blood, T-cell populations even increased above sham levels, proposing proliferation, possibly due to higher IL-2 expression and increased emigration from lymphoid organs (Figure 27B).

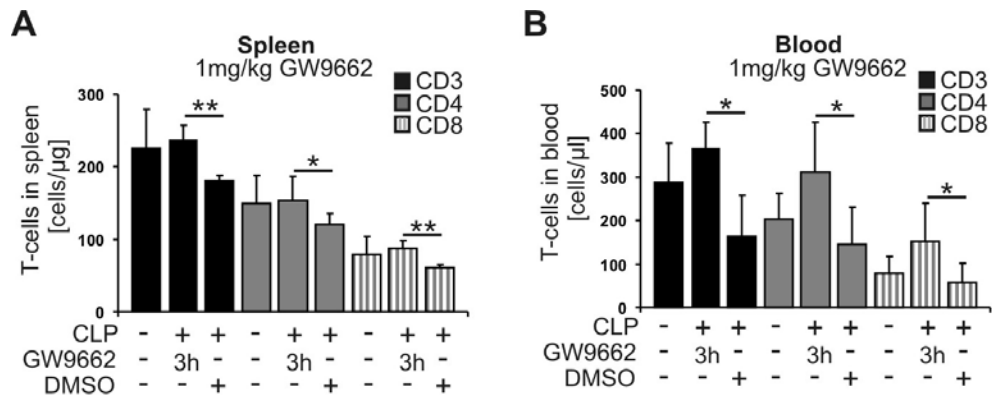


Figure 27: Absolute T-cell count in spleens and blood of WT mice treated with 1 mg/kg GW9662 at 3 h after CLP. WT mice were treated with 1 mg/kg GW9662 at 3 h or with 50  $\mu$ l DMSO (10%) at 3 h or left untreated as controls. (A) T-cell quantification in spleen and (B) blood. Cells were stained with anti-CD3 $\epsilon$ , anti-CD4, as well as anti-CD8a and co-stained using anti-CD45 and Nuclear ORANGE to detect living lymphocytes. Graphs show mean values  $\pm$  SD. \*  $p < 0.05$ ; \*\*  $p < 0.01$ .

To prove efficiency of 1 mg/kg GW9662 on T-cells at 24 h following CLP, I conducted an *in vivo* reporter assay. For this purpose, T-cells from GFP<sup>+/+</sup> mice were isolated and transduced with a lentivector expressing a fluorescent protein (mRuby) upon PPRE activation. By their green fluorescence, transduced GFP<sup>+/+</sup> T-cells can later easily be detected. Upon activation and binding of PPAR $\gamma$  to PPRE in GFP<sup>+/+</sup> T-cells, mRuby is expressed and can be visualized by flow cytometry. During sepsis, PPAR $\gamma$  expression promotes PPRE reporter activity. Figure 28A shows evaluation of PPRE reporter expression versus the T-cell count in GFP<sup>+/+</sup> T-cells depicted as FACS histogram. Reporter activity is increased upon CLP stimulation (green line) compared to sham control (blue line). When GW9662 is administered, the PPRE reporter activity is decreased (red line). Although the reporter construct is not specific for PPAR $\gamma$  and activated upon PPAR $\alpha$  or PPAR $\delta$  agonism as well, I was able to show that PPAR $\gamma$ -specific inhibition with the antagonist GW9662 significantly decreases reporter activation. The quantification of these experiments confirmed this result (Figure 28B). Therefore, when treated with 1 mg/kg GW9662, mice showed a significantly lower PPRE reporter activity in their T-cells compared to untreated or DMSO-treated controls thus, proving effectiveness of the inhibitory potential of GW9662 on PPAR $\gamma$  in T-cells for up to 24 h following CLP surgery.

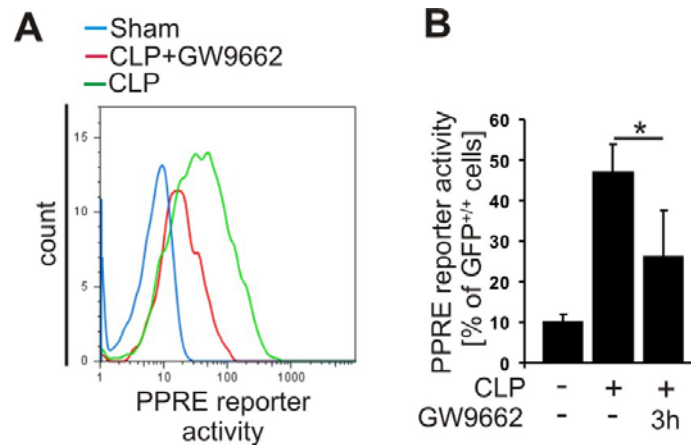


Figure 28: *In vivo* PPRE reporter activity in response to GW9662 stimulation in septic mice. Primary T-cells from GFP<sup>+/+</sup> mice (blood and spleen) were transduced with an mRuby expressing PPRE reporter construct. Subsequently, transduced GFP<sup>+/+</sup> cells were injected into WT mice. 36 h later, CLP was performed and mice were treated with or without 1 mg/kg GW9662 at 3 h after CLP. Sham operated mice were analyzed as controls. (A) Flow cytometric histogram as representative of four experiments performed and (B) bar graph resembling quantification of reporter activity in GFP<sup>+/+</sup> cells. Graphs show mean values  $\pm$  SD. \*  $p < 0.05$ .

### 5.5.2. Detection of T-cell apoptosis

An abrogated T-cell depletion has shown to correlate with less apoptosis of splenic T-cells in Tc-PPAR $\gamma$ <sup>-/-</sup> mice, as well as in IgG-treated mice compared to WT or anti-IL-2 treatment. In line, I provide evidence for increased apoptosis when mice were injected i.p. with DMSO (10%). In contrast, GW9662 application reduced apoptosis in WT mice when given at 3 h post CLP, as visualized by TUNEL assay and active caspase 3 staining (Figure 29).

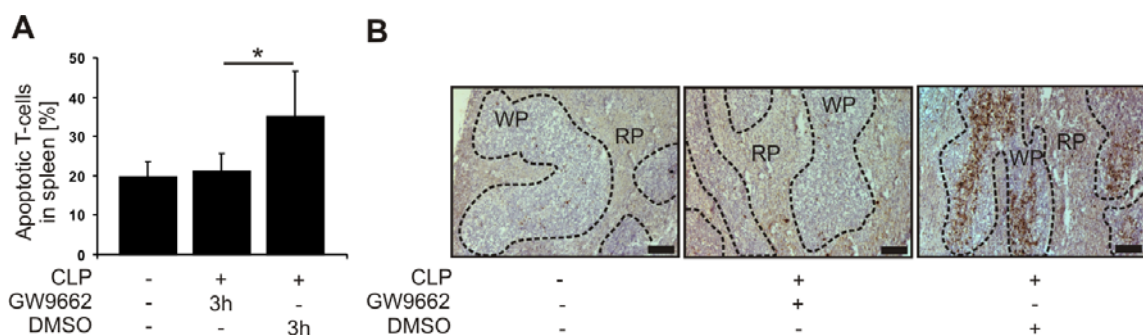


Figure 29: Detection of apoptosis via TUNEL assay and active caspase 3 staining upon GW9662 stimulation. (A) Quantification of apoptotic T-cells in spleens using anti-CD3 $\epsilon$  and TUNEL assay. Values are expressed as mean percentage  $\pm$  SD of apoptotic T-cells of total T-

cell amount in spleens. (B) Histological analysis of CLP-induced splenocyte apoptosis. Spleen sections were stained for active caspase 3 (brown) and counterstained with H&E. Dashed line surrounds T-cell-enriched white pulp (WP). RP, red pulp. Scale bars=100  $\mu\text{m}$ . \*  $p < 0.05$ .

Whether antagonism of PPAR $\gamma$  with GW9662 also affects survival similar to genetic depletion of PPAR $\gamma$  was assessed by survival studies performed for 7 days. GW9662 treatment significantly improved the survival rate to 75% at 7 d after CLP, compared to 8% survival in the solvent control group (Figure 30). This proved to be a statistically significant survival advantage at this time point. The survival rate upon PPAR $\gamma$  antagonism with GW9662 was even higher compared to survival of Tc-PPAR $\gamma^{-/-}$  mice, proposing an additional effect of GW9662 on other cells besides T-cells. This aspect will be further addressed in the discussion.

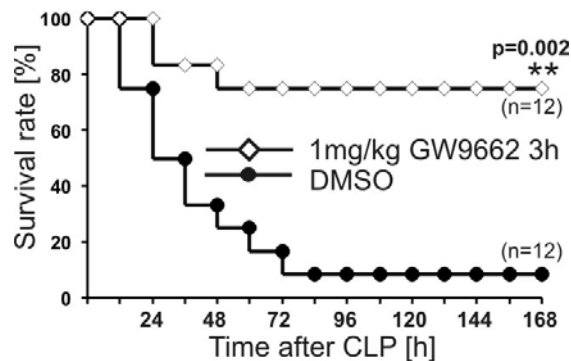


Figure 30: Comparison of survival of GW9662-treated and DMSO-treated WT mice. Mice received either 1 mg/kg GW9662 or 50  $\mu\text{l}$  DMSO (10%) at 3 h after CLP. Survival of mice was observed for 7d. \*\*  $p < 0.01$ .

If increased survival and higher T-cell counts again correlate to less bacterial load and less end organ damage, GW9662 treatment should reduce CFUs in the peritoneum and reduce organ damage markers in the serum of mice subjected to CLP. As seen in Figure 31A, results for bacterial load point to less bacteria, gram-positive as well as gram-negative, in the peritoneum of mice with GW9662 treatment compared to DMSO-treated mice. Furthermore, end organ

damage markers AST, ALT, and LDH were significantly less abundant upon GW9662 treatment compared to the solvent control group (Figure 31B).

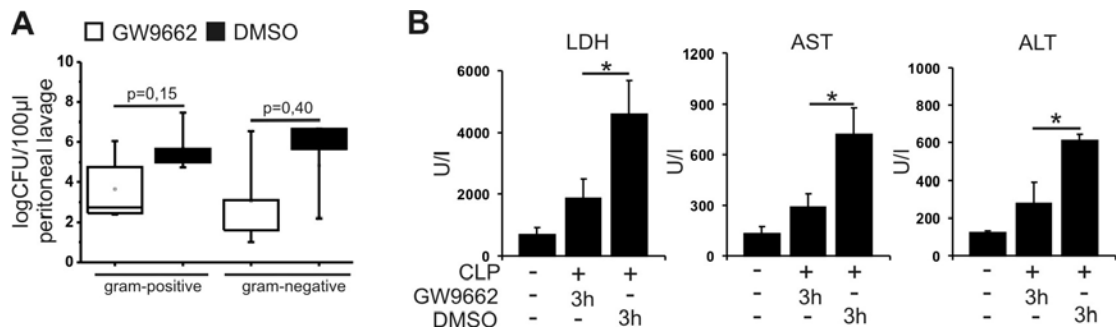


Figure 31: Bacterial clearance and end organ damage quantification in GW9662-treated mice. WT mice were subjected to CLP and treated with 1 mg/kg GW9662 or DMSO (10%) after 3h. (A) Bacterial load presented as colony forming units (CFU) of gram-positive or gram-negative bacteria in 100 µl of peritoneal lavage fluid. (B) Serum activities of lactate dehydrogenase (LDH), alanine aminotransferase (ALT), and aspartate aminotransferase (AST) in serum. \* $p < 0.05$ .

### 5.5.3. PPAR $\gamma$ -dependent apoptotic signaling during sepsis after GW9662

To verify whether the previously identified molecular mechanisms of PPAR $\gamma$ -dependent apoptosis were counteracted by GW9662, I investigated protein and mRNA expression of the previously discussed targets. Two possible apoptosis pathways were identified in the previous experiments in Tc-PPAR $\gamma$ <sup>-/-</sup> mice. The first one is based on increased IL-2 expression and downstream pro-survival signaling when PPAR $\gamma$  is genetically ablated. Upon PPAR $\gamma$  antagonism with GW9662, IL-2 as well as Bcl-2 mRNA expressions were significantly increased. In addition, I identified PPAR $\gamma$  to provoke PTEN expression in WT mice counteracting pro-survival PI3K/Akt signaling with increased Bim expression. GW9662 promotes, similar to Tc-PPAR $\gamma$ <sup>-/-</sup>, reduced PTEN and subsequent lower Bim expression in WT T-cells (Figure 32).

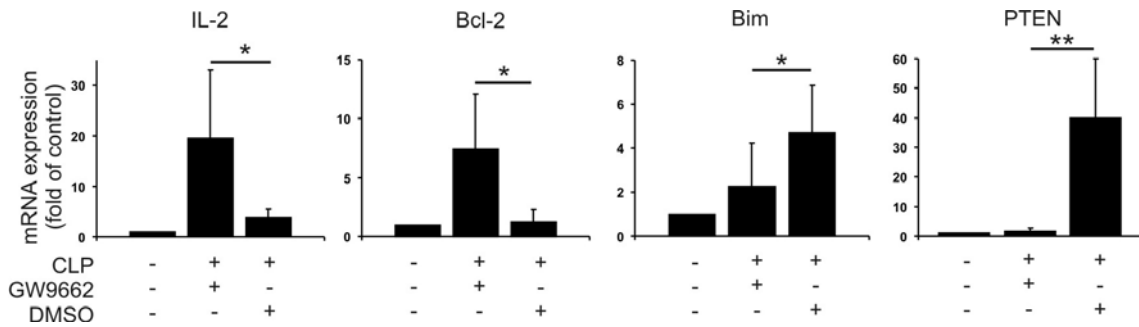


Figure 32: Pro- and anti-apoptotic signaling on mRNA level in WT mice treated with GW9662 or DMSO. WT mice were treated with either 1 mg/kg GW9662 at 3 h, with 50  $\mu$ l DMSO at 3 h or left untreated subsequent to CLP. Mice were sacrificed 24 h following CLP or sham surgery. Spleens were dissected and T-cells were isolated. X-fold mRNA expression of anti-apoptotic IL-2 and Bcl-2, as well as pro-apoptotic Bim and PTEN in T-cells compared to sham control levels detected by real-time PCR. Data are means  $\pm$  SD. \* $p$ <0.05; \*\* $p$ <0.01.

Higher mRNA expression levels also provoked increased protein expression of Bcl-2 and Bim in septic GW9662-treated T-cells compared to WT T-cells (Figure 33A). This coincided with enhanced Akt phosphorylation (Figure 33A), which can be taken as an indicator for decreased PTEN activity. Similar to genetic ablation of PPAR $\gamma$ , GW9662 enhanced NFAT binding to its responsive element in the IL-2 promoter thus, provoking increased IL-2 mRNA (Figure 33B). Enhanced NFAT binding correlated with increased intracellular IL-2 levels (Figure 33C).

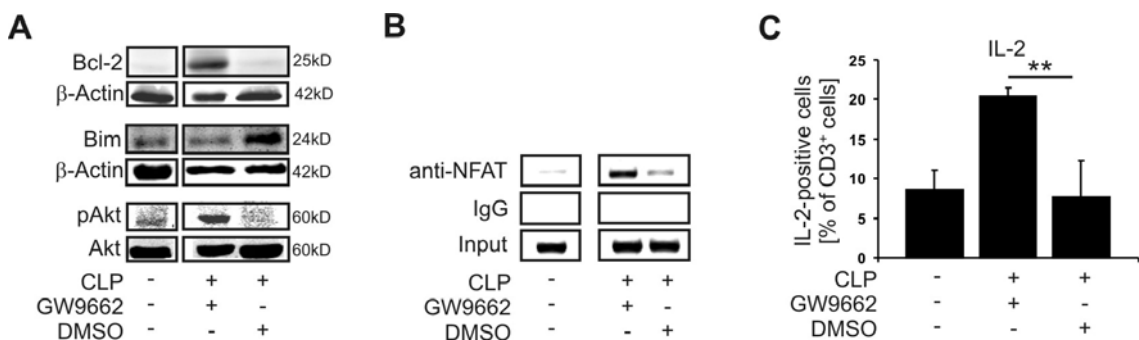


Figure 33: Analysis of apoptosis pathways upon GW9662 or DMSO treatment. WT mice were treated with either 1 mg/kg GW9662 at 3 h, with 50  $\mu$ l DMSO at 3 h or left untreated subsequent to CLP. Mice were sacrificed 24 h following CLP or sham surgery. Spleens were dissected and T-cells were isolated. (A) Western analysis of Bcl-2, Bim, and phosphorylated Akt (pAkt) in T-cells. (B) Association of NFAT with its response element within the IL-2 promoter analyzed by ChIP analysis. (C) Intracellular IL-2 protein amount in T-cells. Cell populations shown are gated



on living, CD45<sup>+</sup>, CD3ε<sup>+</sup> cells and percentage numbers indicate IL-2-expressing T-cells. Data are means ± SD. \*\*p<0.01.

#### 5.5.4. Exploring the therapeutic window of GW9662 medication

As announced previously, the dosing of 1 mg/kg GW9662 did not improve T-cell depletion after 5 h following CLP. Therefore, I questioned whether higher dosing (3 mg/kg) applied 5 h after CLP might improve T-cell counts and possibly also survival. This experimental setup abrogated CD3<sup>+</sup> T-cell depletion. Investigating T-cell subpopulations, I recognized that CD4<sup>+</sup> T-cell counts were decreased, whereas the amount of CD8<sup>+</sup> T-cells was increased (Figure 34).

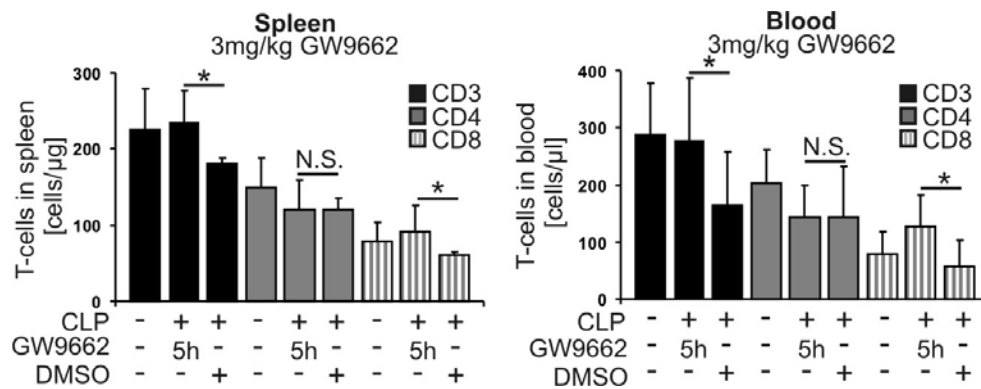


Figure 34: Absolute T-cell count in WT mice treated with 3 mg/kg GW9662 or DMSO at 5 h after CLP. (A) T-cell quantification in spleens and blood of untreated WT mice, with 3 mg/kg GW9662 or with DMSO treatment at 5 h after CLP. Cells were stained with anti-CD3ε, anti-CD4, as well as anti-CD8a and co-stained using anti-CD45 and Nuclear ORANGE to detect living lymphocytes. Data are means ± SD. \*p<0.05. N.S., not significant.

So far, an abrogation of all T-cell populations accounted for increased survival. However, the resulting subpopulation-devided T-cell counts upon treatment with 3 mg/kg GW9662 at 5 h after CLP are very heterogeneous thus no survival rate can be predicted. When performing survival studies for 7 days with this experimental setup I will be able to identify which T-cell type is essential for survival. Considering this treatment regime results in a significantly better survival compared to controls, the depletion of CD4<sup>+</sup> cells is unimportant and surviving CD8<sup>+</sup> T-cells are responsible for pro-survival effects. On the contrary, if mice do not show improved survival with low CD4<sup>+</sup> cell counts and high CD8<sup>+</sup>

counts, the depleted  $CD4^+$  T-cell population would have been important for survival.

The result of this experiment demonstrates that animals treated at 5 h post CLP with 3 mg/kg GW9662 had only minor, at 7 days post-CLP not statistically significant survival advantages of 42% vs. 8% (Figure 35). Thus, my experiment indicates that  $CD4^+$  T-cells contribute to sepsis-related immunodeficiency and thereby reduce survival of the septic host.

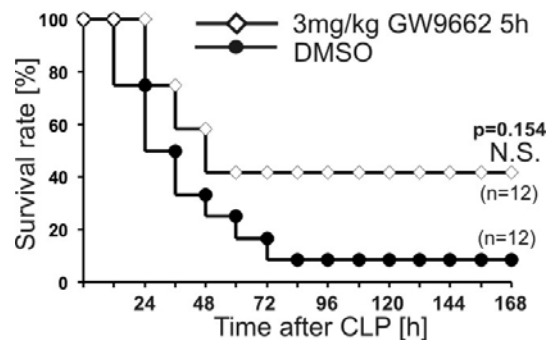


Figure 35: Comparison of survival of GW9662-treated and DMSO-treated Tc-PPAR $\gamma^{-/-}$  mice. Mice received either 3 mg/kg GW9662 or DMSO (10%) at 5 h after CLP. Survival of mice was observed for 7d. N.S., not significant.

In summary, pharmacological antagonism of PPAR $\gamma$  with 1 mg/kg GW9662 given at 3 h after CLP abrogated T-cell depletion and significantly improved survival of WT mice. At a concentration of 3 mg/kg applied at 5 h after CLP, GW9662 failed to improve survival, probably due to decreased  $CD4^+$  T-cell numbers.

## 6. DISCUSSION

The present thesis proposes inhibition of PPAR $\gamma$  as a potential target to achieve protection against the deleterious consequences of T-cell death during sepsis. In the following, the underlying investigation will be discussed and analyzed in a context of problems and findings of current sepsis therapy. Furthermore, the role of T-cell depletion during sepsis, the identified apoptosis pathways, systemic effects of GW9662 application, and the use of the different sepsis models are surveyed. Finally, the consequences of my findings for current sepsis treatment will be discussed.

### 6.1. Problems in current sepsis therapy

Septic patients represent an inhomogenous group, since the individual's immune response can be modulated by a variety of factors, such as the nature of the infectious stimuli, the host genetic makeup (i.e. predisposition to inflammation), comorbidities, and exogenous factors (e.g. medication, blood transfusion, etc.). This heterogeneity makes it difficult for physicians and scientists to design effective therapies. Some patients may need suppression of the first inflammatory response, but most of the patients survive this initial attack of sepsis, and may need therapies that improve their immune system and restore their ability to fight the infection. Despite the development of novel therapeutic entities, eradication of the septic focus, early administration of antibiotics and stabilization of cardiovascular functionality still remains the most effective causal and supportive therapy to treat patients with severe sepsis or septic shock (113). Marginal improvements in survival have recently been observed using adjunctive approaches such as extracorporeal removal of endotoxins (114) or early therapy with activated protein C (115).

The therapeutical treatment regime using PPAR $\gamma$  antagonists proposed in this thesis might represent a novel approach, targeting the deleterious consequences of the second, hypo-inflammatory phase. Thereby, in contrast to

previous investigations, a rescue therapy might be developed that could be applied after the onset of sepsis. Therapies targeting the first, hyper-inflammatory phase on the contrary, have to be given in advance to sepsis, which is mostly difficult to predict.

## **6.2. T-cell apoptosis during sepsis**

During sepsis, the immune response is characterized by changes in circulating lymphocytes. For a long time, it was unclear whether the decrease in the number of lymphocytes in septic patients is due to apoptosis, recruitment from the circulation to the peripheral tissues, changes due to transfusion of blood products, or hemodilution from large crystalloid infusions. Based upon published literature (77, 116-117) and my own data, we proved that the decrease is largely due to apoptosis. Decreases in lymphocyte numbers are thought to contribute to the immunosuppression observed during sepsis and increased susceptibility to infections (118). In my experiments, the control groups (WT mice and DMSO-treated mice), without genetical or pharmacological PPAR $\gamma$  depletion, exhibited a high T-cell apoptosis, which was accompanied by a low survival rate. When inhibiting this deleterious T-cell apoptosis by genetical or pharmacological antagonism of PPAR $\gamma$ , mouse survival was increased.

Currently, the thought is that apoptotic cell death and handling of apoptotic cells by the innate immune system provides a mechanism whereby self-tolerance is maintained by deletion or active immune regulation. Further, exposure of the immune system to a large number of apoptotic cells can induce suppression of immunity. Along with eliciting a compromised immune state, T-cell apoptosis might also induce alterations in other immune cells. Previous publications revealed that uptake of apoptotic cells by phagocytes promotes an immunosuppressive environment that induces anergy and avoids inflammatory responses to pathogens (119). The presence of apoptotic cells during macrophage activation has been shown to increase their secretion of IL-10 and TGF $\beta$  (M2 phenotype) while decreasing the secretion of TNF $\alpha$ , IL-1 and IL-12 (M1 phenotype) (120-121). This shift of pro- to anti-inflammatory cytokines in

response to pathogen contact further impairs the host's response to infection. Transfer of apoptotic splenocytes to animals undergoing CLP resulted in decreased survival compared to untreated animals. Interestingly, in the same studies, transfer of necrotic cells was associated with higher levels of IFN $\gamma$  production by splenocytes and improved survival following CLP (122). Therefore, apoptotic cells and their phagocytosis further promote an immuneparalysed state and reduce the clearance of invading pathogens.

Furthermore, suppression is induced by the induction of immune deviation (e.g. Th1-Th2 shift) and the activation of CD8 $^+$  T $_{regs}$  (123). Therefore, reduced apoptosis might cause an immune stimulation, enhance antimicrobial defenses and limit organ damage.

In my experiments, I discovered CD4 $^+$  cells to be necessary for survival of sepsis. When GW9662 was applied at 5 h after CLP, CD8 $^+$  but not CD4 $^+$  cells survived. This CD4 $^+$  cell-depleted state resulted in a survival rate, which was similar to survival of control mice. This special role of CD4 $^+$  cells has also been discussed in literature previously. Martignoni et al. proposed that CD4 $^+$  T-cells are unexpectedly active in the initial immune response to polymicrobial sepsis such that they promote early bacterial clearance, possibly by influencing neutrophils in an IFN $\gamma$ -dependent manner. A lack of CD4 $^+$  cells is associated with increased IL-6 concentrations, increased bacteremia, and decreased neutrophil activity. Surprisingly, the lack of CD4 $^+$  cells altered survival within the first 30 h of sepsis. Traditionally, T-cells contribute to an effective defense against extracellular bacteria during infections after 48 to 96 h. However, there is emerging evidence that lymphocytes play an early role during acute injuries. This implicates memory CD4 $^+$  T-cells, which can respond to antigens within an acute time frame to be of high importance. In my experiments inducing sepsis, I used the CLP sepsis model. In the CLP model the bacteria released are endogenous and originate from the gut. Herein, it is likely that peritoneal memory CD4 $^+$  cells may be antigenic toward the bacteria released by CLP. If this is the case it is probable they are of a Th1 phenotype. Memory Th1 cells can rapidly secrete IFN $\gamma$  upon recognition of the processed bacterial antigen. IFN $\gamma$  has been reported to activate phagocytes and increase the ability to clear

bacteria (124). During the first 18 h of sepsis, T-cells in the mouse peritoneum secrete  $\text{IFN}\gamma$  or mediators that increase neutrophil  $\text{IFN}\gamma$  production (118).

Recently Lawrence et al. investigated the question why especially  $\text{CD4}^+$  T-cells are dying. They proposed that a lower  $\text{CD4}^+$  ATP content is associated with apoptosis and worsens the clinical outcome of sepsis. They speculate that this lower  $\text{CD4}^+$  ATP content may be due to mitochondrial dysfunction, or to anergy of the lymphocytes to mitogen stimulation. Or it may simply represent another form of organ dysfunction, described as lymphocyte bioenergetic failure in the setting of sepsis (125).

### 6.3. Apoptosis pathways during sepsis modified by $\text{PPAR}\gamma$

I refer to two pro-apoptotic pathways that are highly active during sepsis and are induced upon  $\text{PPAR}\gamma$  activation *in vivo*. The first one proposes limited pro-survival IL-2 signaling during sepsis in activated T-cells. IL-2 is known to activate pathways that lead to proliferation, survival and cytokine production of effector T-cells. IL-2 expression is controlled almost entirely at the transcriptional level. The IL-2 promoter region contains defined binding sites for many inducible transcription factors, such as NFAT,  $\text{NF}\kappa\text{B}$ , AP-1, and CREB (94).  $\text{PPAR}\gamma$  has been shown to suppress IL-2 expression by ligating these important transcription factors (transrepression) (60, 126).

The transcription factor NFAT is in large part responsible for IL-2 transcription. This protein is not the limiting factor for IL-2 starvation during sepsis, which can be explained by its regulation. NFAT is regulated by  $\text{Ca}^{2+}$  and the  $\text{Ca}^{2+}$ /calmodulin-dependent serine phosphatase calcineurin. NFAT protein is phosphorylated and resides in the cytoplasm in resting cells. Upon stimulation, it is dephosphorylated by calcineurin, translocates into the nucleus, and becomes transcriptionally active, thus providing a direct link between intracellular  $\text{Ca}^{2+}$  signaling and gene expression. In activated cells, such as in septic T-cells, it was shown that calcineurin is present in the nucleus of stimulated cells, where it maintains the dephosphorylated status and nuclear localization of NFAT. When  $\text{Ca}^{2+}$  entry is prevented or calcineurin activity is

inhibited, NFAT is rephosphorylated by NFAT kinases and rapidly leaves the nucleus, and NFAT-dependent gene expression of IL-2 is terminated (127). During sepsis, NFAT is located in the nucleus and is there bound to PPAR $\gamma$  and thus not able to promote transcription of IL-2.

IL-2 withdrawal provokes activation of the intrinsic, mitochondrial apoptosis pathway. This so called cytokine withdrawal apoptosis dramatically reduces the expanded T-effector population and is principally regulated by pro- and anti-apoptotic members of the Bcl-2 family. In healthy organisms on the contrary, autocrine IL-2-receptor stimulation initiates intracellular anti-apoptotic signaling pathways, including anti-apoptotic Bcl-2 expression. Tc-PPAR $\gamma$ <sup>-/-</sup> T-cells are protected from apoptosis due to high IL-2 expression levels. These observations were corroborated by my experiments neutralizing IL-2 during peritonitis, which in turn provoked T-cell apoptosis and impaired septic outcome.

Previous reports showed that over-expression of the IL-2-receptor downstream target Bcl-2 improves T-cell survival (80). In 2009 Weber et al. performed a study with patients with early stage severe sepsis, unravelling their expression profile for pro- and anti-apoptotic members of the Bcl-2 family of proteins. They found a similar expression pattern compared to the results described in my thesis. Gene expression of pro-apoptotic Bcl-2 family members Bim, Bad and Bak were induced and a downregulation of the anti-apoptotic Bcl-2 and Bcl-xl proteins was observed in peripheral blood. They also proposed that this constellation affects cellular susceptibility to apoptosis and complex immune dysfunction in sepsis, however, they did not advise a possible target to limit these effects, as it is anticipated in this work by PPAR $\gamma$  (128).

In line with these observations, my work provides evidence for Bcl-2 upregulation on mRNA and protein level. Bcl-2 functions to suppress apoptosis in a variety of cell systems. It is localized in the endoplasmic reticulum, nuclear envelope, and outer mitochondrial membranes. Several mechanisms have been proposed to explain the anti-apoptotic function of Bcl-2. It acts as a regulator of Ca<sup>2+</sup> homeostasis or as an antioxidant. Bcl-2 forms heterodimers with the pro-apoptotic protein Bax and might thereby neutralize its death effector properties. Bcl-2 prevents the release of potent mitochondrial activators

of caspases. The association of Bcl-2 with the mitochondrial apoptosis-activating factor Apaf1 and the blockade of cytochrome c release may inhibit the activation of caspase 9 and 3. Bcl-2 also acts by modulating collapse of the mitochondrial transmembrane potential that occurs during apoptosis (129). Further, Bcl-2 protects against apoptosis by binding to and neutralizing pro-apoptotic Bcl-2 family members such as Bim, Puma, and Noxa (88). It can prevent apoptotic cell death from a wide array of adverse stimuli, including hypoxia, serum and growth factor withdrawal, glucocorticoids, and ionizing irradiation, among others (28). In Figure 36 the proposed pro-apoptotic pathway, described by activated PPAR $\gamma$  ligating NFAT, IL-2 withdrawal and reduced Bcl-2 expression is summarized.

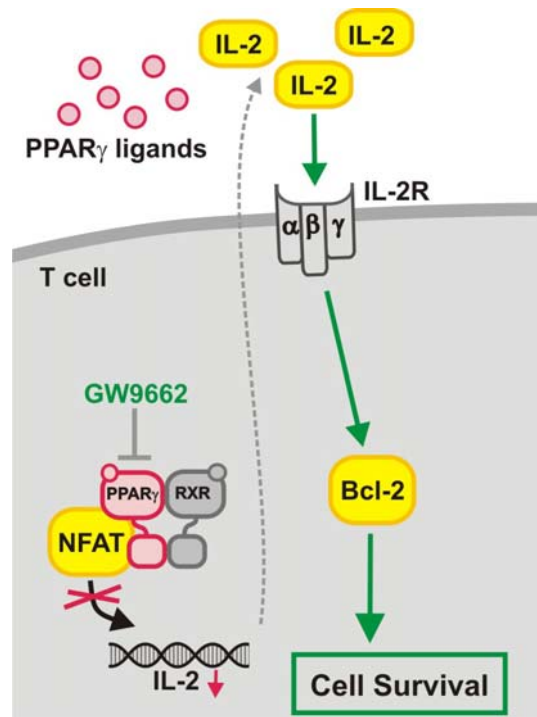


Figure 36: PPAR $\gamma$  binding to NFAT reduces pro-survival IL-2 transcription. Ligand-activated PPAR $\gamma$  transrepresses NFAT by direct ligation thus, preventing NFAT-dependent IL-2 transcription. Pro-survival autocrine IL-2 signaling via the IL-2 receptor (IL-2R) is reduced and subsequently pro-survival Bcl-2 expression is repressed. PPAR $\gamma$  antagonism with GW9662 promotes IL-2 expression and pro-survival Bcl-2 signaling.



The PI3K pathway is one of the major signaling pathways activated upon TCR, IL-2 receptor, and CD28 stimulation, leading to T-cell activation, proliferation, and cell survival. Activation of the pathway is negatively regulated by PTEN, a phosphatidylinositol-phosphatase that is transcriptionally regulated by PPAR $\gamma$ . Several mouse models deficient for the molecules involved in PI3K signaling suggest that impairment of PI3K downstream signals leads to dysregulation of immune responses, and in some cases, autoimmunity (110, 130).

PTEN was originally identified as a tumor suppressor because of its high frequency mutations in various types of tumors. PTEN is regulated on transcriptional level, i.e. by PPAR $\gamma$ , as well as on posttranslational level by phosphorylation. The pro-apoptotic property of PTEN is mainly dependent on its lipid phosphatase activity, which antagonizes the PI3K pathway and inhibits cell survival. PTEN dephosphorylates PIP3 to phosphatidylinositol-diphosphate (PIP2), and consequently reduces Akt phosphorylation (131). Phosphorylated Akt promotes cell survival by phosphorylating its substrates, including the Forkhead transcription factor 3a (FOXO3a). While FOXO3a is phosphorylated by Akt, it will be retained in the cytoplasm. However, is Akt not phosphorylating FOXO3a, during e.g. PTEN-dependent inhibition of the PI3K-pathway, dephosphorylated FOXO3a translocates to the nucleus and induces target gene expression, i.e. for the pro-apoptotic proteins Bim and Fas ligand. Upregulation of Bim in turn promotes cytochrome c release from the mitochondria and caspase-dependent apoptosis (131). Expression of PTEN in activated CD4<sup>+</sup> T-cells inhibits IL-2-dependent proliferation, confirming PTEN as a negative regulator of IL-2 receptor signaling (132). By its effect on PTEN, PPAR $\gamma$  might therefore induce the pro-apoptotic target gene Bim and induce T-cell depletion.

How Bim promotes apoptosis has been the subject of some debate. Bim has been first shown to interact with pro-survival Bcl-2 which has been suggested to be the key ability of Bim to induce apoptosis. However, alternatively it was shown that Bim can bind directly to the pro-apoptotic Bax and Bak proteins to initiate apoptosis. A recent study finally puts this debate to rest and proved Bim to interact with pro-survival Bcl-2, thereby releasing Bax or Bak proteins to promote apoptosis (133). Bim is the most extensively studied pro-apoptotic

Bcl-2 family member and is required for cell death subsequent to cytokine withdrawal, death of autoreactive T-cells and for termination of acute T-cell responses in viral infections. In 2008, the group of Hotchkiss and colleagues showed that Bim knockout mice have nearly complete protection against sepsis-induced lymphocyte apoptosis. They confirmed these experiments by using Bim siRNA which also protected lymphocyte apoptosis and exhibited a better survival of septic mice (88). Bim activation and apoptosis induction in T-cells is considered as one of the most critical pathogenic mechanisms in sepsis (88, 108-109).

In this regard, Williams et al. also suggested that stimulation of the PI3K pathway may be an effective approach for preventing or treating sepsis and/or septic shock (134). In an experimental model of sepsis, this pathway was further confirmed showing that overexpression of pAkt in lymphocytes decreased lymphocyte apoptosis and improved survival during sepsis (135). In my work, I found PPAR $\gamma$ -dependent PTEN expression to reduce phosphorylation of Akt and to induce Bim expression thus, promoting apoptosis (Figure 37).

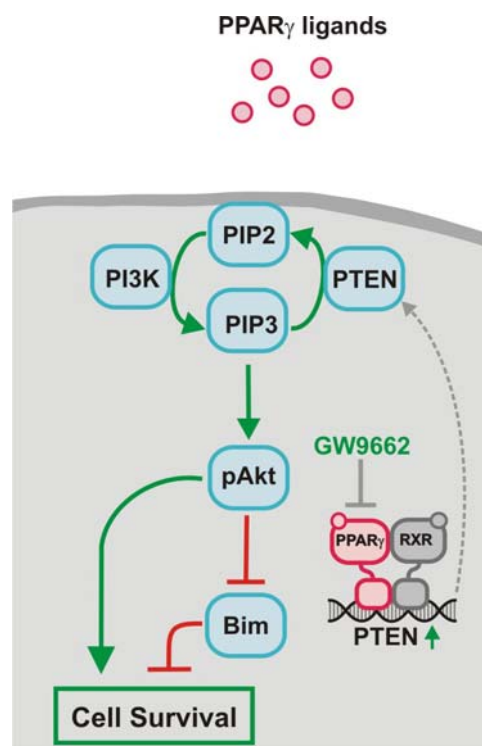


Figure 37: PPAR $\gamma$ -induced PTEN expression promotes pro-apoptotic signaling. Ligand-dependent activation of PPAR $\gamma$  promotes PTEN expression thus, reversing the phosphoinositol-3 kinase (PI3K) dependent phosphatidylinositol-diphosphate (PIP2) to phosphatidylinositol-triphosphate (PIP3) phosphorylation. Akt remains in its unphosphorylated state and promotes Bim expression. If GW9662 is applied, PTEN expression is ablated, PI3K signaling is maintained and phosphorylated Akt (pAkt) prevents pro-apoptotic Bim expression.

Hoogerwerf et al. performed a gene profiling of apoptosis regulators in highly purified monocytes, granulocytes and CD4<sup>+</sup> T-cells. Anti-apoptotic profiles were found in monocytes and granulocytes, while CD4<sup>+</sup> T-cells displayed a foremost pro-apoptotic mRNA profile. In detail, CD4<sup>+</sup> T-cells presented increased expression of Bim, PMAIP1 and BNIP3L in addition to an increased Bax mRNA expression. Furthermore, they discovered no signs of activation of the death receptor pathway, since no alterations were found in death receptor TNFRSF21 expression. Moreover, cFLIP, an inhibitor of death receptor signaling, appeared to be upregulated in CD4<sup>+</sup> lymphocytes (136). However, sepsis is an extremely complex disorder involving activation of numerous intersecting cascades, including pro-inflammatory, anti-inflammatory, coagulation and complement system (76). Thus, it is not surprising that multiple pathways of cell death may be involved in sepsis. Furthermore, different bacteria, such as released by CLP, possess different toxins that may activate unique cell death programs.

#### **6.4. Systemic effects of PPAR $\gamma$ antagonism with GW9662**

GW9662 irreversibly inhibits PPAR $\gamma$  with minor effects on other PPARs (45). To verify GW9662 as therapeutic drug to improve sepsis therapy, its action not only on T-cells needs to be clarified. PPAR $\gamma$  expression patterns during sepsis and possible consequences of inhibition of PPAR $\gamma$  with GW9662 must be taken into consideration.

PPAR $\gamma$  is differentially expressed and exerts diverse action on immune cells during sepsis. In macrophages, PPAR $\gamma$  has been shown to favor an anti-inflammatory phenotype (M2 phenotype) (38), which is characterized by attenuated production of pro-inflammatory mediators, but enhanced secretion of anti-inflammatory ones, such as IL-10, TGF $\beta$ , and PGE<sub>2</sub>. This limits defense

against pathogens thus, when PPAR $\gamma$  is inhibited by GW9662, a pro-inflammatory M1 phenotype might be favored and stimulates macrophages to secrete cytokines and improve pathogen clearance. However, it was recently shown that LPS treatment rapidly down-regulates PPAR $\gamma$  in macrophages after 6 to 15 h by miR-27b-dependent mRNA destabilization, followed by its up-regulation again at later time points (67). Early after the onset of sepsis, I suggest that GW9662 does not exert significant effects on macrophages.

By attenuating NF- $\kappa$ B transactivation, PPAR $\gamma$  inhibits cytokine expression of e.g. TNF $\alpha$  or IL-12 (137), the expression of vascular cell adhesion molecule-1 (VCAM-1) and intercellular adhesion molecule-1 (ICAM-1) (138). Preventing this action with GW9662, more leukocytes are able to enter the site of infection and promote pathogen elimination. Moreover, the expression of the inducible pro-inflammatory proteins, cyclooxygenase-2 (COX-2) (61), cytosolic phospholipase A2, and inducible nitric oxide synthase (iNOS) (139) are blocked (61, 139-141). An inhibition of this pro-inflammatory potential by GW9662 on the contrary might be rather harmful since reduced systemic pro-inflammatory effects might also reduce pathogen killing. *In vivo* studies showed that administration of the PPAR $\gamma$  agonist 15-deoxy- $\Delta^{12,14}$ -prostaglandin J<sub>2</sub> (15d-PGJ<sub>2</sub>) prior to polymicrobial sepsis reduces lung injury and neutrophil trafficking to lung and small intestine (142). 15d-PGJ<sub>2</sub> enhances PPAR $\gamma$  functions in the lung, decreases NF $\kappa$ B activity, and promotes expression of the cytoprotective heat shock protein 70 (HSP70) (143). In turn, the heat shock response is amplified and correlates well with improved lung injury. In this regard, GW9662 application might again be rather harmful, expecting worse lung injury. Agonist treatment might be more effective in this respect, but difficult to handle, since PPAR $\gamma$  agonists must be applied before the onset of sepsis.

The role of PPAR $\gamma$  in T-cells and the effects of GW9662 treatment on T-cell apoptosis were elucidated in detail in this work. There are some additional PPAR $\gamma$ -mediated effects on T-cells that were not taken into consideration in this work so far. PPAR $\gamma$  can inhibit expression of several T-cell cytokines upon activation, including the classical Th1-cell cytokine IFN $\gamma$  (144). Moreover, by reducing IL-12 production in dendritic cells, PPAR $\gamma$  reduces IFN $\gamma$  production by T-cells. This ability indicates that PPAR $\gamma$  might play a role during differentiation

of naïve T-cells into their effector subsets, favoring the anti-inflammatory Th2 cells. Conversely, it was shown that in the presence of IL-4, a cytokine important for the development of Th2 cells (145), monocytes can provide a potential PPAR $\gamma$ -specific ligand through upregulation of the 12/15 lipoxygenase (146). 13-HODE is produced and can be taken up by T-cells to activate PPAR $\gamma$  thus, further promoting a Th2 phenotype (146-147). These observations suggest that GW9662 stimulation reduces anti-inflammatory Th2 phenotype development and promotion of a pro-inflammatory Th1 phenotype that further activates M1 macrophages and indirectly boosts pathogen elimination.

A critical issue of this work was to determine the best time point of therapeutic antagonism of PPAR $\gamma$  with GW9662. Time kinetics revealed that administration of 1 mg/kg GW9662 3 h following CLP not only completely prevented T-cell depletion detected at 24 h post CLP, but increased T-cell counts to ~130% in blood. This effect might be achieved by increased IL-2 expression causing a limited apoptosis and an enhanced proliferation of T-cells. GW9662 administered too early might have no beneficial effect due to low PPAR $\gamma$  expression in T-cells at this time. Applying 3 mg/kg GW9662 at 5 h improved the CD3<sup>+</sup> cell count, but decreased CD4<sup>+</sup> cell numbers, which proved to be deleterious during sepsis, as this treatment regime resulted in low survival rates. Here, PPAR $\gamma$  antagonism might not be advantageous, because T-cell depletion has already proceeded excessively. Therefore, GW9662 is particularly advantageous early after the onset of sepsis, when PPAR $\gamma$  is highly expressed and T-cells have not yet depleted.

Furthermore, markers that define the immunological status of the patient, and that gives information about a possible susceptibility for GW9662 treatment, are highly needed and would be of clinical benefit.

## **6.5. Systemic inflammation vs. sepsis - LPS vs. CLP**

Besides sepsis, also systemic inflammatory conditions provoke T-cell apoptosis and are often developed after i.e. extracorporeal circulation as needed for cardiac bypass surgery (148). In my experiments I used LPS to induce systemic

inflammation. I demonstrated that Tc-PPAR $\gamma$ <sup>-/-</sup> mice exhibited significantly lower T-cell depletion compared to WT mice. Therefore, antagonizing PPAR $\gamma$  following extracorporeal circulation during cardiac surgery might be a promising option to improve immune responses in patients undergoing on-pump cardiac surgery.

During my experiments I decided to change the animal model. There were several arguments that supported my decision: experimentation involving single organisms or even their products, such as LPS, is useful to characterize response patterns and treatments directed against one particular microbe. But models of endotoxemia are of doubtful relevance to clinical sepsis, which is commonly polymicrobial, providing gram-negative and –positive organisms, as well as aerobic and anaerobic bacteria. Typically, an infection that leads to sepsis begins as a focus of microbes that becomes systemic. Mostly pathogens do not originate from the periphery *de novo*. During sepsis, the microbes infecting the patient often originate from the persons own flora, finding their way into wounds, gut perforation, or microbial translocation from the gut (93). Thus, I chose to perform the CLP model. As one of the most widely used models of sepsis and septic shock, the CLP model satisfies many of the criteria listed for an appropriate model: it is polymicrobial, has focal infection origins, produces septicemia, and releases bacterial products into the periphery. And it has the advantage that the microbes are of mixed “host origin” rather than being exogenously introduced. Induced sepsis severity ranges from acute and fatal to chronic and enables a wide range of experimentation (93).

Recent studies suggest immune dysfunction seen after the onset of polymicrobial sepsis, as produced by cecum ligation and puncture, is not caused by endotoxin alone, but may be caused by the combined effect of the necrotic tissue and other microbial components (149).

## **6.6. Possible consequences for sepsis treatment**

In my model, activation of PPAR $\gamma$  contributes to the induction of apoptosis via two important pathways, namely IL-2 repression and PTEN induction. I hypothesize that T-cells undergo apoptosis upon response to an intrinsic signal

and thereby limit self-harmful effects for the host. On the other hand, this effect consequently impairs the host's resistance to continuing infections and might cause or promote organ injury.

Sepsis represents a race to the death of the pathogen and the host immune cells and the pathogens try to find an advantage by inducing death in billions of immune effector cells. The majority of deaths in sepsis occur in the immunosuppressed phase. Simple and rapid tests to identify the immune status of the patient (hyper- vs. hypoinflammatory phase) are needed to guide the immunologic therapy. In this thesis, I propose PPAR $\gamma$  as therapeutic target to improve sepsis therapy, when applied at the hyper-inflammatory phase to prevent the deleterious hypo-inflammatory state. Although I identified a rather narrow time frame for beneficial treatment of septic mice with GW9662, I still believe that the possibility of giving PPAR $\gamma$  antagonists after the onset of sepsis represents a high rescue potential. This treatment regime is of special importance because it displays a method to treat septic patients after the onset of sepsis. Previous studies targeting the pro-inflammatory phase used inhibitors proposing a treatment before the onset of sepsis, which is often difficult to handle. Furthermore, in following experiments it needs to be investigated if a repeated application of antagonists or the application of reversible binding antagonists might broaden the therapeutic window. I do not believe that there is any possibility to improve sepsis pathophysiology with PPAR $\gamma$  antagonists at earlier time points, because activation of the adaptive immune system is needed for high PPAR $\gamma$  expression levels in T-cells. If the antagonist is given too early, no effect is seen at later time points either, probably due to interception of the antagonists by cells highly expressing PPAR $\gamma$  at this time. GW9662 binds irreversibly and is thus, not available for T-cells at later stages.

I hypothesize that in order to save patients with severe sepsis and septic shock from the vicious circle of secondary infection, chronic multiple organ failure, and death, it will be of high importance to concentrate on the underlying immune pathophysiology in the hypimmune phase (Figure 38). In the next steps, GW9662 treatment should be tested for its ability for widespread routine use.

Therefore, I suggest that my findings might open novel “therapeutic windows” in the treatment of sepsis by targeting two apoptosis pathways using only one blocking agent.

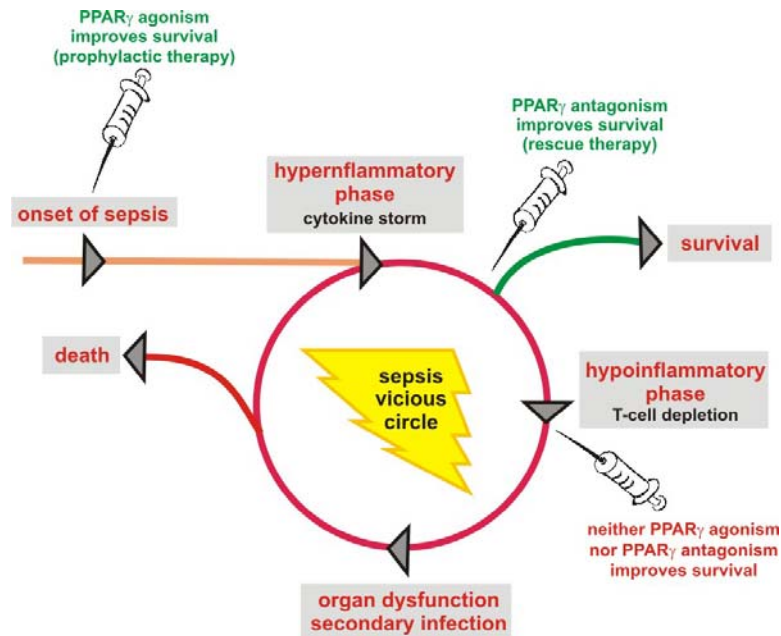


Figure 38: Therapeutical timing regime for treatment with PPAR $\gamma$  agonists and antagonists during the course of sepsis. Before or at the onset of sepsis, treatment with PPAR $\gamma$  agonists is beneficial, blocking the hyperinflammatory phase. During the hyperinflammatory phase, application with PPAR $\gamma$  antagonists improved survival. In the hyperinflammatory phase, neither PPAR $\gamma$  agonism nor its antagonism would be advantageous in preventing organ dysfunction, secondary infections and eventually death.

## 6.7. Outlook

### 6.7.1. The role of PTEN during sepsis progression

In this thesis, I provide evidence for increased expression of PTEN upon PPAR $\gamma$  activation in T-cells. If mice are treated with GW9662, PPAR $\gamma$  activation is inhibited and PTEN expression is decreased. Using GW9662, the subsequent PI3K/Akt signaling pathway is not suppressed anymore and promotes pro-survival signals. But the direct link between PTEN expression and the PI3K/Akt signaling is still missing. Possibly, inhibition of the PI3K/Akt pathway results



from diminished autocrine IL-2 receptor signaling. To analyze this alternative, a dominant negative PTEN construct, as well as a WT PTEN expressing construct will be lentivirally transduced into primary mouse T-cells. Transduced T-cells will be injected i.v. into WT mice and CLP will be performed. If my hypothesis of PTEN as crucial for apoptosis induction is true, cells overexpressing PTEN will have reduced pro-survival PI3K/Akt signaling and die by apoptosis. In contrast, T-cells carrying the dominant negative mutant of PTEN will have no reduction in PI3K/Akt pathway. This experimental setup should clarify the question whether the tumor suppressor PTEN, regulated by PPAR $\gamma$ , plays an important role during sepsis-induced T-cell depletion. PTEN might then represent another target, besides PPAR $\gamma$ , to reduce T-cell apoptosis and to improve the immune suppressed status of septic patients.

### **6.7.2. Impact of GW9662 on T-cells from septic patients**

In my experiments I proved efficacy of the specific PPAR $\gamma$  antagonist GW9662 in an animal model of sepsis. However, it remains unclear whether GW9662 promotes the same effects in human T-cells. Therefore, I propose that T-cells from septic patients should be isolated and treated with GW9662. In previous experiments with T-cells from septic patients, stimulation with PPAR $\gamma$  agonists, such as rosiglitazone, resulted in apoptosis. Further, PPAR $\gamma$  ligands were identified in serum of patients blood (89), suggesting active PPAR $\gamma$  to promote apoptosis of T-cells during sepsis in humans. To confirm my hypothesis of PPAR $\gamma$ -induced T-cell apoptosis during sepsis, primary human T-cells from septic patient blood should be analyzed for apoptosis induction and PPAR $\gamma$  activation upon GW9662 treatment. Furthermore, it is still questionable whether primary human T-cells react similar in concerns of apoptosis induction, cytokine regulation, and Bcl-2 family member expression when treated with the PPAR $\gamma$  antagonist. If these experiments mirror the results of the underlying work, sepsis therapy with GW9662 (or a comparable PPAR $\gamma$  antagonist) is getting one step forward.

### **6.7.3. Antagonism of S1P to improve peripheral T-cell counts during sepsis**

In my experiments I detected apoptosis of splenic T-cells. This led to reduced peripheral T-cell counts and impaired resistance against pathogens. Another organ where apoptosis of T-cells occurs and which might be another target to improve peripheral T-cell availability and subsequently improve survival might be the thymus. The thymus is the main provider for naïve T-cells during life. It decreases in size and functionality throughout the lifespan. This phenomenon is called thymus involution. For a long time it has been assumed that the thymic function gradually decreases after puberty. By the age of 18, the periphery was thought to be filled with a complete repertoire of antigen-reactive T-cells. In recent years, more and more data have contradicted this dogmatic view and provided demonstrative evidence that the adult thymus remains active late in life and still generates functional T-cells for the peripheral lymphoid repertoire (150-151). During acute inflammatory conditions such as sepsis, a similar pattern of thymus involution can be recognized. In contrast to age-dependent thymus involution, this acute modification is transient, reversible and followed by a phase of hyperproliferation of the thymus. It is called acute thymus involution (152). In addition to the so far identified T-cell apoptosis in the blood and spleen of septic patients, this mechanism adds dramatically to the immunosuppression and subsequent bad outcome of sepsis. Very recently, acute thymus involution has attracted attention for another disease that is accompanied by a massive T-cell depletion, the infection with the HI-virus. HIV infection leads primarily to an infection and subsequent depletion of CD4<sup>+</sup> T-cells. Similar to sepsis, HIV infected patients suffer from immunosuppression and are likely dying by secondary diseases. For HIV infection, it was recently shown that inhibition of the underlying thymus involution reduces the viral load and increases the amount of viable T-cells in the periphery (153). In line with this finding, the underlying mechanism for sepsis-related T-cell depletion should be clarified.

The main emigration factor for naïve T-cells is the lipid sphingosine-1-phosphate (S1P). T-cells follow a S1P gradient out of the thymus in the lymph and blood (upper part of Figure 39) (154-155). S1P is usually secreted by

thrombocytes and erythrocytes, but recent findings also proposed S1P release from apoptotic cells (156-157). During sepsis, there is abundant evidence for apoptosis in the thymus (158). Here, especially  $CD4^+$ ,  $CD8^+$  double positive thymocytes are dying. The expression of the  $S1P_1$  receptor on the surface of thymic endothelial cells as well as T-cells is necessary for emigration of naïve T-cells. However, high concentrations of S1P promote internalization of the  $S1P_1$  receptor and T-cells are not able to overcome the endothelial barrier anymore (159-160). In mice whose haematopoietic stem cells lack the  $S1P_1$  receptor no T-cells are in the periphery because mature T-cells are unable to exit the thymus (160). The underlying hypothesis for this project is that apoptotic cells that occur in the thymus during sepsis secrete S1P thus, destroying the S1P gradient and promoting internalization of the  $S1P_1$  receptor, which is important for emigration of T-cells (lower part of Figure 39).

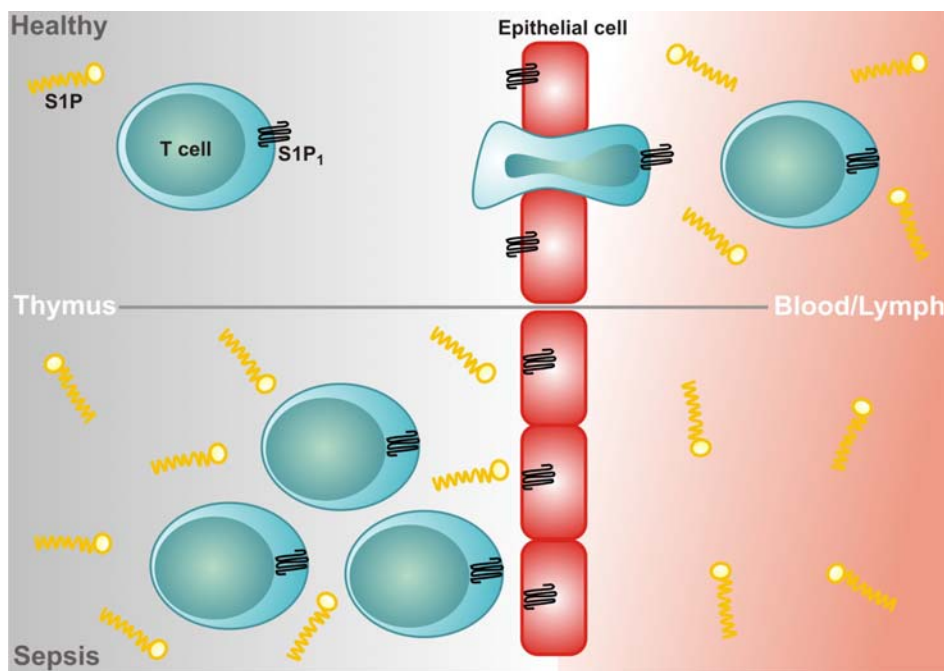


Figure 39: Acute thymus involution as hypothetical mechanism for decreased peripheral T-cell count. In a healthy organism, sphingosine-1-phosphate (S1P) is highly expressed in the blood and lymph and rarely expressed in lymphoid tissue, such as the thymus. Naïve, mature T-cells follow the S1P-gradient out of the tissue into the blood/lymph. Expression of the  $S1P_1$  receptor ( $S1P_1$ ) on thymic endothelial cells as well as T-cells is necessary for emigration of naïve T-cells. During sepsis, thymic S1P promotes internalization of the  $S1P_1$  receptor thus, inhibiting emigration of naïve T-cells.

Targets to reduce acute thymus involution and increase emigration of naïve T-cells are the S1P forming enzymes sphingosine kinase (SphK) 1 and 2. By experiments using SphK1 and SphK2 knockout mice during sepsis, it might be possible to identify the responsible kinase for S1P production in the thymus. Furthermore, there are inhibitors for SphK1 and SphK2 available which might be useful therapeutic agents. Previous publications demonstrated a critical role of SphK1 in endotoxin signaling and sepsis-induced inflammatory responses and suggest that inhibition of SphK1 is a potential therapy for septic shock by reducing phagocyte cytokine production (161). However, they did not take the role of SphK1 or SphK2 during thymus involution into consideration.

In addition, it was proposed that IL-6 is a critical mediator associated with aging and septic shock, and that thymic tissue can produce this cytokine (152, 162). On the contrary, it was shown that IL-7 and leptin protect against thymic remodeling during endotoxemia-induced thymus involution (150, 162-164). For macrophages, it was already shown that they can produce IL-6 upon S1P stimulation (165), leading to the following hypothesis: Sepsis induces thymocyte apoptosis, thereby releasing S1P and promoting thymus involution either by internalization of the S1P<sub>1</sub> receptor and/or indirectly by induction of IL-6 secretion by thymocytes.

If the underlying hypotheses turn out to be correct, another possible target to improve peripheral T-cell count, besides PPAR<sub>γ</sub>, is identified. Targeting one of the S1P-producing SphKs or even S1P itself to limit thymus involution and improve thymic naïve T-cell output might then further improve immunosuppression. The restoration of thymic function in ageing and in various disorders seems thus to be an important objective in the elderly, in AIDS and in a series of haematooncological disorders.

## 7. REFERENCES

1. Nathens AB, Marshall JC. Sepsis, SIRS, and MODS: what's in a name? *World J Surg.* May 1996;20(4):386-391.
2. Deutsche Sepsis Gesellschaft. History of Sepsis. 2011; [www.sepsis-gesellschaft.de](http://www.sepsis-gesellschaft.de).
3. Eichacker PQ, Parent C, Kalil A, et al. Risk and the efficacy of antiinflammatory agents: retrospective and confirmatory studies of sepsis. *Am J Respir Crit Care Med.* Nov 1 2002;166(9):1197-1205.
4. Groesdonk HV, Wagner F, Hoffarth B, Georgieff M, Senftleben U. Enhancement of NF-kappaB activation in lymphocytes prevents T cell apoptosis and improves survival in murine sepsis. *J Immunol.* Dec 15 2007;179(12):8083-8089.
5. Riedemann NC, Guo RF, Ward PA. The enigma of sepsis. *J Clin Invest.* Aug 2003;112(4):460-467.
6. Barke RA, Roy S, Chapin RB, Charboneau R. The role of programmed cell death (apoptosis) in thymic involution following sepsis. *Arch Surg.* Dec 1994;129(12):1256-1261; discussion 1261-1252.
7. Guo RF, Huber-Lang M, Wang X, et al. Protective effects of anti-C5a in sepsis-induced thymocyte apoptosis. *J Clin Invest.* Nov 2000;106(10):1271-1280.
8. Busse M. *Die Rolle der CD4+ T-Lymphozyten bei Sepsis - Untersuchungen in einem Peritonitismodell der Maus.* Dissertation. Greifswald: Mathematisch-Naturwissenschaftliche Fakultät, Ernst-Moritz-Arndt-Universität; 2007.
9. Aßfalg V. *Einfluss des CC-Chemokinrezeptor 4 Knockouts auf die abdominelle Sepsis im Mausmodell der Colon Ascendens Stent Peritonitis.* Dissertation. München: Fakultät für Medizin, Technische Universität München; 2005.
10. Offermann K. *Hydrocortison im septischen Schock: Einfluss auf Inflammation und Hämodynamik.* Dissertation. Berlin: Medizinische Fakultät, Charité-Universitätsmedizin Berlin; 2007.

11. Knaus WA, Wagner DP, Draper EA, et al. The APACHE III prognostic system. Risk prediction of hospital mortality for critically ill hospitalized adults. *Chest*. Dec 1991;100(6):1619-1636.
12. Vincent JL, Moreno R, Takala J, et al. The SOFA (Sepsis-related Organ Failure Assessment) score to describe organ dysfunction/failure. On behalf of the Working Group on Sepsis-Related Problems of the European Society of Intensive Care Medicine. *Intensive Care Med*. Jul 1996;22(7):707-710.
13. Medzhitov R, Janeway CA, Jr. Innate immunity: the virtues of a nonclonal system of recognition. *Cell*. Oct 31 1997;91(3):295-298.
14. Medzhitov R, Janeway CA, Jr. Innate immunity: impact on the adaptive immune response. *Curr Opin Immunol*. Feb 1997;9(1):4-9.
15. Murphy KM, Travers P, Walport M. *Janeway Immunologie*. 7. Auflage ed: Spektrum Akademischer Verlag; 2009.
16. Cohen J. The immunopathogenesis of sepsis. *Nature*. Dec 19-26 2002;420(6917):885-891.
17. van der Poll T, van Deventer SJ. Cytokines and anticytokines in the pathogenesis of sepsis. *Infect Dis Clin North Am*. Jun 1999;13(2):413-426.
18. Faust SN, Levin M, Harrison OB, et al. Dysfunction of endothelial protein C activation in severe meningococcal sepsis. *N Engl J Med*. Aug 9 2001;345(6):408-416.
19. Hotchkiss RS, Nicholson DW. Apoptosis and caspases regulate death and inflammation in sepsis. *Nat Rev Immunol*. Nov 2006;6(11):813-822.
20. Adib-Conquy M, Cavillon JM. Compensatory anti-inflammatory response syndrome. *Thromb Haemost*. Jan 2009;101(1):36-47.
21. Le Tulzo Y, Pangault C, Gacouin A, et al. Early circulating lymphocyte apoptosis in human septic shock is associated with poor outcome. *Shock*. Dec 2002;18(6):487-494.
22. Wesche DE, Lomas-Neira JL, Perl M, Chung CS, Ayala A. Leukocyte apoptosis and its significance in sepsis and shock. *J Leukoc Biol*. Aug 2005;78(2):325-337.

23. Reim D, Westenfelder K, Kaiser-Moore S, Schlautkotter S, Holzmann B, Weighardt H. Role of T cells for cytokine production and outcome in a model of acute septic peritonitis. *Shock*. Mar 2009;31(3):245-250.
24. White JC, Nelson S, Winkelstein JA, Booth FV, Jakab GJ. Impairment of antibacterial defense mechanisms of the lung by extrapulmonary infection. *J Infect Dis*. Feb 1986;153(2):202-208.
25. Wang TS, Deng JC. Molecular and cellular aspects of sepsis-induced immunosuppression. *J Mol Med*. May 2008;86(5):495-506.
26. Hotchkiss RS, Swanson PE, Cobb JP, Jacobson A, Buchman TG, Karl IE. Apoptosis in lymphoid and parenchymal cells during sepsis: findings in normal and T- and B-cell-deficient mice. *Crit Care Med*. Aug 1997;25(8):1298-1307.
27. Hotchkiss RS, Tinsley KW, Swanson PE, et al. Sepsis-induced apoptosis causes progressive profound depletion of B and CD4+ T lymphocytes in humans. *J Immunol*. Jun 1 2001;166(11):6952-6963.
28. Hotchkiss RS, Tinsley KW, Swanson PE, et al. Prevention of lymphocyte cell death in sepsis improves survival in mice. *Proc Natl Acad Sci U S A*. Dec 7 1999;96(25):14541-14546.
29. Hotchkiss RS, Karl IE. The pathophysiology and treatment of sepsis. *N Engl J Med*. Jan 9 2003;348(2):138-150.
30. Peck-Palmer OM, Unsinger J, Chang KC, et al. Modulation of the Bcl-2 family blocks sepsis-induced depletion of dendritic cells and macrophages. *Shock*. Apr 2009;31(4):359-366.
31. Wheeler DS, Zingarelli B, Wheeler WJ, Wong HR. Novel pharmacologic approaches to the management of sepsis: targeting the host inflammatory response. *Recent Pat Inflamm Allergy Drug Discov*. 2009;3(2):96-112.
32. Hotchkiss RS, Opal S. Immunotherapy for sepsis--a new approach against an ancient foe. *N Engl J Med*. Jul 1 2010;363(1):87-89.
33. Mason PE, Al-Khafaji A, Milbrandt EB, Suffoletto BP, Huang DT. CORTICUS: the end of unconditional love for steroid use? *Crit Care*. 2009;13(4):309-311.
34. Buras JA, Holzmann B, Sitkovsky M. Animal models of sepsis: setting the stage. *Nat Rev Drug Discov*. Oct 2005;4(10):854-865.

35. Wang T, Xu J, Yu X, Yang R, Han ZC. Peroxisome proliferator-activated receptor gamma in malignant diseases. *Crit Rev Oncol Hematol*. Apr 2006;58(1):1-14.
36. Issemann I, Green S. Activation of a member of the steroid hormone receptor superfamily by peroxisome proliferators. *Nature*. Oct 18 1990;347(6294):645-650.
37. Zhang F, Lavan BE, Gregoire FM. Selective Modulators of PPAR-gamma Activity: Molecular Aspects Related to Obesity and Side-Effects. *PPAR Res*. 2007; 2007:32696.
38. Schmidt MV, Brune B, von Knethen A. The nuclear hormone receptor PPARgamma as a therapeutic target in major diseases. *ScientificWorldJournal*. 2010;10:2181-2197.
39. Straus DS, Glass CK. Anti-inflammatory actions of PPAR ligands: new insights on cellular and molecular mechanisms. *Trends Immunol*. Dec 2007;28(12):551-558.
40. Clark RB, Bishop-Bailey D, Estrada-Hernandez T, Hla T, Puddington L, Padula SJ. The nuclear receptor PPAR gamma and immunoregulation: PPAR gamma mediates inhibition of helper T cell responses. *J Immunol*. Feb 1 2000;164(3):1364-1371.
41. Sundvold H, Lien S. Identification of a novel peroxisome proliferator-activated receptor (PPAR) gamma promoter in man and transactivation by the nuclear receptor RORalpha1. *Biochem Biophys Res Commun*. Sep 21 2001;287(2):383-390.
42. Zhou J, Wilson KM, Medh JD. Genetic analysis of four novel peroxisome proliferator activated receptor-gamma splice variants in monkey macrophages. *Biochem Biophys Res Commun*. Apr 26 2002;293(1):274-283.
43. Nolte RT, Wisely GB, Westin S, et al. Ligand binding and co-activator assembly of the peroxisome proliferator-activated receptor-gamma. *Nature*. Sep 10 1998;395(6698):137-143.
44. Henke BR, Blanchard SG, Brackeen MF, et al. N-(2-Benzoylphenyl)-L-tyrosine PPARgamma agonists. 1. Discovery of a novel series of potent antihyperglycemic and antihyperlipidemic agents. *J Med Chem*. Dec 3 1998;41(25):5020-5036.



45. Leesnitzer LM, Parks DJ, Bledsoe RK, et al. Functional consequences of cysteine modification in the ligand binding sites of peroxisome proliferator activated receptors by GW9662. *Biochemistry*. May 28 2002;41(21):6640-6650.
46. Hamuro Y, Coales SJ, Morrow JA, et al. Hydrogen/deuterium-exchange (H/D-Ex) of PPARgamma LBD in the presence of various modulators. *Protein Sci*. Aug 2006;15(8):1883-1892.
47. Chandra V, Huang P, Hamuro Y, et al. Structure of the intact PPAR-gamma-RXR-alpha nuclear receptor complex on DNA. *Nature*. Oct 29 2008:350-356.
48. Bishop-Bailey D, Wray J. Peroxisome proliferator-activated receptors: a critical review on endogenous pathways for ligand generation. *Prostaglandins Other Lipid Mediat*. Apr 2003;71(1-2):1-22.
49. Gilroy DW, Colville-Nash PR, Willis D, Chivers J, Paul-Clark MJ, Willoughby DA. Inducible cyclooxygenase may have anti-inflammatory properties. *Nat Med*. Jun 1999;5(6):698-701.
50. Chatterjee PK. On the road to discovering protective endogenous peroxisome proliferator-activator receptor-gamma ligands for endotoxemia: are we there yet? *Crit Care Med*. Apr 2006;34(4):1277-1279.
51. Szeles L, Torocsik D, Nagy L. PPARgamma in immunity and inflammation: cell types and diseases. *Biochim Biophys Acta*. Aug 2007;1771(8):1014-1030.
52. Varga T, Nagy L. Nuclear receptors, transcription factors linking lipid metabolism and immunity: the case of peroxisome proliferator-activated receptor gamma. *Eur J Clin Invest*. Oct 2008;38(10):695-707.
53. Pourcet B, Fruchart JC, Staels B, Glineur C. Selective PPAR modulators, dual and pan PPAR agonists: multimodal drugs for the treatment of type 2 diabetes and atherosclerosis. *Expert Opin Emerg Drugs*. Sep 2006;11(3):379-401.
54. Lehrke M, Lazar MA. The many faces of PPARgamma. *Cell*. Dec 16 2005;123(6):993-999.

55. Pascual G, Glass CK. Nuclear receptors versus inflammation: mechanisms of transrepression. *Trends Endocrinol Metab.* Oct 2006;17(8):321-327.
56. Ricote M, Glass CK. PPARs and molecular mechanisms of transrepression. *Biochim Biophys Acta.* Aug 2007;1771(8):926-935.
57. Chen F, Wang M, O'Connor JP, He M, Tripathi T, Harrison LE. Phosphorylation of PPARgamma via active ERK1/2 leads to its physical association with p65 and inhibition of NF-kappabeta. *J Cell Biochem.* Nov 1 2003;90(4):732-744.
58. Gupta RA, Polk DB, Krishna U, et al. Activation of peroxisome proliferator-activated receptor gamma suppresses nuclear factor kappa B-mediated apoptosis induced by Helicobacter pylori in gastric epithelial cells. *J Biol Chem.* Aug 17 2001;276(33):31059-31066.
59. Wang P, Anderson PO, Chen S, Paulsson KM, Sjogren HO, Li S. Inhibition of the transcription factors AP-1 and NF-kappaB in CD4 T cells by peroxisome proliferator-activated receptor gamma ligands. *Int Immunopharmacol.* Apr 2001;1(4):803-812.
60. Yang XY, Wang LH, Chen T, et al. Activation of human T lymphocytes is inhibited by peroxisome proliferator-activated receptor gamma (PPARgamma) agonists. PPARgamma co-association with transcription factor NFAT. *J Biol Chem.* Feb 18 2000;275(7):4541-4544.
61. Subbaramaiah K, Lin DT, Hart JC, Dannenberg AJ. Peroxisome proliferator-activated receptor gamma ligands suppress the transcriptional activation of cyclooxygenase-2. Evidence for involvement of activator protein-1 and CREB-binding protein/p300. *J Biol Chem.* Apr 13 2001;276(15):12440-12448.
62. Shipley JM, Waxman DJ. Down-regulation of STAT5b transcriptional activity by ligand-activated peroxisome proliferator-activated receptor (PPAR) alpha and PPARgamma. *Mol Pharmacol.* Aug 2003;64(2):355-364.
63. Daynes RA, Jones DC. Emerging roles of PPARs in inflammation and immunity. *Nat Rev Immunol.* Oct 2002;2(10):748-759.

64. Ramos YF, Hestand MS, Verlaan M, et al. Genome-wide assessment of differential roles for p300 and CBP in transcription regulation. *Nucleic Acids Res.* Sep 2010;38(16):5396-5408.
65. Sahar S, Reddy MA, Wong C, Meng L, Wang M, Natarajan R. Cooperation of SRC-1 and p300 with NF-kappaB and CREB in angiotensin II-induced IL-6 expression in vascular smooth muscle cells. *Arterioscler Thromb Vasc Biol.* Jul 2007;27(7):1528-1534.
66. Pascual G, Fong AL, Ogawa S, et al. A SUMOylation-dependent pathway mediates transrepression of inflammatory response genes by PPAR-gamma. *Nature.* Sep 29 2005;437(7059):759-763.
67. Jennewein C, Kuhn AM, Schmidt MV, et al. Sumoylation of peroxisome proliferator-activated receptor gamma by apoptotic cells prevents lipopolysaccharide-induced NCoR removal from kappaB binding sites mediating transrepression of proinflammatory cytokines. *J Immunol.* Oct 15 2008;181(8):5646-5652.
68. Park JY, Bae MA, Cheon HG, et al. A novel PPARgamma agonist, KR62776, suppresses RANKL-induced osteoclast differentiation and activity by inhibiting MAP kinase pathways. *Biochem Biophys Res Commun.* Jan 16 2009;378(3):645-649.
69. Ji H, Wang H, Zhang F, Li X, Xiang L, Aiguo S. PPARgamma agonist pioglitazone inhibits microglia inflammation by blocking p38 mitogen-activated protein kinase signaling pathways. *Inflamm Res.* Nov 2010;59(11):921-929.
70. Desreumaux P, Dubuquoy L, Nutten S, et al. Attenuation of colon inflammation through activators of the retinoid X receptor (RXR)/peroxisome proliferator-activated receptor gamma (PPARgamma) heterodimer. A basis for new therapeutic strategies. *J Exp Med.* Apr 2 2001;193(7):827-838.
71. Johann AM, von Knethen A, Lindemann D, Brune B. Recognition of apoptotic cells by macrophages activates the peroxisome proliferator-activated receptor-gamma and attenuates the oxidative burst. *Cell Death Differ.* Sep 2006;13(9):1533-1540.
72. Perzzutto A, Ulrichs T, Burmester GR, Wirth J. *Taschenatlas der Immunologie.* 2. Auflage. Stuttgart: Georg Thieme Verlag; 2007.

73. Scharl MG, von Eckardstein, A. *Biochemie und Molekularbiologie des Menschen*. 1. Auflage. München: Elsevier GmbH; 2009.
74. Wu JS, Lin TN, Wu KK. Rosiglitazone and PPAR-gamma overexpression protect mitochondrial membrane potential and prevent apoptosis by upregulating anti-apoptotic Bcl-2 family proteins. *J Cell Physiol*. Jul 2009;220(1):58-71.
75. Petros AM, Olejniczak ET, Fesik SW. Structural biology of the Bcl-2 family of proteins. *Biochim Biophys Acta*. Mar 1 2004;1644(2-3):83-94.
76. Hotchkiss RS, Osmon SB, Chang KC, Wagner TH, Coopersmith CM, Karl IE. Accelerated lymphocyte death in sepsis occurs by both the death receptor and mitochondrial pathways. *J Immunol*. Apr 15 2005;174(8):5110-5118.
77. Ayala A, Chung CS, Xu YX, Evans TA, Redmond KM, Chaudry IH. Increased inducible apoptosis in CD4+ T lymphocytes during polymicrobial sepsis is mediated by Fas ligand and not endotoxin. *Immunology*. May 1999;97(1):45-55.
78. Oberholzer C, Oberholzer A, Bahjat FR, et al. Targeted adenovirus-induced expression of IL-10 decreases thymic apoptosis and improves survival in murine sepsis. *Proc Natl Acad Sci U S A*. Sep 25 2001;98(20):11503-11508.
79. Iwata A, Stevenson VM, Minard A, et al. Over-expression of Bcl-2 provides protection in septic mice by a trans effect. *J Immunol*. Sep 15 2003;171(6):3136-3141.
80. Hotchkiss RS, Swanson PE, Knudson CM, et al. Overexpression of Bcl-2 in transgenic mice decreases apoptosis and improves survival in sepsis. *J Immunol*. Apr 1 1999;162(7):4148-4156.
81. Haendeler J, Messmer UK, Brune B, Neugebauer E, Dimmeler S. Endotoxic shock leads to apoptosis in vivo and reduces Bcl-2. *Shock*. Dec 1996;6(6):405-409.
82. Bilbault P, Lavaux T, Lahlou A, et al. Transient Bcl-2 gene down-expression in circulating mononuclear cells of severe sepsis patients who died despite appropriate intensive care. *Intensive Care Med*. Mar 2004;30(3):408-415.

83. Willis SN, Fletcher JI, Kaufmann T, et al. Apoptosis initiated when BH3 ligands engage multiple Bcl-2 homologs, not Bax or Bak. *Science*. Feb 9 2007;315(5813):856-859.
84. Strasser A. The role of BH3-only proteins in the immune system. *Nat Rev Immunol*. Mar 2005;5(3):189-200.
85. Abrams MT, Robertson NM, Yoon K, Wickstrom E. Inhibition of glucocorticoid-induced apoptosis by targeting the major splice variants of BIM mRNA with small interfering RNA and short hairpin RNA. *J Biol Chem*. Dec 31 2004;279(53):55809-55817.
86. Bouillet P, Purton JF, Godfrey DI, et al. BH3-only Bcl-2 family member Bim is required for apoptosis of autoreactive thymocytes. *Nature*. Feb 21 2002;415(6874):922-926.
87. Chang KC, Unsinger J, Davis CG, et al. Multiple triggers of cell death in sepsis: death receptor and mitochondrial-mediated apoptosis. *FASEB J*. Mar 2007;21(3):708-719.
88. Schwulst SJ, Muenzer JT, Peck-Palmer OM, et al. Bim siRNA decreases lymphocyte apoptosis and improves survival in sepsis. *Shock*. Aug 2008;30(2):127-134.
89. Soller M, Tautenhahn A, Brune B, et al. Peroxisome proliferator-activated receptor gamma contributes to T lymphocyte apoptosis during sepsis. *J Leukoc Biol*. Jan 2006;79(1):235-243.
90. Akiyama TE, Sakai S, Lambert G, et al. Conditional disruption of the peroxisome proliferator-activated receptor gamma gene in mice results in lowered expression of ABCA1, ABCG1, and apoE in macrophages and reduced cholesterol efflux. *Mol Cell Biol*. Apr 2002;22(8):2607-2619.
91. Hennet T, Hagen FK, Tabak LA, Marth JD. T-cell-specific deletion of a polypeptide N-acetylgalactosaminyl-transferase gene by site-directed recombination. *Proc Natl Acad Sci U S A*. Dec 19 1995;92(26):12070-12074.
92. Wang HY, Xu X, Ding JH, Bermingham JR, Jr., Fu XD. SC35 plays a role in T cell development and alternative splicing of CD45. *Mol Cell*. Feb 2001;7(2):331-342.
93. Hubbard WJ, Choudhry M, Schwacha MG, et al. Cecal ligation and puncture. *Shock*. Dec 2005;24 Suppl 1:52-57.

94. Wang J, Barke RA, Roy S. Transcriptional and epigenetic regulation of interleukin-2 gene in activated T cells by morphine. *J Biol Chem*. Mar 9 2007;282(10):7164-7171.
95. Harris SG, Phipps RP. The nuclear receptor PPAR gamma is expressed by mouse T lymphocytes and PPAR gamma agonists induce apoptosis. *Eur J Immunol*. Apr 2001;31(4):1098-1105.
96. Doi K, Leelahavanichkul A, Yuen PS, Star RA. Animal models of sepsis and sepsis-induced kidney injury. *J Clin Invest*. Oct 2009;119(10):2868-2878.
97. Unsinger J, Kazama H, McDonough JS, Hotchkiss RS, Ferguson TA. Differential lymphopenia-induced homeostatic proliferation for CD4+ and CD8+ T cells following septic injury. *J Leukoc Biol*. Mar 2009;85(3):382-390.
98. Miyaji T, Hu X, Yuen PS, et al. Ethyl pyruvate decreases sepsis-induced acute renal failure and multiple organ damage in aged mice. *Kidney Int*. Nov 2003;64(5):1620-1631.
99. Doi K, Yuen PS, Eisner C, et al. Reduced production of creatinine limits its use as marker of kidney injury in sepsis. *J Am Soc Nephrol*. Jun 2009;20(6):1217-1221.
100. Kim EJ, Cho D, Hwang SY, Kim TS. Interleukin-2 fusion protein with anti-CD3 single-chain Fv (sFv) selectively protects T cells from dexamethasone-induced apoptosis. *Vaccine*. Nov 12 2001;20(3-4):608-615.
101. Blattman JN, Grayson JM, Wherry EJ, Kaech SM, Smith KA, Ahmed R. Therapeutic use of IL-2 to enhance antiviral T-cell responses in vivo. *Nat Med*. May 2003;9(5):540-547.
102. Chung SW, Kang BY, Kim TS. Inhibition of interleukin-4 production in CD4+ T cells by peroxisome proliferator-activated receptor-gamma (PPAR-gamma) ligands: involvement of physical association between PPAR-gamma and the nuclear factor of activated T cells transcription factor. *Mol Pharmacol*. Nov 2003;64(5):1169-1179.
103. Feau S, Facchinetti V, Granucci F, et al. Dendritic cell-derived IL-2 production is regulated by IL-15 in humans and in mice. *Blood*. Jan 15 2005;105(2):697-702.

104. Downes CP, Bennett D, McConnachie G, et al. Antagonism of PI 3-kinase-dependent signalling pathways by the tumour suppressor protein, PTEN. *Biochem Soc Trans.* Nov 2001;29(Pt 6):846-851.
105. Patel L, Pass I, Coxon P, Downes CP, Smith SA, Macphee CH. Tumor suppressor and anti-inflammatory actions of PPARgamma agonists are mediated via upregulation of PTEN. *Curr Biol.* May 15 2001;11(10):764-768.
106. Suzuki A, Nakano T, Mak TW, Sasaki T. Portrait of PTEN: messages from mutant mice. *Cancer Sci.* Feb 2008;99(2):209-213.
107. Teresi RE, Waite KA. PPARgamma, PTEN, and the Fight against Cancer. *PPAR Res.* 2008; 2008:932632.
108. Strasser A, Pellegrini M. T-lymphocyte death during shutdown of an immune response. *Trends Immunol.* Nov 2004;25(11):610-615.
109. Snow AL, Oliveira JB, Zheng L, Dale JK, Fleisher TA, Lenardo MJ. Critical role for BIM in T cell receptor restimulation-induced death. *Biol Direct.* 2008;3:34-52.
110. Lan RY, Selmi C, Gershwin ME. The regulatory, inflammatory, and T cell programming roles of interleukin-2 (IL-2). *J Autoimmun.* Aug 2008;31(1):7-12.
111. Washida K, Ihara M, Nishio K, et al. Nonhypotensive dose of telmisartan attenuates cognitive impairment partially due to peroxisome proliferator-activated receptor-gamma activation in mice with chronic cerebral hypoperfusion. *Stroke.* Aug 2010;41(8):1798-1806.
112. De Backer O, Elinck E, Priem E, Leybaert L, Lefebvre RA. Peroxisome proliferator-activated receptor gamma activation alleviates postoperative ileus in mice by inhibition of Egr-1 expression and its downstream target genes. *J Pharmacol Exp Ther.* Nov 2009;331(2):496-503.
113. Reinhart K, Brunkhorst FM, Bone HG, et al. Prevention, diagnosis, therapy and follow-up care of sepsis: 1st revision of S-2k guidelines of the German Sepsis Society (Deutsche Sepsis-Gesellschaft e.V. (DSG)) and the German Interdisciplinary Association of Intensive Care and Emergency Medicine (Deutsche Interdisziplinäre Vereinigung für Intensiv- und Notfallmedizin (DIVI)). *Ger Med Sci.* 2010;8:Doc14.

114. Ronco C, Piccinni P, Kellum J. Rationale of extracorporeal removal of endotoxin in sepsis: theory, timing and technique. *Contrib Nephrol.* 2010;167:25-34.
115. Marti-Carvajal A, Salanti G, Cardona AF. Human recombinant activated protein C for severe sepsis. *Cochrane Database Syst Rev.* 2008(1):CD004388.
116. Ayala A, Perl M, Venet F, Lomas-Neira J, Swan R, Chung CS. Apoptosis in sepsis: mechanisms, clinical impact and potential therapeutic targets. *Curr Pharm Des.* 2008;14(19):1853-1859.
117. Hotchkiss RS, Swanson PE, Freeman BD, et al. Apoptotic cell death in patients with sepsis, shock, and multiple organ dysfunction. *Crit Care Med.* Jul 1999;27(7):1230-1251.
118. Martignoni A, Tschop J, Goetzman HS, et al. CD4-expressing cells are early mediators of the innate immune system during sepsis. *Shock.* May 2008;29(5):591-597.
119. Peng Y, Martin DA, Kenkel J, Zhang K, Ogden CA, Elkon KB. Innate and adaptive immune response to apoptotic cells. *J Autoimmun.* Dec 2007;29(4):303-309.
120. Barker RN, Erwig L, Pearce WP, Devine A, Rees AJ. Differential effects of necrotic or apoptotic cell uptake on antigen presentation by macrophages. *Pathobiology.* 1999;67(5-6):302-305.
121. Voll RE, Herrmann M, Roth EA, Stach C, Kalden JR, Girkontaite I. Immunosuppressive effects of apoptotic cells. *Nature.* Nov 27 1997;390(6658):350-351.
122. Hotchkiss RS, Chang KC, Grayson MH, et al. Adoptive transfer of apoptotic splenocytes worsens survival, whereas adoptive transfer of necrotic splenocytes improves survival in sepsis. *Proc Natl Acad Sci U S A.* May 27 2003;100(11):6724-6729.
123. Unsinger J, Kazama H, McDonough JS, Griffith TS, Hotchkiss RS, Ferguson TA. Sepsis-induced apoptosis leads to active suppression of delayed-type hypersensitivity by CD8+ regulatory T cells through a TRAIL-dependent mechanism. *J Immunol.* Jun 15 2010;184(12):6766-6772.



124. Foulds KE, Wu CY, Seder RA. Th1 memory: implications for vaccine development. *Immunol Rev.* Jun 2006;211:58-66.
125. Lawrence KL, White PH, Morris GP, et al. CD4+ lymphocyte adenosine triphosphate determination in sepsis: a cohort study. *Crit Care.* Jun 11 2010;14(3):110-115.
126. Rockwell CE, Snider NT, Thompson JT, Vanden Heuvel JP, Kaminski NE. Interleukin-2 suppression by 2-arachidonyl glycerol is mediated through peroxisome proliferator-activated receptor gamma independently of cannabinoid receptors 1 and 2. *Mol Pharmacol.* Jul 2006;70(1):101-111.
127. Hogan PG, Chen L, Nardone J, Rao A. Transcriptional regulation by calcium, calcineurin, and NFAT. *Genes Dev.* Sep 15 2003;17(18):2205-2232.
128. Weber SU, Schewe JC, Lehmann LE, et al. Induction of Bim and Bid gene expression during accelerated apoptosis in severe sepsis. *Crit Care.* 2008;12(5):128-142.
129. Breitschopf K, Haendeler J, Malchow P, Zeiher AM, Dimmeler S. Posttranslational modification of Bcl-2 facilitates its proteasome-dependent degradation: molecular characterization of the involved signaling pathway. *Mol Cell Biol.* Mar 2000;20(5):1886-1896.
130. Kashiwada M, Lu P, Rothman PB. PIP3 pathway in regulatory T cells and autoimmunity. *Immunol Res.* 2007;39(1-3):194-224.
131. Li D, Qu Y, Mao M, et al. Involvement of the PTEN-AKT-FOXO3a pathway in neuronal apoptosis in developing rat brain after hypoxia-ischemia. *J Cereb Blood Flow Metab.* Dec 2009;29(12):1903-1913.
132. Walsh PT, Buckler JL, Zhang J, et al. PTEN inhibits IL-2 receptor-mediated expansion of CD4+ CD25+ Tregs. *J Clin Invest.* Sep 2006;116(9):2521-2531.
133. Ewings KE, Wiggins CM, Cook SJ. Bim and the pro-survival Bcl-2 proteins: opposites attract, ERK repels. *Cell Cycle.* Sep 15 2007;6(18):2236-2240.
134. Williams DL, Li C, Ha T, et al. Modulation of the phosphoinositide 3-kinase pathway alters innate resistance to polymicrobial sepsis. *J Immunol.* Jan 1 2004;172(1):449-456.

135. Bommhardt U, Chang KC, Swanson PE, et al. Akt decreases lymphocyte apoptosis and improves survival in sepsis. *J Immunol.* Jun 15 2004;172(12):7583-7591.
136. Hoogerwerf JJ, van Zoelen MA, Wiersinga WJ, et al. Gene expression profiling of apoptosis regulators in patients with sepsis. *J Innate Immun.* 2010;2(5):461-468.
137. Chung SW, Kang BY, Kim SH, et al. Oxidized low density lipoprotein inhibits interleukin-12 production in lipopolysaccharide-activated mouse macrophages via direct interactions between peroxisome proliferator-activated receptor-gamma and nuclear factor-kappa B. *J Biol Chem.* Oct 20 2000;275(42):32681-32687.
138. Zapolska-Downar D, Naruszewicz M. Propionate reduces the cytokine-induced VCAM-1 and ICAM-1 expression by inhibiting nuclear factor-kappa B (NF-kappaB) activation. *J Physiol Pharmacol.* Jun 2009;60(2):123-131.
139. Li M, Pascual G, Glass CK. Peroxisome proliferator-activated receptor gamma-dependent repression of the inducible nitric oxide synthase gene. *Mol Cell Biol.* Jul 2000;20(13):4699-4707.
140. Lin TH, Yang RS, Tang CH, Lin CP, Fu WM. PPARgamma inhibits osteogenesis via the down-regulation of the expression of COX-2 and iNOS in rats. *Bone.* Oct 2007;41(4):562-574.
141. Liu JJ, Liu PQ, Lin DJ, et al. Downregulation of cyclooxygenase-2 expression and activation of caspase3 are involved in peroxisome proliferator-activated receptor-gamma agonists induced apoptosis in human monocyte leukemia cells in vitro. *Ann Hematol.* Mar 2007;86(3):173-183.
142. Kaplan JM, Cook JA, Hake PW, O'Connor M, Burroughs TJ, Zingarelli B. 15-Deoxy-delta(12,14)-prostaglandin J(2) (15D-PGJ(2)), a peroxisome proliferator activated receptor gamma ligand, reduces tissue leukosequestration and mortality in endotoxic shock. *Shock.* Jul 2005;24(1):59-65.
143. Lee KJ, Ha ES, Kim MK, et al. CD36 signaling inhibits the translation of heat shock protein 70 induced by oxidized low density lipoprotein through

- activation of peroxisome proliferators-activated receptor gamma. *Exp Mol Med*. Dec 31 2008;40(6):658-668.
144. Cunard R, Ricote M, DiCampi D, et al. Regulation of cytokine expression by ligands of peroxisome proliferator activated receptors. *J Immunol*. Mar 15 2002;168(6):2795-2802.
145. Schmitz J, Thiel A, Kuhn R, et al. Induction of interleukin 4 (IL-4) expression in T helper (Th) cells is not dependent on IL-4 from non-Th cells. *J Exp Med*. Apr 1 1994;179(4):1349-1353.
146. Yang XY, Wang LH, Mihalic K, et al. Interleukin (IL)-4 indirectly suppresses IL-2 production by human T lymphocytes via peroxisome proliferator-activated receptor gamma activated by macrophage-derived 12/15-lipoxygenase ligands. *J Biol Chem*. Feb 8 2002;277(6):3973-3978.
147. Chtanova T, Kemp RA, Sutherland AP, Ronchese F, Mackay CR. Gene microarrays reveal extensive differential gene expression in both CD4(+) and CD8(+) type 1 and type 2 T cells. *J Immunol*. Sep 15 2001;167(6):3057-3063.
148. Yamazaki S, Inamori S, Nakatani T, Suga M. Activated protein C attenuates cardiopulmonary bypass-induced acute lung injury through the regulation of neutrophil activation. *J Thorac Cardiovasc Surg*. Jul 3 2010. in Press.
149. Ayala A, Song GY, Chung CS, Redmond KM, Chaudry IH. Immune depression in polymicrobial sepsis: the role of necrotic (injured) tissue and endotoxin. *Crit Care Med*. Aug 2000;28(8):2949-2955.
150. Lynch HE, Goldberg GL, Chidgey A, Van den Brink MR, Boyd R, Sempowski GD. Thymic involution and immune reconstitution. *Trends Immunol*. Jul 2009;30(7):366-373.
151. Geenen V, Poulin JF, Dion ML, et al. Quantification of T cell receptor rearrangement excision circles to estimate thymic function: an important new tool for endocrine-immune physiology. *J Endocrinol*. Mar 2003;176(3):305-311.
152. Gruver AL, Sempowski GD. Cytokines, leptin, and stress-induced thymic atrophy. *J Leukoc Biol*. Oct 2008;84(4):915-923.

153. Napolitano LA, Schmidt D, Gotway MB, et al. Growth hormone enhances thymic function in HIV-1-infected adults. *J Clin Invest.* Mar 2008;118(3):1085-1098.
154. Pappu R, Schwab SR, Cornelissen I, et al. Promotion of lymphocyte egress into blood and lymph by distinct sources of sphingosine-1-phosphate. *Science.* Apr 13 2007;316(5822):295-298.
155. Schwab SR, Cyster JG. Finding a way out: lymphocyte egress from lymphoid organs. *Nat Immunol.* Dec 2007;8(12):1295-1301.
156. Weigert A, Johann AM, von Knethen A, Schmidt H, Geisslinger G, Brune B. Apoptotic cells promote macrophage survival by releasing the antiapoptotic mediator sphingosine-1-phosphate. *Blood.* Sep 1 2006;108(5):1635-1642.
157. Johann AM, Weigert A, Eberhardt W, et al. Apoptotic cell-derived sphingosine-1-phosphate promotes HuR-dependent cyclooxygenase-2 mRNA stabilization and protein expression. *J Immunol.* Jan 15 2008;180(2):1239-1248.
158. Feng H, Guo L, Song Z, et al. Caveolin-1 protects against sepsis by modulating inflammatory response, alleviating bacterial burden, and suppressing thymocyte apoptosis. *J Biol Chem.* Aug 13 2010;285(33):25154-25160.
159. Thangada S, Khanna KM, Blaho VA, et al. Cell-surface residence of sphingosine 1-phosphate receptor 1 on lymphocytes determines lymphocyte egress kinetics. *J Exp Med.* Jul 5 2010;207(7):1475-1483.
160. Matloubian M, Lo CG, Cinamon G, et al. Lymphocyte egress from thymus and peripheral lymphoid organs is dependent on S1P receptor 1. *Nature.* Jan 22 2004;427(6972):355-360.
161. Puneet P, Yap CT, Wong L, et al. SphK1 regulates proinflammatory responses associated with endotoxin and polymicrobial sepsis. *Science.* Jun 4 2010;328(5983):1290-1294.
162. Hick RW, Gruver AL, Ventevogel MS, Haynes BF, Sempowski GD. Leptin selectively augments thymopoiesis in leptin deficiency and lipopolysaccharide-induced thymic atrophy. *J Immunol.* Jul 1 2006;177(1):169-176.

163. Broers AE, Posthumus-van Sluijs SJ, Spits H, et al. Interleukin-7 improves T-cell recovery after experimental T-cell-depleted bone marrow transplantation in T-cell-deficient mice by strong expansion of recent thymic emigrants. *Blood*. Aug 15 2003;102(4):1534-1540.
164. Unsinger J, McGlynn M, Kasten KR, et al. IL-7 promotes T cell viability, trafficking, and functionality and improves survival in sepsis. *J Immunol*. Apr 1 2010;184(7):3768-3779.
165. Price MM, Kapitonov D, Allegood J, Milstien S, Oskeritzian CA, Spiegel S. Sphingosine-1-phosphate induces development of functionally mature chymase-expressing human mast cells from hematopoietic progenitors. *FASEB J*. Oct 2009;23(10):3506-3515.

## 8. APPENDIX

### Phosphate buffered saline (PBS)

NaCl	137 mM
KCl	2.7 mM
Na <sub>2</sub> HPO <sub>4</sub>	8.1 mM
KH <sub>2</sub> PO <sub>4</sub>	1.5 mM
→ pH 7.4	

### Western Lysis buffer

TRIS	50 mM
NaCl	150 mM
EDTA	5 mM
NP-40	0.5% (v/v)
→ pH 7.9	
Freshly added:	
DTT	1 mM
PIM	1 x
PhosStop	1 x

### SDS running buffer

Tris/HCl	25 mM
Glycine	192 mM
SDS	0.7 mM
→ pH 8.3	

### TBS (Tris buffered saline)

Tris/HCl	50 mM
NaCl	140 mM
→ pH 7.4	

### Upper Tris buffer (4 x)

Tris/HCl	0.5 M
→ pH 6.8	

### Lower Tris buffer (4 x)

Tris/HCl	1.5 M
----------	-------

### SDS sample buffer (4 x)

Tris/HCl	250 mM
SDS	8% (w/v)
Glycerol	40% (v/v)
Bromophenol blue	0.02% (w/v)
β-mercaptoethanol	10% (v/v)
→ pH 6.8	

### Blotting buffer

Tris-HCl	25 mM
Glycine	192 mM
Methanol	20% (v/v)
→ pH 8.3	

### TTBS

Tween-20	0.06% (v/v)
→ in TBS	

### Neutralizing buffer for genotyping

Tris-HCl	40 mM
→ pH 5	

**DEPC-treated water**

1 ml Diethylpyrocarbonate (DEPC) in  
1 l distilled H<sub>2</sub>O  
→ stir overnight and autoclave

**Urea lysis buffer**

Urea	6.65 M
Glycerol	10% (v/v)
SDS	1% (v/v)
Tris-HCl	10 mM
deionized water	ad 50 ml

→ pH 7.4

**Erythrocyte lysis buffer**

NH <sub>4</sub> Cl	155 mM
KHCO <sub>3</sub>	10 mM
EDTA	0.1 mM

**autoMACS rinsing buffer**

EDTA	2 mM
------	------

→ in PBS

**ChIP lysis buffer**

NaCl	150 mM
Tris-HCl	50 mM
NP-40	1% (m/v)

→ pH 8.0

**Lysis buffer for genotyping**

NaOH	25 mM
EDTA	0.2 mM

→ pH 12

**autoMACS running buffer**

EDTA	2 mM
BSA	0.5% (w/v)

→ in PBS

**ChIP elution buffer**

NaHCO <sub>3</sub>	0.1 M
SDS	1% (v/v)

→ deionized water ad 4.5 ml

**Zinc fixative**

Tris Base	12.1 g
Deionized water	900 ml
HCl	1.0 M
Ca(C <sub>2</sub> H <sub>3</sub> O <sub>2</sub> ) <sub>2</sub>	0.5 g
Zn(C <sub>2</sub> H <sub>3</sub> O <sub>2</sub> ) <sub>2</sub>	5.0 g
ZnCl <sub>2</sub>	5.0 g

**Antibody diluent**

NaCl	100 mM
BSA	3% (m/v)
Triton X-100	1% (m/v)
NaPO <sub>4</sub>	50 mM

→ pH 7.4

**Sodium dodecyl sulfate (SDS)-polyacrylamide gel**

	10% (Separation)	4% (Stacking)
40% Acrylamide/Bis-acrylamide (37.5% : 1.0% w/v)	2.5 ml	300 µl
Lower Tris buffer (4 x)	2.5 ml	
Upper Tris buffer (4 x)		750 µl
H <sub>2</sub> O distilled	4.9 ml	1.95 ml
10% SDS	100 µl	30 µl
TEMED	10 µl	2.5 µl
10% (w/v) ammonium persulfate	100 µl	25 µl



## 9. PUBLICATIONS

### PAPER

**Schmidt MV**, Paulus P, Kuhn AM, Weigert A, Morbitzer V, Zacharowski K, Kempf VAJ, Brüne B, von Knethen A

PPAR $\gamma$ -induced T-cell apoptosis reduces survival during polymicrobial sepsis  
American Journal of Respiratory and Critical Care Medicine.

2011 Feb 25. (In Press)

**Schmidt MV**, Brüne B, von Knethen A

The nuclear hormone receptor PPAR $\gamma$  as therapeutic target in major diseases  
ScientificWorldJournal 10:2181-97, 2010

Kuhn AM, Tzieply N, **Schmidt MV**, von Knethen A, Namgaladze D, Yamamoto M, Brüne B

Antioxidant signaling via Nrf2 counteracts lipopolysaccharide-mediated inflammatory responses in foam cell macrophages

Free Radical Biology and Medicine. 2011 Mar 4. (In Press)

Von Knethen A, Neb H, Meilladec-Jullig V, **Schmidt MV**, Kuhn AM, Weis N, Brüne B

ROS-driven PPAR $\gamma$  activation increased HO-1 mRNA stability in monocytes/macrophages

Free Radical Biology and Medicine (In Revision)

Weigert A, Cremer S, **Schmidt MV**, von Knethen A, Brüne B

Cleavage of sphingosine kinase 2 by caspase 1 provokes its release from apoptotic cells

Blood 115(17):3531-40, 2010

Jennewein C, Kuhn AM, **Schmidt MV**, Meilladec-Jullig V, von Knethen A, Gonzales FJ, Brüne B

Sumoylation of peroxisome proliferator-activated receptor gamma by apoptotic cells prevents lipopolysaccharide-induced NCoR removal from kappaB binding sites mediating transrepression of proinflammatory cytokines  
Journal of Immunology 181(8):5646-52, 2008

## **ABSTRACTS & POSTER**

**Schmidt MV**, Paulus P, Kuhn AM, Morbitzer V, Zacharowski K, Brüne B, von Knethen A

T-cells determine the fate of sepsis (Abstract)

T-cells Subsets & Functions. Marburg, Germany 2010

**Schmidt MV**, Paulus P, Kuhn AM, Morbitzer V, Zacharowski K, Brüne B, von Knethen A

Nuclear receptor PPAR $\gamma$  promotes T-cell apoptosis during sepsis (Abstract & Poster)

Keystone Symposium: Nuclear Receptors. Keystone, MO, USA 2010

**Schmidt MV**, Paulus P, Kuhn AM, Meilladec-Jullig V, Zacharowski K, Brüne B, von Knethen A

T-cell-specific PPAR $\gamma$  depletion inhibits T-cell apoptosis and improves survival of septic mice via an IL-2-dependent mechanism (Abstract & Poster)

Sepsis 2009. Amsterdam, Netherlands 2009

**Schmidt MV**, Paulus P, Kuhn AM, Meilladec-Jullig V, Zacharowski K, Brüne B, von Knethen A

PPAR $\gamma$  induces T-cell apoptosis during sepsis via NFAT ligation, consequently inhibits IL-2 expression and downstream signaling (Abstract & Poster)

Sepsis and multipleorgan dysfunctions. Weimar, Germany, 2009

**Schmidt MV**, von Knethen A, Brüne B

The role of peroxisome proliferator-activated receptor gamma in the progression of sepsis (Abstract & Poster)

Joint Annual Meeting of Immunology. Vienna, Austria, 2008

## 10. ACKNOWLEDGMENTS

An dieser Stelle möchte ich einigen Personen danken, die jeder auf seine/ihre Weise grundlegend an der Entstehung dieser Doktorarbeit teilhatten.

Mein besonderer Dank gilt:

PD Dr. Andreas von Knethen für die Überlassung des interessanten Themas, die Betreuung und anregenden Diskussionen über die Ergebnisse, die Möglichkeit der selbständigen Forschung, die Ermöglichung und Unterstützung meiner diversen Kongressreisen, die humorvollen Retreatabende und sein Vertrauen in mich und meine Arbeit.

Prof. Dr. Bernhard Brüne für die Möglichkeit der Promotion an seinem Institut, für das große Interesse an meiner Arbeit und die zuverlässige, regelmäßige Diskussionsbereitschaft mit stets konstruktiver Kritik.

Prof. Dr. Dr. Kai Zacharowski und Dr. Patrick Paulus für die Ermöglichung der Durchführung des ZLP-Modells, die kompetente Unterstützung in allen Sepsis-Fragen, die stete Diskussions- und Korrekturbereitschaft sowie für die zukunftsorientierte Hilfestellung.

Prof. Dr. Volkhard Kempf für die Ermöglichung der peritonealen CFU-Messung und den großartigen Ruderunterricht.

meinen Eltern und meiner Schwester für ihr anhaltendes Interesse an meiner Forschung und ihre bedingungslose, vertrauensvolle Unterstützung in jeder Hinsicht.

Andreas Völker, der meine Doktorarbeitszeit in all ihren Facetten mit mir durchlebt hat, für seine liebevolle und optimistische Unterstützung durch Worte, Taten und zusammenverbrachte Zeit.

Sebastian Barzen für sein wohlthuend sonniges Gemüt, seine unermüdliche Hilfsbereitschaft, sein umfassendes Interesse unter anderem auch an meiner Arbeit und für eine großartige und stets kommunikative WG-Zeit und Freundschaft.

meinen ehemaligen Kommilitoninnen Derya, Mascha, Anne und Mirella für ihre intensive Freundschaft und die ausgesprochen schöne, amüsante und abwechslungsreiche Zeit bei vielen Stammtischen, Urlauben und Feiern neben dem Forschungsalltag.

meinen Mitstreitern des „PPAR $\gamma$ -Teams“ Anne-Marie, Carla, Nico und Vera für eine tolle Laborzeit, für viele erheiternde und ebenso fachlich höchst prägnante, fordernde und fruchtende Gespräche und für eine Freundschaft die über den Laboralltag hinaus besteht.

Johanna Blees für den sportlichen Ausgleich beim abendlichen Joggen oder Rudern, die intensiven Gespräche, ihr ansteckendes Lachen und die gute, wiederaufgelebte Freundschaft.

Danny, Kathrin, Lisa, Steffi und Barbara für die freundschaftliche Laborgemeinschaft und viele erheiternde Gesprächsrunden.

Nadja Wallner und Meggie Wiebe für die jederzeit tatkräftige und zuverlässige Unterstützung in Mausangelegenheiten und Histo-Färbungen.

allen weiteren Mitarbeitern der AG Brüne für das gute Arbeitsklima, die ständige Hilfsbereitschaft und die durchweg schöne Zeit.

## 11. CURRICULUM VITAE

Name Martina Victoria Schmidt

### Promotion

09/2007 bis 03/2011 Promotion im Fachbereich Medizin,  
Institut für Biochemie I - Pathobiochemie  
Goethe-Universität Frankfurt am Main

### Studienverlauf

09/2009 Diplom in Pharmazie (Dipl.-Pharm.)  
Institut für Pharmazeutische Technologie  
Martin-Luther-Universität, Halle-Wittenberg

08/2007 Appobation zur Apothekerin  
Fachbereich Pharmazie,  
Goethe-Universität, Frankfurt am Main

12/2006 bis 05/2007 Praktisches Jahr bei Merck KGaA, Darmstadt  
Erstellung einer Diplomarbeit

05/2006 bis 11/2006 Praktisches Jahr in der Apotheke am Weißen Stein,  
Frankfurt am Main

10/2001 bis 05/2006 Studium der Pharmazie,  
Goethe-Universität, Frankfurt am Main

### Schulische Laufbahn

1992 bis 2001 Städtisches Gymnasium, Haan  
Abschluss: Abitur

1998 bis 1999 Auslandsschuljahr, Marshall Senior High School  
Marshall, Minnesota, USA; Abschluss: Graduation

1988 bis 1992 Grundschule Unterhaan, Haan

Frankfurt am Main, den

## 12. ERKLÄRUNG

Ich erkläre ehrenwörtlich, dass ich die dem Fachbereich Medizin der Goethe-Universität Frankfurt am Main zur Promotionsprüfung eingereichte Arbeit mit dem Titel

**“The role of peroxisome proliferator-activated receptor  $\gamma$   
during sepsis-induced lymphopenia“**

am Institut für Biochemie I – Pathobiochemie unter Betreuung und Anleitung von PD Dr. Andreas von Knethen ohne sonstige Hilfe selbst durchgeführt und bei der Abfassung der Arbeit keine anderen als die in der Dissertation angeführten Hilfsmittel benutzt habe. Darüber hinaus versichere ich, nicht die Hilfe einer kommerziellen Promotionsvermittlung in Anspruch genommen zu haben.

Ich habe bisher an keiner in- oder ausländischen Universität ein Gesuch um Zulassung zur Promotion eingereicht. Die vorliegende Arbeit wurde bisher nicht als Dissertation eingereicht.

Teile der vorliegenden Arbeit wurden in folgenden Publikationsorganen veröffentlicht:

American Journal of Respiratory and Critical Care Medicine. 2011 Feb 25.  
[In Press]

ScientificWorldJournal 10:2181-97, 2010

Frankfurt am Main, den